INCIPIENT FAILURE DETECTION IN BUS ENGINE COMPONENTS

William B. Ribbens
Mitra Naaseh

Center for Transit Research and Management Development
University of Michigan Transportation Research Institute
2901 Baxter Road
Ann Arbor, MI 48109

MARCH 1987

FINAL REPORT

Document is available to the U.S. public through the
National Technical Information Service
Springfield, Virginia 22161

Prepared for
U.S. DEPARTMENT OF TRANSPORTATION
URBAN MASS TRANSPORTATION ADMINISTRATION
Office of Technical Assistance
Washington, D.C. 20590

NOTICE

Technical Report Documentation Page

1. Report No.	2. Government Accession No.	3. Recipient's Catalog No.

4. Title and Subtitle	5. Report Date
Incipient Failure Detection in Bus Engine Components	March 1987
	6. Performing Organization Code
7. Author(s)	8. Performing Organization Report No.
W. B. Ribbens and M. Naaseh	UMTRI-87-16
9. Performing Organization Name and Address	10. Work Unit No.
Vehicular Electronics Lab University of Michigan Ann Arbor, MI	11. Contract or Grant No. UMTA-MI-0009
	13. Type of Report and Period Covered
12. Sponsoring Agency Name and Address U.S. Department of Technical Urban Mass Transportation Administration Office of Technical Assistance Washington, D.C. 20590	Final Report August 1985 - March 1987
	14. Sponsoring Agency Code URT-33

15. Supplementary Notes

16. Abstract

This report summarizes technical progress in a study of incipient fault detection in bus engines. The type of failures to which this method is applicable are those for which there is a gradual deterioration to failure over a relatively long time. The fundamental basis of predicting such a fault is real time measurements of engine performance in the form of instantaneous brake torque and the nonuniformity in that torque. In addition to predicting component failure this method can also detect the failure once it has occurred.

The present study has used instrumentation which was developed at Vehicular Electronics Lab of Univ. of Mich. for measurement of engine torque. For our studies a number of buses were instrumented for real time performance measurements in simulated route operation. A database was established from these measurements from which the statistical model for predicting failure has been developed.

This report explains: the theory of the method, the instrumentation, the experimental results and the statistical model upon which failure prediction is based. The experimental results are interpreted within the framework of the failure prediction model. In addition the report explains the optimum strategy for using the method to optimize maintenance scheduling.

17. Key Words	18. Distribution Statement
Failure detection Optimal Bus Maintenance Scheduling	

19. Security Classif. (of this report)	20. Security Classif. (of this page)	21. No. of Pages	22. Price
Unclassified	Unclassified	74	

Table of Contents

1. INTRODUCTION

This report presents the results of a study which has had, as its goal, the development of instrumentation and procedures for detecting incipient failures in bus diesel engines. The class of failures toward which this research was aimed is characterized by gradual deterioration of performance to failure. In this context failure means unacceptable level of performance. A typical example of a component for which such gradual deterioration might be expected is a fuel injector or an injector pump.

In addition, it has been a goal of this research to provide diagnostic assistance to mechanics. The instrumentation developed for the primary goal for this project has the capability of isolating individual cylinders having relatively low performance, thereby helping the mechanic quickly locate a corresponding fault. An explanation of this 'side-benefit' to our studies is presented later in this report.

There are numerous applications for detection of incipient failure in optimizing scheduled bus maintenance. Whenever a failure is anticipated in a bus, it can be scheduled for repair before the performance reaches unacceptable levels. Moreover, unnecessary routine maintenance operations can be reduced.

One of the issues addressed by the present project is the feasibility and desirability of onboard instrumentation for direct performance measurements. Although it is desirable to have onboard instrumentation for maintaining continuous performance measurements, it is far less costly and perhaps adequate to perform the measurements in the shop using off-board instrumentation.

In this latter case, performance variables are measured once each day, possibly during fueling or bus checkout times. Once per day performance measurements represent sampling of the relevant performance variable. However, once/day sampling is sufficient, provided the deterioration of performance is sufficiently gradual.

The concept for early detection of incipient failure of engine components is based upon continuous, real-time measurements

of engine performance. Early detection of component failure is derived from these measurements.

Figure 1 illustrates a typical deterioration to failure for a component based upon the measurement of a performance variable P(t).

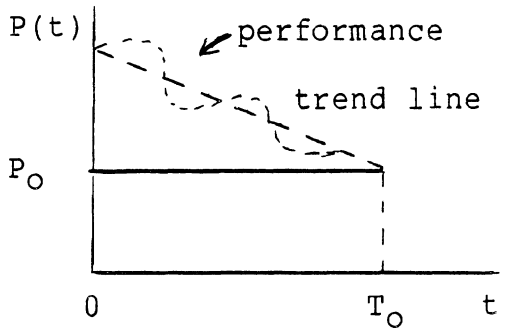

Figure 1.

In the present example, a performance variable decreases with time as a component deteriorates. Failure is defined as performance $P(t) \leq P_o$. A trend line is obtained (statistically) using one of the standard prediction methods. An estimated time-to-failure T_o is continuously computed based upon P(t) at the present time and the history up to the present time. In addition to estimated time-to-failure, confidence limits can be computed for T_o.

The present project has concentrated on continuous, real-time measurements of performance to establish the feasibility of the concept. In particular the present project has concentrated on measurements of a specific performance variable and the feasibility of using these measurements to sense degraded performances.

The present project has established the feasibility of continuous, real-time performance measurements using onboard instrumentation as explained in this report.

This report is organized into 4 sections including: 1) theory of concept for real-time performance measurement, 2) description of instrumentation, 3) description of experiments and procedures, and 4) summary of results and conclusions.

2. THEORY OF METHOD

The present method of measuring torque nonuniformity is based upon the relationship between torque and crankshaft angular speed and upon noncontacting measurements of that speed. This relationship is nonlinear and relatively complex. However, for the purpose of explaining the theory of the present measurement method, it is convenient to assume a simplified linear model for the relationship. This model is approximately valid at steady RPM in the small signal case and provides valuable insight into the present method.

A linear model for the engine/drivetrain can be understood with reference to Figure 2 which is an equivalent circuit for the engine/drivetrain (first introduced in ref. 1; see Bibliography below, p. 68).

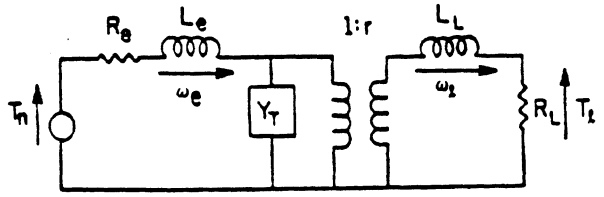

Figure 2. Equivalent circuit for engine/drivetrain

In this equivalent circuit torque is analogous to voltage and angular speed is analogous to current. This equivalent circuit represents an engine which is delivering torque T_ℓ to a load through a transmission. In the particular experimental studies which are reported in this paper the vehicle is equipped with an automatic transmission.

In this figure the generator voltage $T_n(t)$ is analogous to the torque which is applied at the crankshaft. This torque results from cylinder pressure during the power stroke less cylinder frictional losses, pumping losses, and losses due to the forces required to accelerate the reciprocating components. The crankshaft angular speed is denoted $\omega_e(t)$ and the transmission output angular speed is denoted ω_ℓ.

The various circuit parameters have the following physical correspondence:

circuit element	physical equivalent
transformer	transmission
Y_T	torsional isolator
R_e	frictional loss which is proportional to angular speed
L_e	moment of inertia of engine rotating parts
L_L	load moment of inertia
R_L	load power absorber

The torsional isolator is a component which isolates the load from the torque fluctuations resulting from each cylinder power stroke. In the case of a manual transmission this isolation is provided by a set of springs in the clutch plate. The corresponding equivalent circuit is a shunt combination of a capacitor with a series resistance.

In the case of an automatic transmission the required isolation is provided by the torque converter. The circuit equivalence for the torque converter is a relatively complex function of frequency. (Note: The fundamental frequency of the torque fluctuations is cylinder firing frequency). The frequency components of the torque fluctuation are proportional to engine angular speed or RPM. For the purposes of the present discussion of the shunt admittance the torque converter can be modelled as an ideal isolator.

$Y_T = 0$ for steady torque component

$Y_T \to \infty$ for torque fluctuations

This latter model is presumed for the present discussion because the experimental measurements were made in a bus having an automatic transmission, and because most buses use automatic transmissions.

The equivalent circuit for the engine drivetrain with respect to torque fluctuations (at steady RPM) is depicted in Figure 3. In this reduced equivalent circuit the torque deviation from the average (d-c) value is denoted τ_n.

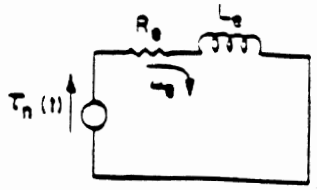

Figure 3. Equivalent circuit for engine

$$\tau_n = T_n(t) - T_n$$
$$T_n = \text{steady average torque}$$

Similarly the angular speed fluctuations are conveniently denoted $\eta(t)$:

$$\eta(t) = \omega_e(t) - \Omega$$

where

$$\Omega = \text{steady average crankshaft angular speed} = \frac{2\pi \cdot (RPM)}{60}$$

The relationship between torque fluctuation and crankshaft angular speed is expressed by the following equation which is applicable within the validity of the small signal linear approximation:

$$\eta(t) = \tau_n(t) * h(t)$$

where

$h(t)$ = impulse response for the equivalent circuit of figure 3.

$*$ $\longrightarrow$ convolution

The relationship between $\tau_n(t)$ and $\eta(t)$ can also be expressed in the frequency domain

$$n(j\lambda) = \tau_n(j\lambda)H(j\lambda)$$

where

$H(j\lambda)$ = frequency response

λ = radian frequency

$\tau_n^*(j\lambda)$ = complex amplitude of torque

$n(j\lambda)$ = complex amplitude of angular speed.

For the equivalent circuit of figure 3 the transfer function for torque vs angular speed is given by:

$$H(j\lambda) = \frac{1}{R_e + j\lambda L_e}$$

The relationship between crankshaft angular speed fluctuation and torque fluctuation is RPM dependent as shown in the above equation. This result can be readily seen from $H(j\lambda)$ and from the fact that the Fourier components of τ_n are at frequencies λ which are proportional to RPM.

Nevertheless, measurements of angular speed fluctuation provide a means of measuring torque fluctuations. This paper presents a scalar index for torque nonuniformity which is computed once for each engine cycle and experimental results of measurements of this variable.

Moreover, the sinusoidal frequency response is given approximately by the following expression for sufficiently high RPM.

$$H(j\lambda) \simeq \frac{1}{j\lambda L_e}$$

For the buses involved in the experimental studies for the present project this approximation is valid at idle and higher RPM's.

2.1 Nonuniformity Index

The concept for the nonuniformity index is based upon the presumption that the essential nonuniformity is represented by the extrema of the torque or crankshaft angular speed. Previous experimental studies (refs. 2 and 3) have confirmed this conjecture of the relative importance of the extrema in ω_e. The

present method uses nonuniformity in crankshaft angular speed as an index of torque nonuniformity.

The present work is an extension of a concept which was first presented in (ref. 4). The nonuniformity metric presented in that paper is constructed from relative maxima and relative minima of torque. Recent research (ref. 2 and 3) has shown that an index of nonuniformity can be constructed from relative minima of angular speed. However, relative maxima are equally suitable for measuring torque nonuniformity.

This study uses the latter method for obtaining nonuniformity index. This index is computed from a block of N consecutive relative minima in $\omega_e(t)$ and is in fact a metric on an N dimensional vector space.

The nonuniformity metric is obtained from an N dimensional vector $\underline{\omega}(k)$ which is obtained by sampling the measured angular speed $\omega_e(t)$ at extremal values:

$$\underline{\omega}'(k) = [\omega_1(k) \ldots . \omega_N(k)] = \text{transpose of } \underline{\omega}(k)$$

where

$$\omega_m(k) = \omega_e[t_m(k)] \qquad m = k, k+1, \ldots k+N-1$$
$$k = 0, N, 2N \ldots$$

and where

$t_m(k)$ = time of mth relative minima of $\omega_e(t)$ within the kth block of data. Prime refers to transpose. Note: a similar vector could be constructed using relative maxima of $\omega_e(t)$.

The average value of the N components of $\underline{\omega}(k)$ is denoted $\omega_a(k)$ and is computed

$$\omega_a(k) = \frac{1}{N} \sum_{n=1}^{N} \omega_n(k)$$

Then a nonuniformity vector $\underline{n}(k)$ is computed:

$$\underline{n}(k) = \underline{\omega}(k) - \omega_a(k) * \underline{u}$$

where $\underline{u}$ is an N dimensional vector each component of which is unity:

$$\underline{u}' = [1, 1, \ldots 1] \text{ N dimensional}$$

The nonuniformity metric which we denote n(k) for each data block is obtained from the L_1 norm of $\underline{n}(k)$ which is denoted $||\underline{n}(k)||_1$

$$n(k) = \frac{1}{N} ||n(k)||_1$$

This nonuniformity index is a random variable having several interesting properties. For example, it is identically zero for maximally uniform torque. In this case each relative minimum contributes identically to $\underline{\omega}(k)$ and

$$\underline{\omega}(k) = \underline{u}\ \omega_a(k)$$

However, the above case represents an ideal which is never achieved exactly in practice. There is always cylinder-to-cylinder and cycle-to-cycle variation in torque production. This torque variation produces a corresponding angular speed variation which is measured in the present method. The nonuniformity index, n(k) increases with nonuniformity in $\omega_e(t)$ for each cycle. Thus n(k) serves as an index of torque nonuniformity.

This study reports the results of experimental studies of the statistics for the n(k). These statistics are very useful for characterizing the engine 'roughness' in actual vehicle operation.

2.2 Choice of Index Period

Although the choice of N in the definition for the nonuniformity index is arbitrary, there are certain choices which are useful for particular applications. For diagnostic applications it is often advantageous to compute the nonuniformity index for each engine cycle. In this case N should be chosen as

the number of cylinders for which choice k becomes the number of engine cycles. For such a choice of N the data on torque nonuniformity is available to the controller on a cycle by cycle basis. We have made this choice in the present study for which N = 6.

At this point we have demonstrated theoretically that crankshaft speed variations are proportional to torque variation (at each RPM). We have also presented an index n for the speed fluctuations which serves as an index for torque nonuniformity. A goal of this study is to ascertain the feasibility of representing torque nonuniformity with n and to be able to detect abnormal engine operation (as characterized by excessively nonuniform torque generation) from measurements of n. The feasibility of detecting abnormal engine operation depends upon the statistics for random variable n under abnormal operation relative to normal operation.

Although there are many criteria for assessing the feasibility of this application, in general all of these criteria involve the relationship between the main value, standard deviation, skew and kurtosis, for n under normal and abnormal conditions. The present experimental investigation has studied these statistical parameters for a variety of operating conditions in a specific vehicle.

We have postulated that the statistics for n shift to larger values for abnormal operation compared to normal operation. To be useful for detecting abnormal engine operation, the shift in mean value for $\langle n \rangle$ should be large compared to the standard deviation for the normal and abnormal cases. It is shown in this report that abnormal engine operation can be detected from measurements of n(k) for certain operating conditions.

In the present project experimental studies have been conducted of n for various operating conditions of a bus on the road in simulated service along a typical urban route. The influence of defective components have been simulated in order to examine the influence on n of deteriorated component performance.

One of the goals of this study has been to determine the operating conditions which give maximum variation in the statistical parameters for n for simulated defects relative to normal operation. Another goal of this study is to develop an algorithm for detecting incipient engine failure based upon measurements of n (as explained in the introduction).

In conducting these experimental studies a pair of buses were instrumented for measurements of n as explained in the next section of this report. The experimental data was collected for the buses operating in simulated actual routes and in the maintenance area. The data was stored in internal memory of the onboard instrumentation for later retrieval. The onboard memory has sufficient capacity to collect data for an entire day's operation in service. This provides the capability to obtain performance measurements while the bus is in service.

However, in our experimental studies the data retrieval was accomplished by means of a portable computer. The onboard stored data was transferred at the end of each experimental run to the portable computer.

The portable computer has the capability to conduct limited data analysis which has proven useful during the experimental phase of this project. However, the primary data reduction and analysis for the experimental studies have been performed on a DEC 11-23 computer. Data was transferred to the DEC computer from the portable computer at the end of each experimental test. In the next section of this report the instrumentation and experimental procedures are explained.

3. INSTRUMENTATION

Figure 4 depicts a block diagram of the set up of all the units of the instrumentation for this experiment.

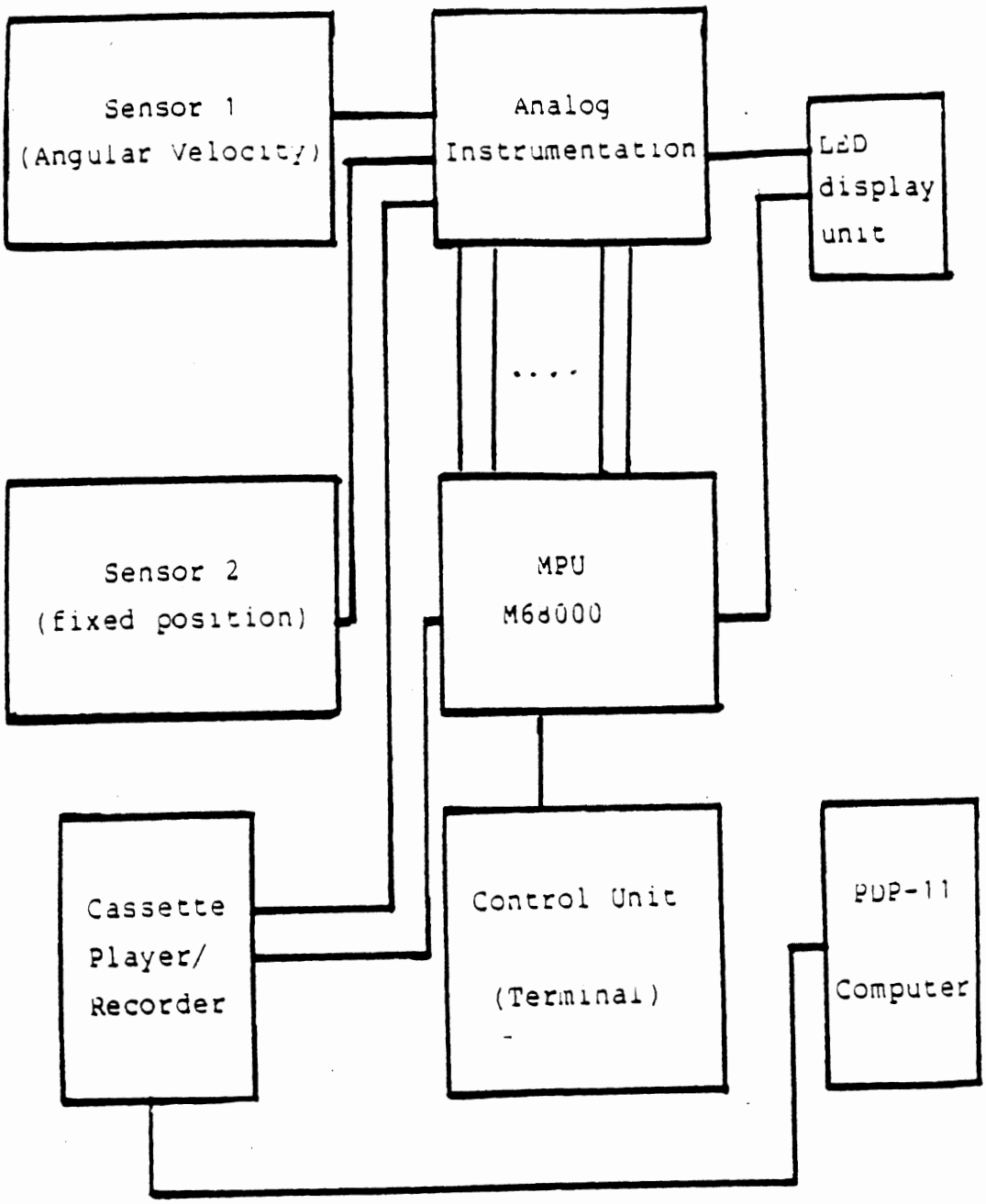

Figure 4. Instrumentation block diagram

Two inductive sensors are used; one to sense engine instantaneous angular velocity, another to mark the beginning of each engine cycle. The two signals are processed through the analog hardware portion of the instrument as shown in the figure. The output is sent to the microprocessor (mpu)(M68000) through the interface.

The appropriate program is loaded on the computer using a cassette player/recorder, the interface, and a terminal (control/unit). The program is designed to compute the torque non-uniformity metric given the needed signals from the analog instrument.

Finally, the data is stored in RAM and displayed on an LED display unit.

The main objective is to design an instrument capable of processing the crankshaft angular velocity signal in order to provide the information concerning cycle-to-cycle and cylinder-to-cylinder fluctuations in engine performance.

This section describes in detail the sensor, the analog and microprocessor interface hardware, as well as the essential features of the software.

3.1 Sensors

Two sensor inputs are required by the instrument; one provides a signal related to instantaneous engine angular position, the other provides a fixed position reference. Both sensors are of the inductive type.

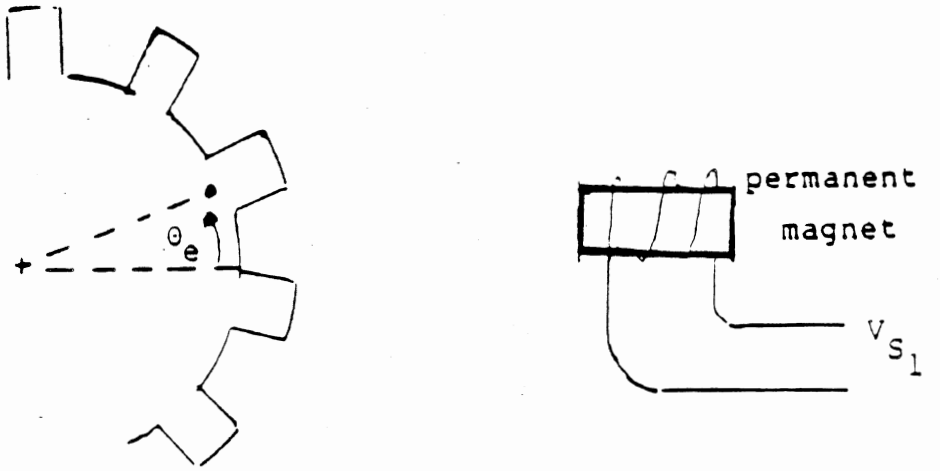

Figure 5. Inductive sensor for instantaneous angular position.

Figure 5 is a sketch of the sensor providing the instantaneous engine angular position which is mounted directly over the starter ring gear.

The sensor consists of a permanent magnet around which a coil is wound. The magnetic field of the permanent magnet couples to the steel starter ring gear. The magnetic flux linkage of the coil varies with crankshaft angular position being influenced by the spacing between the magnet and the ring gear and by the ring gear profile.

Figure 6 is a sketch of the sensor which provides a fixed position reference. The same type of inductive sensor is used which is mounted over the accessory pulley with minor adjustments. A slot with dimensions of approximately 0.5 cm width and 0.5 cm depth is made on the pulley.

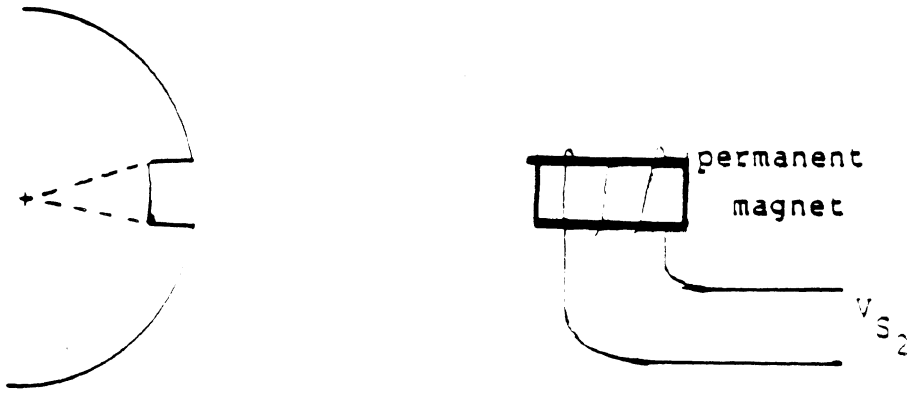

Figure 6. Inductive sensor for fixed position reference.

The magnetic field of the magnet couples to the steel pulley. The magnetic flux linkage is influenced by the slot angular position relative to the permanent magnet.

The gap between the inductive sensor and the metal plates should be set between 1.5 and 2.0 mm.

Some simple signal models for the sensor signals are discussed prior to examining the details of the hardware.

3.2 Characteristics of the Sensor Signals.

The engine angular velocity signal, obtained from the non-contacting measurement of angular position at the ring gear on the

flywheel appears as a frequency modulation component on a carrier proportional to the average speed of the engine. The sensor voltage is approximately given by

$$V_s(t) = V \sin [\theta(t) + \phi] \qquad (1)$$

where $\theta(t)$ is the instantaneous angular position of the flywheel, for a ring-gear with m teeth, the average frequency of the sensor signal is given by

$$\lambda_S = 2\pi M \frac{RPM}{60}$$

where

M = number of teeth on ring gear

The firing frequency of an N-cylinder two-stroke cycle engine is given by

$$\lambda_f = 2\pi N \frac{RPM}{60} \qquad (2)$$

and is therefore related to λs by

$$\lambda_s = \frac{m}{N} \cdot \lambda_f \qquad (3)$$

The individual cylinder firing events cause the crankshaft (hence the flywheel) to accelerate and decelerate about its mean speed, so that at steady-state we may express the angular velocity $\theta(t)$, as the sum of AC and DC components, i.e.:

$$\theta(t) = \Omega(t) = \Omega + \omega(t) \qquad (4)$$

with

Ω = average engine speed

and

$\omega(t)$ = speed variations about Ω.

Any non-uniformity in the generation of engine torque (and hence angular velocity), as would be caused by fluctuations in the combustion process from cylinder to cylinder and from cycle to

cycle, will appear in the spectrum of $\Omega(t)$ as subharmonic components of the fundamental frequency of oscillation, λ_f.

As was mentioned earlier, $\Omega(t)$ appears as a frequency modulation component in the sensor output, $V_s(t)$, at a carrier frequency λ_s. The dynamic range of the engine is such that the carrier frequency, which is itself proportional to RPM, varies over a wide range. In addition, normal engine operation causes relatively large changes in λ_s (and in Ω) to occur at all times, due to changes in load caused by inputs to the throttle or transmission. This in practice makes $V_s(t)$ an extremely wide-band FM signal and precludes the use of conventional phase-locked FM-demodulation techniques as was observed during the early stages of this project. The limited lock range on the PLL introduces problems in the demodulation of the sensor signal.

Among the possible solutions to this FM demodulation problem, a frequency-to-voltage (F-V) conversion scheme based on a charge-pump was found to be the best approach.

This demodulation scheme separates the $\Omega(t)$ signal from the carrier by shifting it back to baseband.

Let $V_{out}(\lambda)$ be the Fourier transform of the signal after the F-V conversion, then

$$V_{out}(\lambda) = V_{\Omega} + V_{\omega}(\lambda_f) + V_c(\lambda_s) \qquad (6)$$

where

V_{Ω} = quasi-steady-state component
V_{ω} = oscillations at harmonic and subharmonics of λ_f
V_c = vestigial carrier components at sensor frequency

Since some of the carrier frequency component remains in the signal spectrum after the frequency to voltage conversion, some RPM dependent filtering scheme must be implemented in order to obtain good separation between the desired signal and the undesired high frequency component. This will be discussed in later subsections.

3.3 Instrumentation Objectives

Having examined the characteristics of the sensor signal, we are ready to define a set of goals for the data acquisition instrumentation. The instrument is required to:

a) perform a frequency to voltage conversion on the raw output of a non-contacting angular position sensor placed near the flywheel. The dynamic range of the F-V converter must cover the full range of the engine RPM;

b) provide RPM dependent filtering, so as to have a constant bandwidth for the $\Omega(t)$ signal in the face of changes in RPM, and to minimize carrier leakage;

c) sample the extrema of the filtered $\Omega(t)$ waveform and provide timing pulses corresponding to the occurrence of the extrema;

d) use the output of the inductive sensor placed near the accessory pulley to identify the beginning of each new engine cycle and provide timing pulses to mark this event;

e) convert the analog extrema to a corresponding 8-bit digital equivalent;

f) interface the timing information in c) and d) and the 8-bits of information regarding the extrema of e) with an available microprocessor (Motorola 68000);

g) perform the computation of the nonuniformity metric [i.e., n(k)] for a selectable number of engine cycles by means of the 68000 microprocessor and store the results for later access;

h) display the nonuniformity metric for immediate monitoring;

i) be as operator-independent as possible, so as to enable experiments to be performed by relatively unskilled operators in a variety of environments.

3.4 The analog instrument

The essential features of the analog portion of the instrument are shown in the block diagram of Figure 7. The following subsections examine the details of each block.

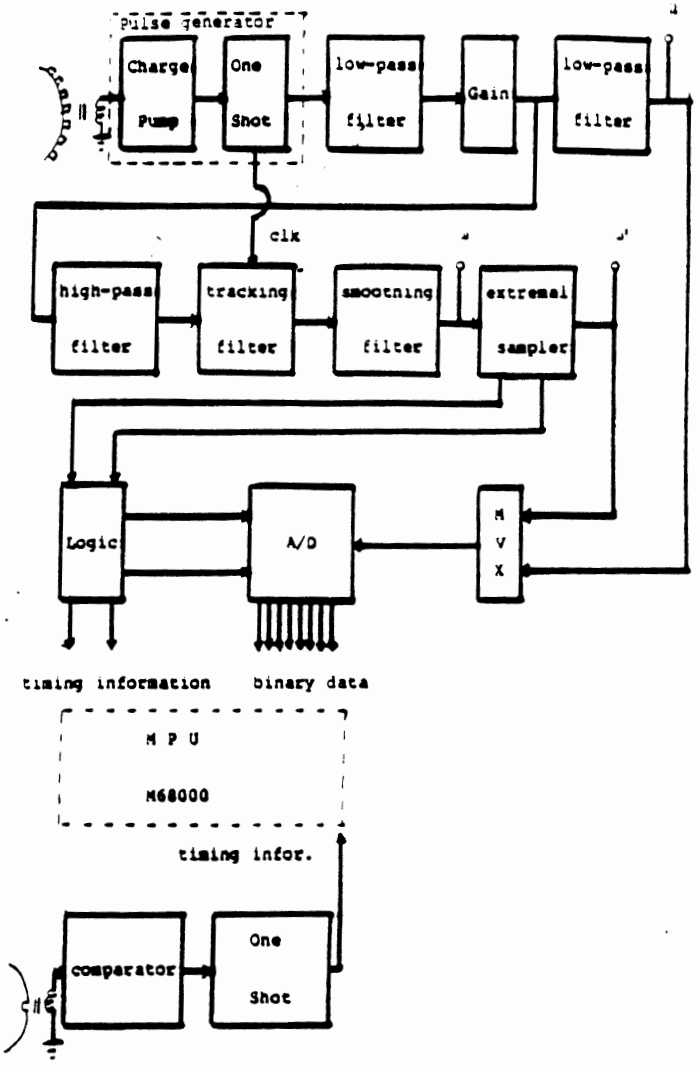

Figure 7. Block diagram of the analog instrument

3.4.1 Pulse Generation

The first step in the conversion of frequency to voltage is achieved by pulse generation. A fixed duration pulse is required with frequency proportional to that of the sensor signal. For this purpose, a commercially available F-V converter (LM2907) is used as a charge pump which generates a fixed duration pulse at each zero crossing of the sensor waveform.

To achieve a duration τ for the pulse which is insensitive to environmental factors and device variations, the pulse at the

output of the charge pump is fed to a highly stable CMOS one-shot (CD 4538). For a detailed schematic of the circuitry, refer to Appendix A.

It is easily shown (derivation in Appendix B) that the average value of this pulse is proportional to the input waveform frequency (sensor frequency) by

$$V_{out} = 2\tau V_{DD} \cdot f_{in} \tag{7}$$

where

τ = fixed pulse width of one-shot
V_{DD} = supply voltage
f_{in} = input signal frequency

3.4.2 Filtering

In the next stage, we use filtering in order to achieve maximum carrier rejection without the distortion of the $\omega(t)$ signal. A filter with a fixed cutoff frequency is inadequate for the purpose of eliminating the ripple due to the vestigial carrier component at the lower signal frequencies. Recall that the ratio between carrier and signal frequency is fixed at

$$\frac{\lambda_s}{\lambda_f} = \frac{m}{N} \tag{8}$$

where

m = number of teeth on the ring gear
N = number of cylinders

Thus with m = 102 teeth and N = 6 cylinders we have

$$\frac{\lambda_s}{\lambda_f} = 17.0 \tag{9}$$

Calculations are therefore made according to the wide range of 350-3500 RPM. In order to satisfy the dynamic range of signal and carrier frequencies, a filter with RPM controlled cutoff frequency is required. A three pole active filter is used. Details for the filter are shown in Appendix A.

The next issue in obtaining an analog of $\omega(t)$ is that the separation between low frequency components due to the throttle and load transients, Ω, and the subharmonics of firing frequency generated by the presence of torque (velocity) non-uniformity. Throttle transients, especially with the engine unloaded or lightly loaded, can cause large 'steps' in average engine speed while the oscillations at the firing frequency remain relatively small in amplitude, in particular in a smoothly running engine.

After a gain stage following the first low pass filter, we separate $\Omega(t)$ into AC and quasi-DC paths by means of two three-pole filters: one a high-pass with cutoff frequency around 5 rps, the other a low pass with the same cutoff frequency of 5 rps. The signal at the output of the high-pass filter is ideally equal to $\omega(t)$, while the low-pass filter produces a signal proportional to the Ω DC term at steady-state.

Following the analog filter just described, the signal $V\omega(t)$ is still contaminated by a ripple component at the carrier frequency. In order to eliminate this distortion, a tunable filter is implemented using a switched-capacitor (sampled) filter with a four-pole Butterworth characteristic followed by a smoothing filter (three-pole low-pass). The latter is needed to smooth out the step-like output of the former which is essentially a sampling device.

The switched capacitor filter has a cutoff frequency which is related to an external clock frequency by a constant, i.e.:

$$f_3 db = \frac{f_{clock}}{M} \qquad (10)$$

By using an RPM derived clock signal, such as is available at the output of the one-shot following the pulse generator, the filter will have an instantaneous bandwidth proportional to the instantaneous RPM. Recall that the sensor frequency, λ_s (converted into a pulse train by the charge pump) is larger than the firing frequency, λ_f, by a factor of 17 as calculated earlier.

A nominal M of 20 for the filter will then maintain the filter bandwidth above λ_f, maximally rejecting the undesired carrier component. For a detailed diagram of circuitry and design procedures for the switched capacitor filter (MF-10) refer to Appendix C.

3.4.3 External Sampling

The sampled relative maxima and minima values of the $V\omega(t)$ waveform which will be used for metric calculations are obtained by a simple extremal sampler, constituted of a differentiator, comparator, and track-and-hold circuit. In order to avoid any delay caused by the presence of hysteresis in the comparators (which is necessary for noise rejection), use was made of two comparators, one for detection of the relative maxima, one for the relative minima. The track-and-hold circuit is implemented by means of an operational transconductance-amplifier (OTA), with gain controlled by an external current.

The pulse generated by the occurrence of either extremum turns on the track-and-hold circuit for an appropriate length of time. Figure 8 shows a detailed diagram of the circuit.

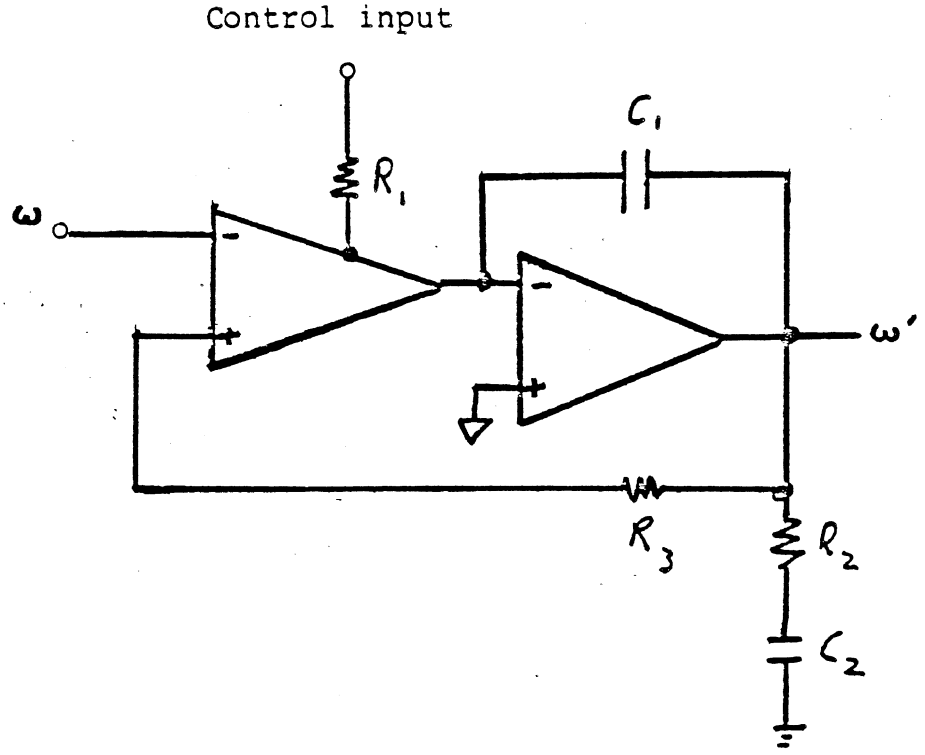

Figure 8. Track & hold circuit

Logic and A/D Conversion

The track-and-hold signal, V_ω, is then multiplexed with the signal V_Ω, so that either can be fed to an A/D converter by an appropriate decoding scheme. Simple logic allows the user to perform A/D conversions for four different experimental conditions simply by setting a DIP switch:

1) convert just maxima of V_ω;
2) convert just minima of V_ω;
3) convert both maxima and minima of V_ω;
4) convert both maxima and minima of V_ω and a sample of V_Ω after every V_ω sample.

Option 4) is potentially useful in that it automatically provides a measurement of the average RPM for each engine cycle. A detailed schematic of the logic circuitry is available in Appendix A.

Along with the data output of the A/D converter (8-bit word), the end of conversion (EOC) pulse provides a timing reference to signal the occurance of an available sample to the MPU on an interrupt line.

A separate interrupt signal is also provided to indicate the beginning of a new cycle. This is obtained by means of an inductive sensor signal (described earlier). The signal is processed through a comparator and a one-shot so that a clean data cycle pulse is obtained. The circuit details are shown in Appendix A. A detailed timing diagram is shown in Figure 9.

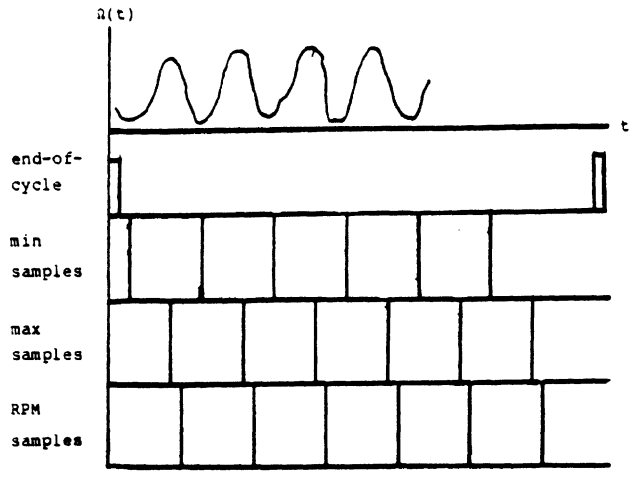

Figure 9. Timing Diagram.

LED Display

For the purpose of visual monitoring of the nonuniformity metric while the instrument is being used, an LED display unit is designed. This unit uses the EOC pulse to latch or enable two 7-segment displays. The computed metric obtained from the MPU is shown in Hexadecimal representation and is updated every 3-4 seconds.

Interface with Motorola 68000 Microprocessor.

The two interrupts, indicating the beginning of a cycle and the availability of a sample at the A/D converter output, as well as the 8 bits of data corresponding to each sample of an extremum, are interfaced with the 68000 MPU by means of a Peripheral Interface Adapter (PIA).

Port B of the PIA is employed as an input port to the MPU for the A/D converter data line. The EOC interrupt signal is connected to Port C (H3-H4). Port C is used to process the beginning/end-of-cycle interrupt. Port A of the PIA is employed as an output port to the LED metric display unit.

In addition, there are two other signals available at the digital hardware outputs which indicate whether the current information on the sampled extrema is about the maxima or the minima. (They are shown as Flag0, Flag1 in the schematic, Appendix A). These signals could be used as software flags which would be obtained by interfacing the signals with the MPU through Port C (H1-H2) if desired. The current version of the software however, does not make use of this option.

The individual connections for the MPU interface are made by exactly following the instructions from the MC68000 Educational Computer Board User's Manual. For further details please refer to this manual.

Power Supply

The analog circuit and the digital interface, along with the MPU operate on +12, -12, +5 voltage supplies. A voltage of approximately +14V is obtained from the power distribution unit of the bus underneath the driver's seat. This single power supply is

transient protected and regulated (using an Intronics II-DC12/12/D DC-DC converter) to provide adequate current, and is insensitive to load changes such as engagng the A/C, the starter motor or turning the ignition off.

3.4.4 Software

The software performs the computation of the metrics and stores the results in a RAM so as to generate a distribution (histogram) of values for the metric.

Programs are recorded and stored on special cassettes and are loaded onto the computer through an interface with a cassette player/recorder. The results (non-uniformity metric) can also be loaded onto a cassette through the same interface to be recorded permanently.

Figure 10a and 10b show flowcharts of the current version of the software with the essential features of the program. A detailed listing of the program in Assembly 68000 Language is available in Appendix D.

4. EXPERIMENTAL FACILITIES

All of the experimental work described in this section was performed on two GMC RTS04 1981 buses made available to us by the Ann Arbor Transportation Authority. Both buses have a V671N engine.

Throughout the course of study, both buses were still operating on a regular schedule, on regular route. Thus, the tuneups and other maintenance work on these buses were similar to all the others in service.

Buses had to be reserved ahead of time for any particular test. For this phase of the study, the two inductive sensors were installed on the buses with minor adjustments as described earlier. The set up and wiring for these sensors and for the power supply from the power distribution unit required an average of 4-6 hours per bus. The sensors and the wiring were left on the buses throughout the study. The monitoring instrumentation,

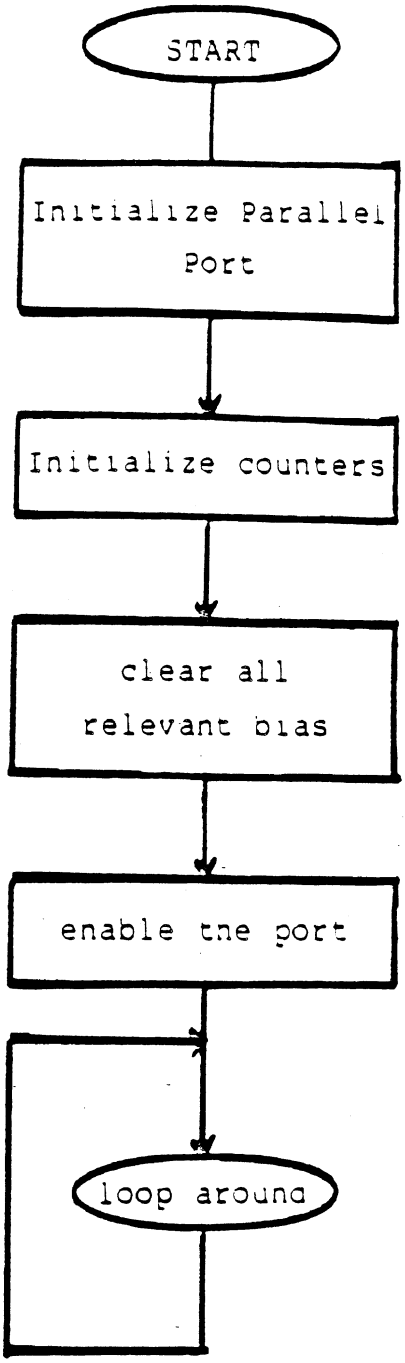

Figure 10a. Flow chart for the main routine of the program. Note: The processor stays in the routine until an interrupt either due to the new data or new cycle occurs.

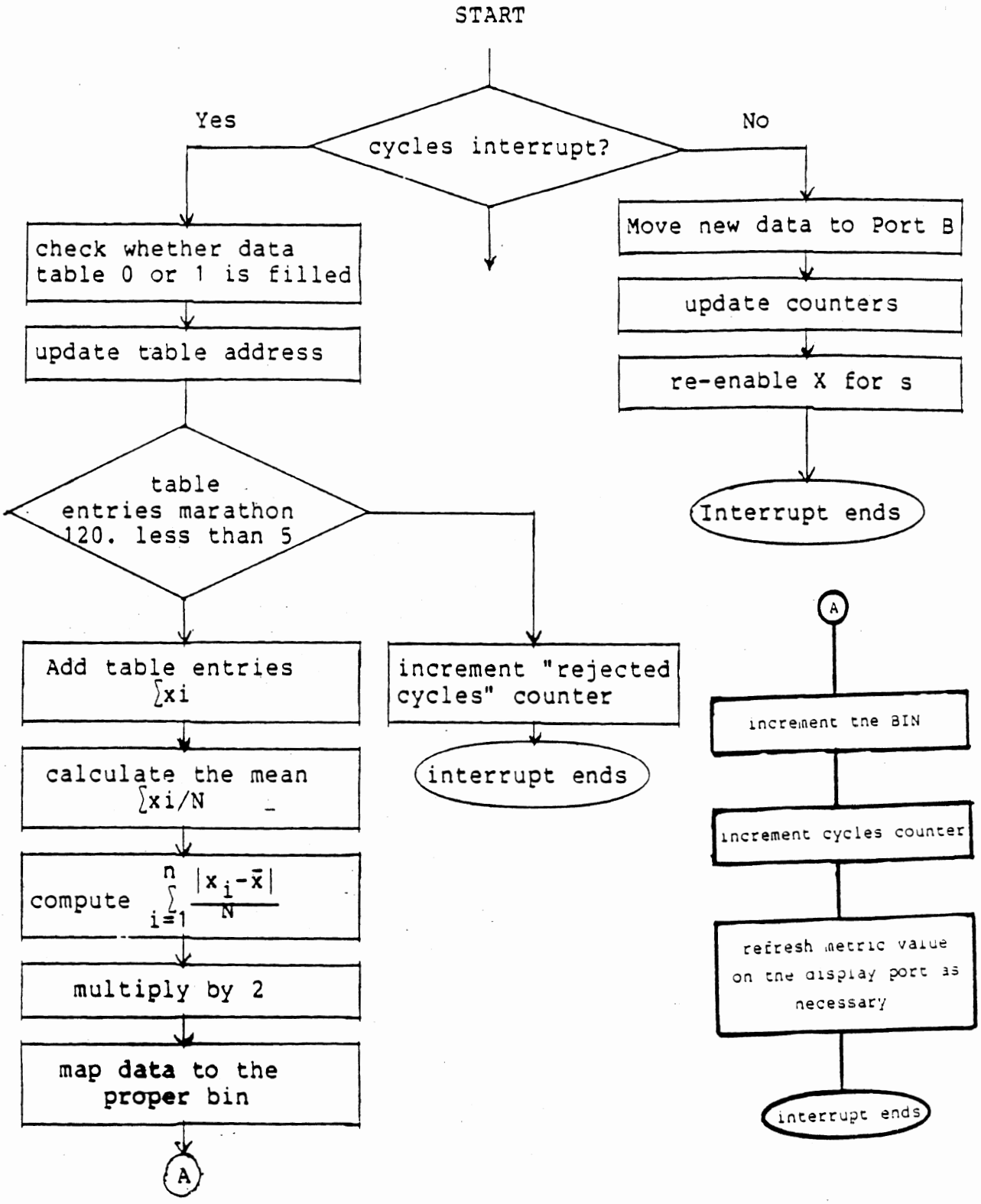

Figure 10b. Flow chart for signal analysis.

however, was carried on the bus and easily installed for each test.

4.1 Experimental Conditions

Experiments were performed both on the road and in the AATA garage. The test conditions were mainly ruled by two major variables:

a. RPM and Load

b. engine torque nonuniformity level.

RPM and Load

Road Tests:

On a normal AATA route, the buses cover a range of 10-45 mph. Thus, to simulate these conditions as closely as possible, we designed tests at constant RPM's and constant loads. This was done by choosing routes which allowed the bus to travel at a constant RPM without the use of the brakes or a shift in gear for a long enough period to obtain adequate data. Also, the load was kept fairly constant on all tests by choosing roads with the same roughness and the same grading (all of the chosen routes were flat).

A speed range of 15-50 mph was covered on each test. The number of engine cycles of data collected for each case varied somewhat with each individual test condition, but was kept around 5000 cycles/run.

4.2 Garage Tests

On a normal run, the buses spend a considerable amount of time in idle conditions in the garage (waiting to be parked, tuned, or fueled, etc.). In order to simulate these conditions, a series of tests were performed in the garage while the buses were idling. The various tests consisted of 4 break-loaded idle conditions:

1) idle in Neutral;

2) idle in Drive;

3) idle in Reverse;

4) fast idle in Neutral.

The parking brakes on the bus were used (just as would be in normal runs) and using the manual gear, the first 3 conditions were tested. Fast idle in Neutral is an available option on all the buses.

The number of engine cycles collected on these runs were more controllable (around 4000-5000 cycles) and took an average of 3-5 min to obtain.

Engine torque nonuniformity level

In order to show the effects of engine nonuniformity on the metric calculations, all of the tests described above were run for normal and extremely nonuniform engine conditions. In order to achieve a condition of extreme torque non-uniformity, the engine was operated with one fuel injector (lower left) disconnected. This condition is, in fact, far worse than would be encountered in any normal engine operation, but illustrates the distinction clearly.

For all operating conditions a permanent record was made of the computed nonuniformity metric histogram and, when possible, the analog velocity waveform was also recorded.

The next section includes the series of repeated tests as described above and the resulting nonuniformity metric histograms.

5.SUMMARY OF EXPERIMENTAL RESULTS

In this section of the report the detailed results of experimental measurements are presented. These data are presented in both graphical and tabular form. On each page the results of both normal and abnormal operating conditions are presented side by side for each operating condition. In this way the statistical distributions for normal and abnormal operating conditions can most easily be compared. Particular attention should be paid to the shift in the distribution for these extreme operating conditions.

In addition, the statistical parameters are presented for each measured distribution in tabular form. Here, as in the graphical presentation comparison of performance of normal and abnormal engine operation, the statistical parameters are readily comparable. Each table and each graph is identified with respect to the actual operating condition.

TABLE 1

Summary of Data

DATA SET #1.1: BUS A

General Operating Conditions: Idle in various Gears (5 min.)

	ID# (Description)	1st moment	2nd moment	3rd moment Normalized	4th moment Normalized
NORMAL	102300•4AM Idle - Neutral	9.43	13.58	-.26	2.10
ABNORMAL	102500•1AM Idle - Neutral	11.87	10.74	-.18	2.51
NORMAL	102300•2AM Idle - Drive	10.57	22.50	-.38	1.95
ABNORMAL	120500•2AM Idle - Drive	24.22	17.70	.07	2.58
NORMAL	102300•5AM Idle - Reverse	10.33	21.54	-.38	2.07
ABNORMAL	120500•3AM Idle - Reverse	24.14	10.15	.71	2.74
NORMAL	102601•1AM Fast Idle	7.35	8.20	-.18	2.20
ABNORMAL	120501•1AM Fast Idle	9.12	6.50	1.17	11.53

TABLE 1 (Continued)

DATA SET #2.1: BUS A

General Operating Conditions: Constant Speeds at 15-50 mph (3-5 min.)

	ID# (Description)	1st moment	2nd moment	3rd moment Normalized	4th moment Normalized
NORMAL	102615-1AM 15 mph	7.34	6.11	.16	2.71
ABNORMAL	120515-1AM 15 mph	10.33	7.55	0.37	5.83
NORMAL	102620-1AM 20 mph	7.09	6.10	1.40	12.45
ABNORMAL	120520-1AM 20 mph	9.13	6.92	-0.01	3.09
NORMAL	102625-1AM	7.24	5.59	0.64	7.51
ABNORMAL	120525-1AM 25 mph	10.52	8.37	0.28	5.98
NORMAL	102630-1AM 30 mph	7.18	5.97	0.37	4.79
ABNORMAL	120530-1AM 30 mph	11.37	6.30	-0.13	2.28
NORMAL	102635-1AM 35 mph	7.38	5.95	0.26	4.05
ABNORMAL	120535-1AM 35 mph	9.95	9.24	0.46	4.64
NORMAL	102640-1AM 40 mph	7.40	6.14	0.27	4.73
ABNORMAL	120540-1AM 40 mph	12.19	11.84	-0.18	3.65
NORMAL	102645-1AM 45 mph	8.14	6.73	0.12	2.85
ABNORMAL	120545-1AM 45 mph	11.73	11.91	0.16	3.60
NORMAL	102650-1AM 50 mph	8.16	5.95	0.15	2.86
ABNORMAL	120550-1AM 50 mph	9.60	7.31	0.35	3.59

TABLE 1 (continued)

DATA SET #3.1: BUS B

General Operating Conditions: Idle in various gears (5 min).

	ID# (Description)	1st moment	2nd moment	3rd moment Normalized	4th moment Normalized
NORMAL	103100-3BM IDLE - NEUTRAL	13.38	21.81	-0.03	1.93
ABNORMAL	112800-4BM IDLE - NEUTRAL	13.13	8.88	0.35	3.14
NORMAL	103100-2BM IDLE - DRIVE	14.46	28.6	-0.12	1.91
ABNORMAL	112800-5BM IDLE - DRIVE	18.51	22.57	0.20	3.18
NORMAL	103100-1BM IDLE - REVERSE	14.37	28.93	-0.14	1.88
ABNORMAL	112800-6BM IDLE - REVERSE	22.84	13.08	-1.01	5.85
NORMAL	103101-1BM FAST - IDLE	7.99	7.55	0.08	2.76
ABNORMAL	112801-2BM FAST - IDLE	8.32	6.06	2.20	20.48

TABLE 1 (Continued)

DATA SET #4.1: Bus B
General Operating Conditions: Constant speeds at 15-50 mph (3-5 min)

	ID# (Description)	1st moment	2nd moment	3rd moment Normalized	4th moment Normalized
NORMAL	102815-1BM 15 mph	7.59	5.61	1.30	11.95
ABNORMAL	112815-2BM 15 mph	9.57	7.85	1.42	11.52
NORMAL	102820-1BM 20 mph	7.32	4.57	1.54	13.74
ABNORMAL	112820-2BM 20 mph	5.59	6.45	0.77	7.81
NORMAL	102825-1BM 25 mph	7.57	6.84	1.35	13.37
ABNORMAL	112825-2BM 25 mph	8.84	6.72	1.40	12.26
NORMAL	103130-2BM 30 mph	7.40	7.75	0.61	6.01
ABNORMAL	112830-2BM 30 mph	10.43	9.82	0.51	4.61
NORMAL	103135-2BM 35 mph	7.88	7.55	1.16	9.99
ABNORMAL	112835-2BM 35 mph	10.25	11.90	0.50	3.62
NORMAL	103140-1BM 40 mph	7.66	7.42	0.35	4.30
ABNORMAL	112840-2BM 40 mph	11.82	13.47	0.10	3.68
NORMAL	103145-1BM 45 mph	7.63	7.31	0.22	3.78
ABNORMAL	112845-2BM 45 mph	13.09	16.81	-0.18	3.01
NORMAL	103150-1BM 50 mph	9.25	5.98	-0.07	3.12
ABNORMAL	112850-1BM 50 mph	11.55	12.45	0.05	3.07

TABLE 1 (Continued)

DATA SET #1.2: Bus B
General Operating Conditions: Idle in various gears (5 min)

	ID# (Description)	1st moment	2nd moment	3rd moment Normalized	4th moment Normalized
NORMAL	092500-1AM Idle-Neutral	9.37	17.38	-0.01	4.30
ABNORMAL	110700-1AM Idle-Neutral	8.87	7.38	0.79	5.04
NORMAL	102300-2AM Idle-Drive	10.57	22.50	-0.38	1.95
ABNORMAL	110700-2AM Idle-Drive	21.03	20.38	-0.35	3.32
NORMAL	102300-5AM Idle-Reverse	10.33	21.54	-0.38	2.07
ABNORMAL	110700-3AM Idle-Reverse	19.85	19.22	-0.41	3.10
NORMAL	092501-1AM Fast-Idle	7.42	8.14	0.48	7.66
ABNORMAL	110701-1AM Fast-Idle	16.66	26.28	2.47	19.68

TABLE 1 (Continued)

DATA SET #2.2: Bus A
General Operating Conditions: Constant speeds at 15-50 mph (3-5 min)

	ID# (Description)	1st moment	2nd moment	3rd moment Normalized	4th moment Normalized
NORMAL	092515-1AM 15 mph	8.58	14.34	1.28	6.43
ABNORMAL	110715-1AM 15 mph	10.18	9.77	0.54	6.08
NORMAL	092520-1AM 20 mph	7.22	6.53	1.53	13.96
ABNORMAL	110720-1AM 20 mph	9.01	7.54	1.04	9.44
NORMAL	0925250-1AM 25 mph	7.19	6.24	1.25	11.73
ABNORMAL	110725-2BM 25 mph	12.39	13.18	0 09	3.66
NORMAL	092530-2BM 30 mph	7.22	7.23	0.97	7.70
ABNORMAL	110730-1AM 30 mph	10.75	10.16	0.48	4.62
NORMAL	092535-1AM 35 mph	7.43	6.40	1.26	15.48
ABNORMAL	110735-1AM 35 mph	10.0	7.36	0.41	6.69
NORMAL	092540-1BM 40 mph	7.28	6.47	0.84	8.57
ABNORMAL	110740-1AM 40 mph	12.38	11.92	0.19	4.56
NORMAL	092545-1AM 45 mph	7.82	6.76	0.30	4.25
ABNORMAL	110745-1AM 45 mph	11.09	9.61	0.34	3.76
NORMAL	092550-1AM 50 mph	8.38	6.24	0.20	2.93
ABNORMAL	110750-1AM 50 mph	10.0	7.31	0.08	3.76

TABLE 1 (Continued)

DATA SET #3.2: Bus B
General Operating Conditions: Idle in various gears (5 min)

	ID# (Description)	1st moment	2nd moment	3rd moment Normalized	4th moment Normalized
NORMAL	092300-1BM Idle-Neutral	11.48	16.73	0.17	2.67
ABNORMAL	112800-1BM Idle-Neutral	12.60	6.74	0.26	3.56
NORMAL	103100-2BM Idle-Drive	14.46	28.69	-0.12	1.91
ABNORMAL	112800-2BM Idle-Drive	20.49	29.10	0.12	3.06
NORMAL	103100-1BM Idle-Reverse	14.37	28.93	-0.14	1.88
ABNORMAL	112800-3BM Idle-Reverse	18.23	24.30	0.55	3.84
NORMAL	092301-1BM Fast-Idle	8.74	13.87	0.91	4.47
ABNORMAL	112801-1BM Fast-Idle	8.29	5.30	1.69	16.35

TABLE 1 (Continued)

DATA SET #4.2: Bus B
General Operating Conditions: Constant speeds at 15-50 mph (3-5 min)

	ID# (Description)	1st moment	2nd moment	3rd moment Normalized	4th moment Normalized
NORMAL	093515-1BM 15 mph	7.54	5.59	0.75	6.52
ABNORMAL	112815-1BM 15 mph	9.69	8.25	8.85	7.73
NORMAL	093520-1BM 20 mph	7.07	5.79	1.01	6.34
ABNORMAL	112820-1BM 20 mph	8.45	6.55	1.78	14.86
NORMAL	093525-1BM 25 mph	7.24	6.62	0.47	4.39
ABNORMAL	112825-1BM 25 mph	8.34	8.27	1.13	8.31
NORMAL	093530-2BM 30 mph	7.52	5.69	0.42	3.49
ABNORMAL	112830-1BM 30 mph	10.07	9.83	0.46	4.40
NORMAL	093535-1BM 35 mph	7.26	5.27	0.14	3.17
ABNORMAL	112835-2BM 35 mph	10.19	10.64	0.49	3.71
NORMAL	093540-1BM 40 mph	8.01	6.67	0.44	3.70
ABNORMAL	112840-1BM 40 mph	10.59	14.30	0.44	3.60
NORMAL	093545-1BM 45 mph	7.87	5.94	0.22	3.24
ABNORMAL	112845-1BM 45 mph	11.86	13.96	0.05	3.43
NORMAL	093550-1BM 50 mph	7.50	4.79	0.37	3.25
ABNORMAL	112850-1BM 50 mph	11.98	12.23	0.00	3.21

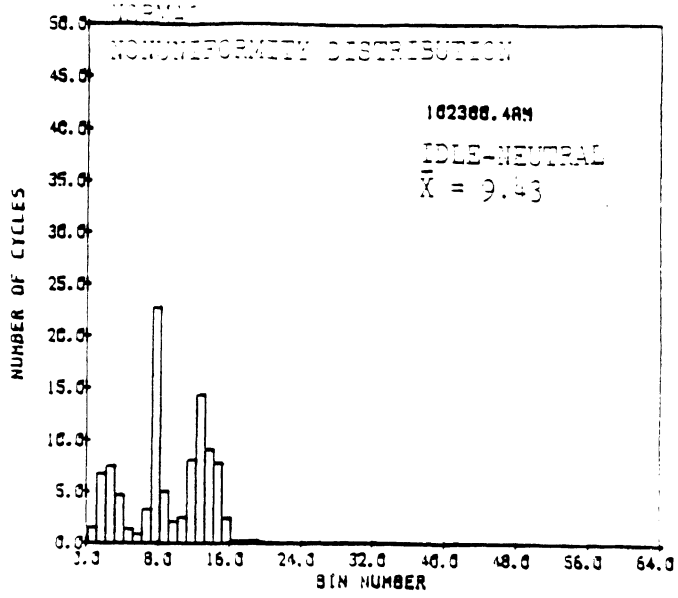
NONUNIFORMITY DISTRIBUTION
162300.4AM
IDLE-NEUTRAL
X̄ = 9.43
NUMBER OF CYCLES
BIN NUMBER

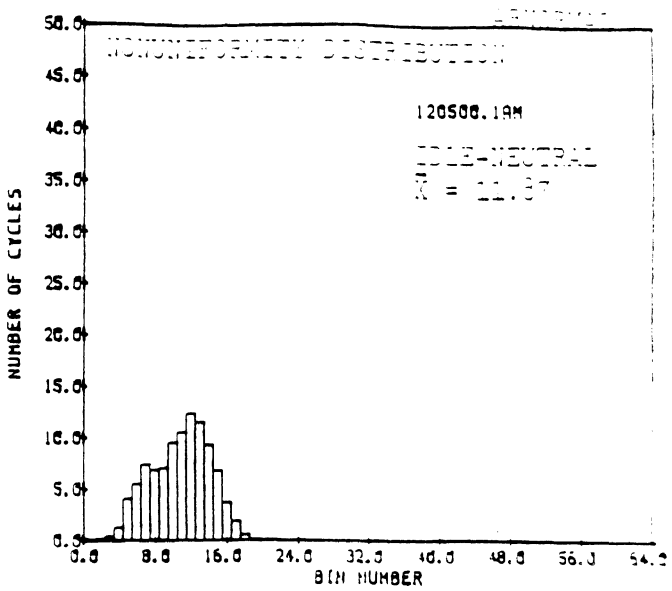
NONUNIFORMITY DISTRIBUTION
120500.1AM
IDLE-NEUTRAL
X̄ = 11.37
NUMBER OF CYCLES
BIN NUMBER

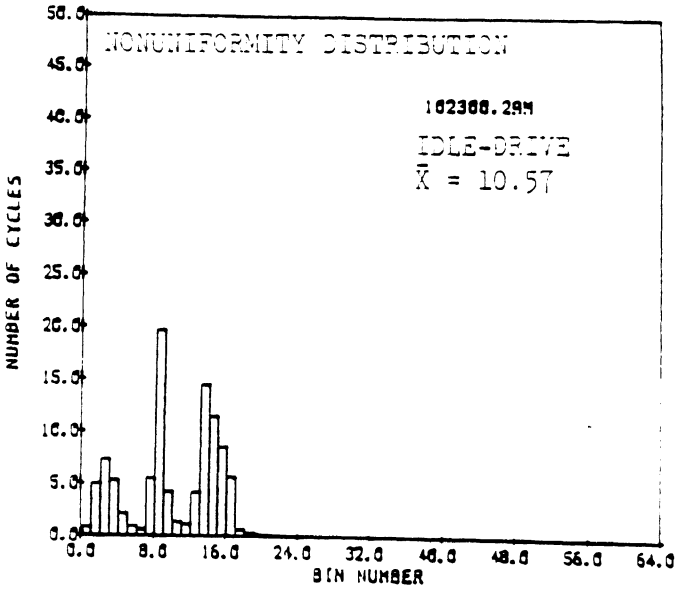
NONUNIFORMITY DISTRIBUTION
162300.2AM
IDLE-DRIVE
X̄ = 10.57
NUMBER OF CYCLES
BIN NUMBER

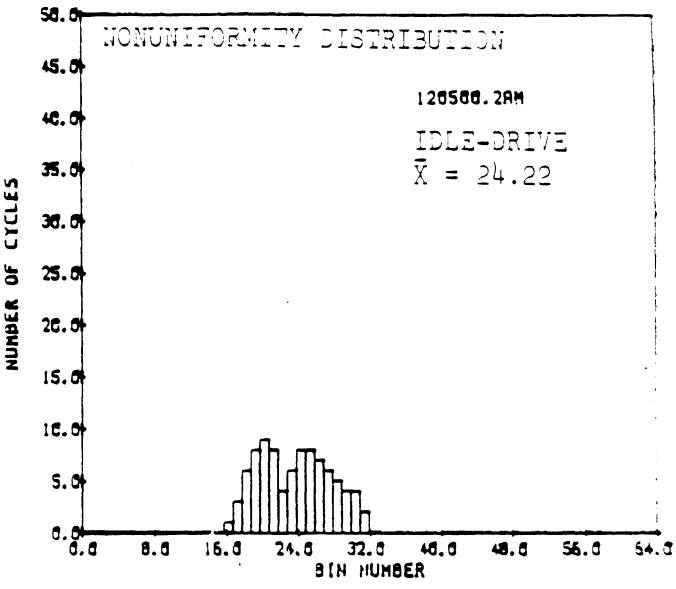
NONUNIFORMITY DISTRIBUTION
120500.2AM
IDLE-DRIVE
X̄ = 24.22
NUMBER OF CYCLES
BIN NUMBER

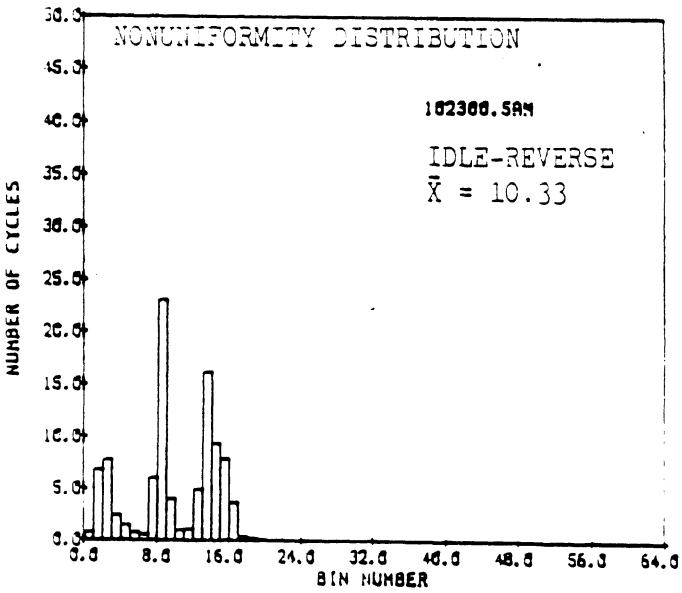
NONUNIFORMITY DISTRIBUTION
162300.5AM
IDLE-REVERSE
X̄ = 10.33
NUMBER OF CYCLES
BIN NUMBER

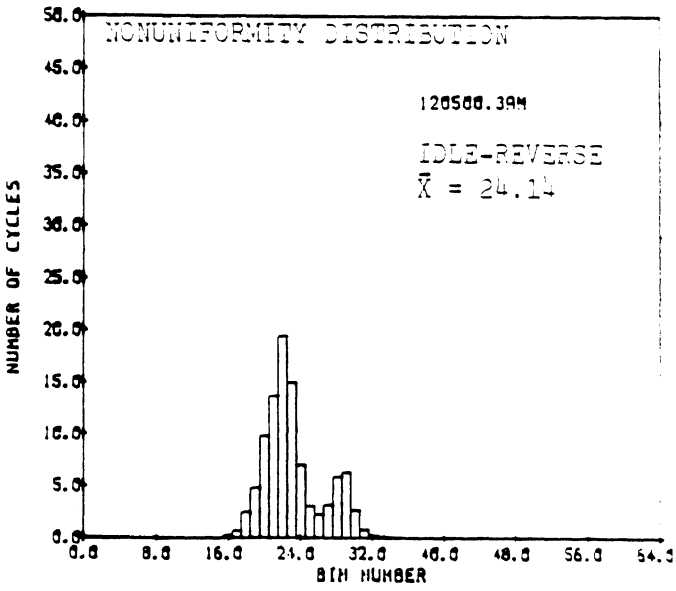
NONUNIFORMITY DISTRIBUTION
120500.3AM
IDLE-REVERSE
X̄ = 24.14
NUMBER OF CYCLES
BIN NUMBER

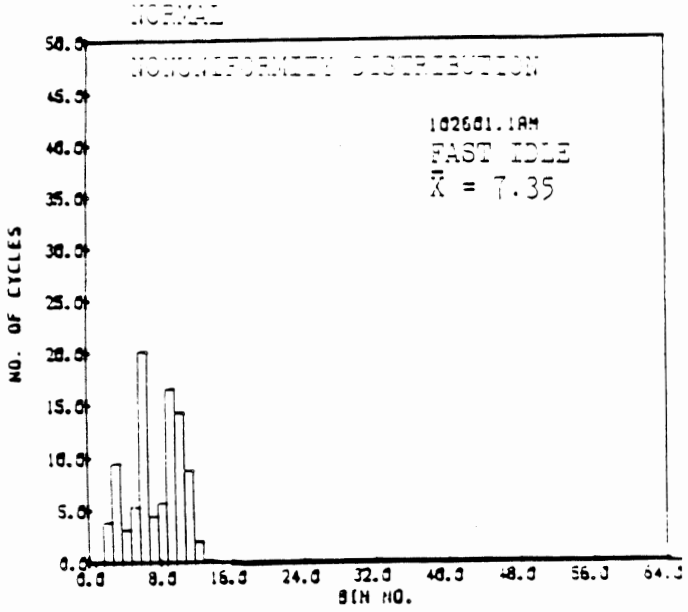
NORMAL
NONUNIFORMITY DISTRIBUTION
102681.1AM
FAST IDLE
X̄ = 7.35
NO. OF CYCLES
BIN NO.

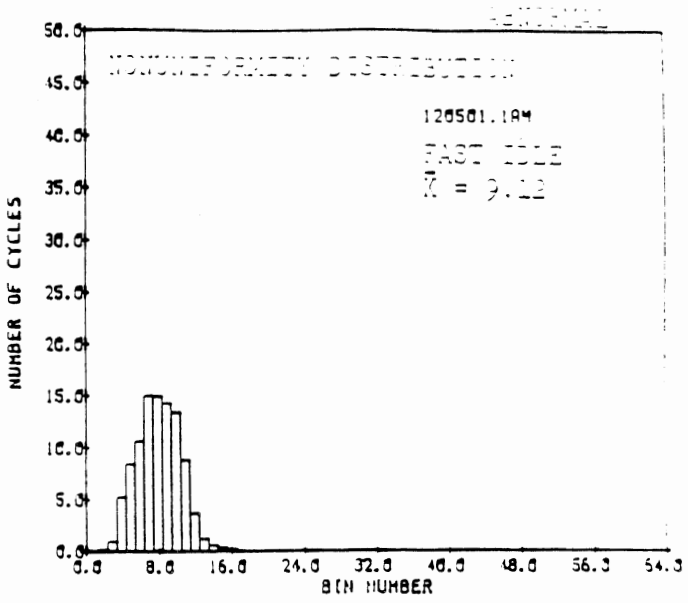
NORMAL
NONUNIFORMITY DISTRIBUTION
120581.1AM
FAST IDLE
X̄ = 9.12
NUMBER OF CYCLES
BIN NUMBER

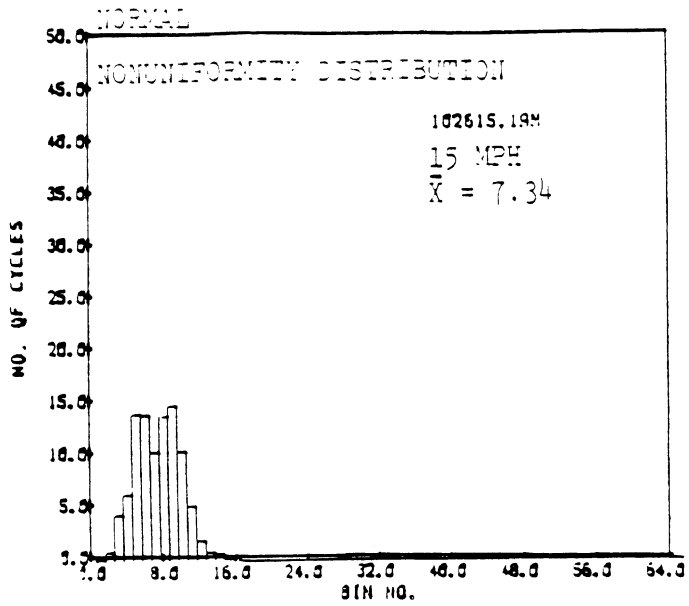
NONUNIFORMITY DISTRIBUTION
102615.1AM
15 MPH
X̄ = 7.34
NO. OF CYCLES
BIN NO.

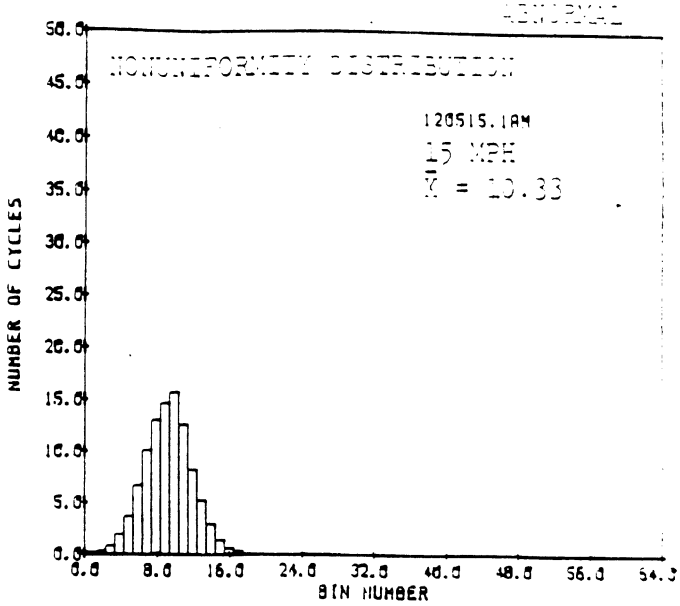
NONUNIFORMITY DISTRIBUTION
120515.1AM
15 MPH
X̄ = 10.33
NUMBER OF CYCLES
BIN NUMBER

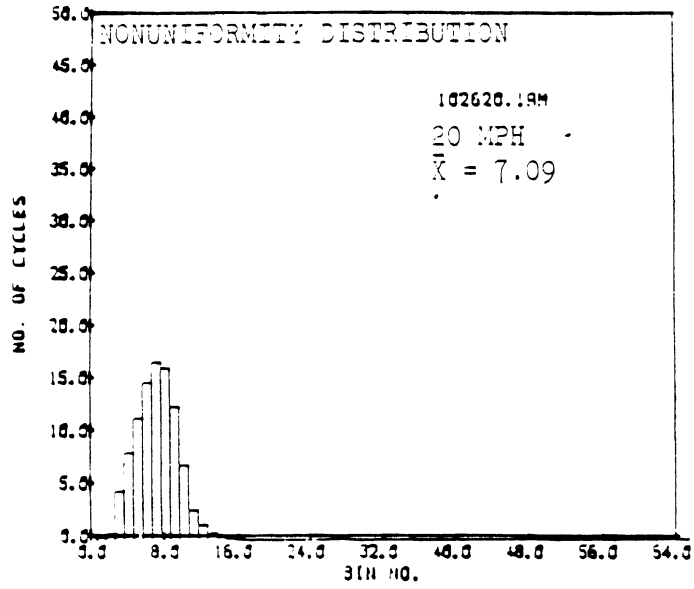
NONUNIFORMITY DISTRIBUTION
102620.1AM
20 MPH
X̄ = 7.09
NO. OF CYCLES
BIN NO.

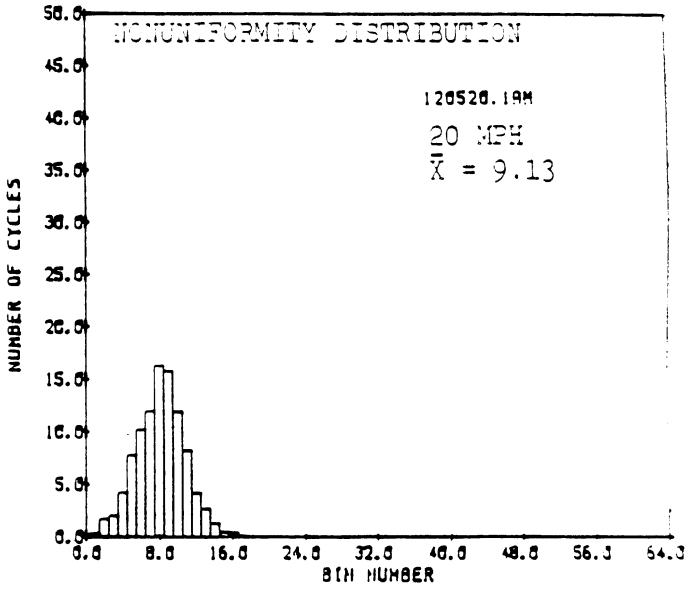
NONUNIFORMITY DISTRIBUTION
120520.1AM
20 MPH
X̄ = 9.13
NUMBER OF CYCLES
BIN NUMBER

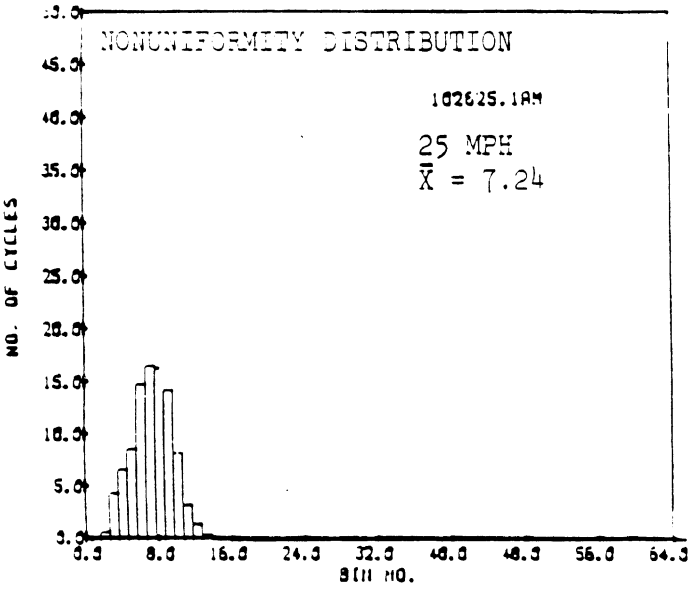
NONUNIFORMITY DISTRIBUTION
102625.1AM
25 MPH
X̄ = 7.24
NO. OF CYCLES
BIN NO.

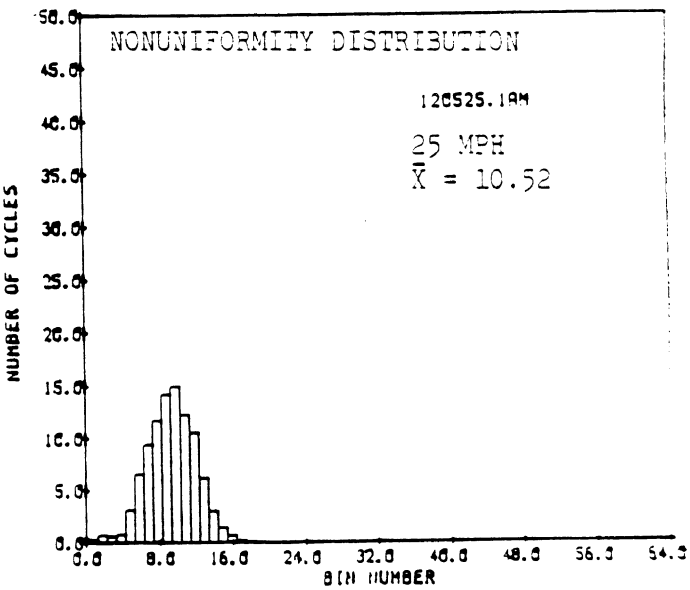
NONUNIFORMITY DISTRIBUTION
120525.1AM
25 MPH
X̄ = 10.52
NUMBER OF CYCLES
BIN NUMBER

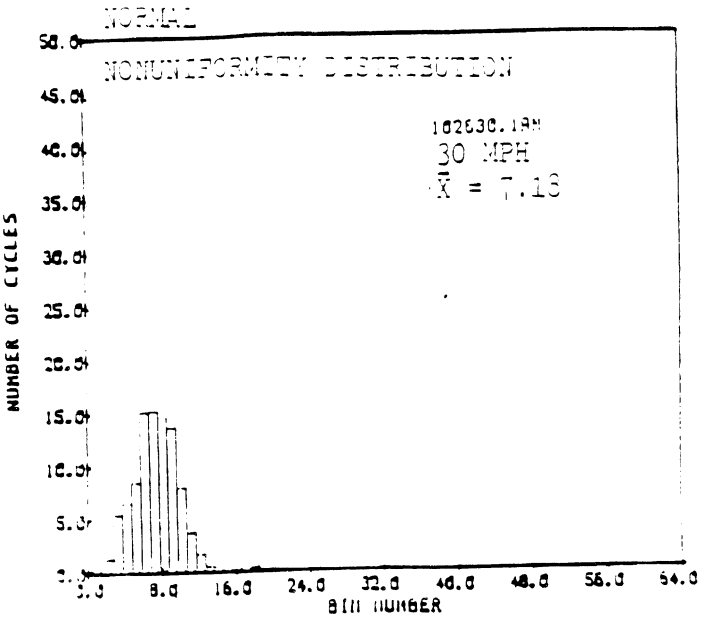
NORMAL
NONUNIFORMITY DISTRIBUTION
102630.1AM
30 MPH
$\bar{X}$ = 7.18
NUMBER OF CYCLES
BIN NUMBER

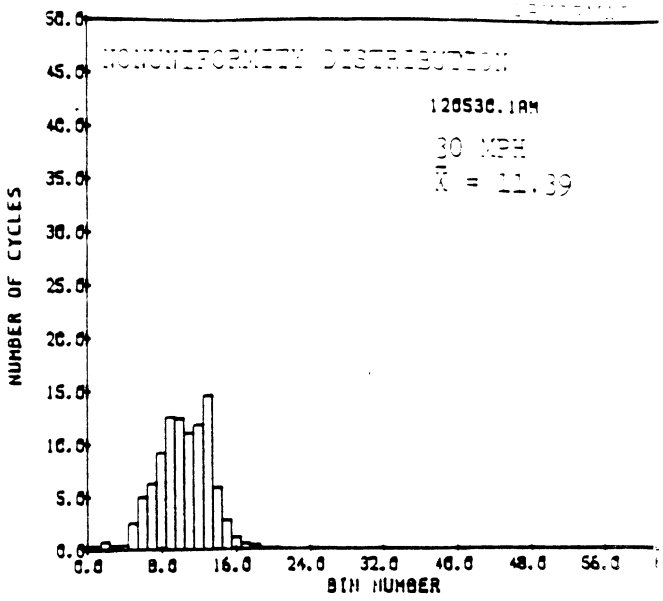
NONUNIFORMITY DISTRIBUTION
120530.1AM
30 MPH
$\bar{X}$ = 11.39
NUMBER OF CYCLES
BIN NUMBER

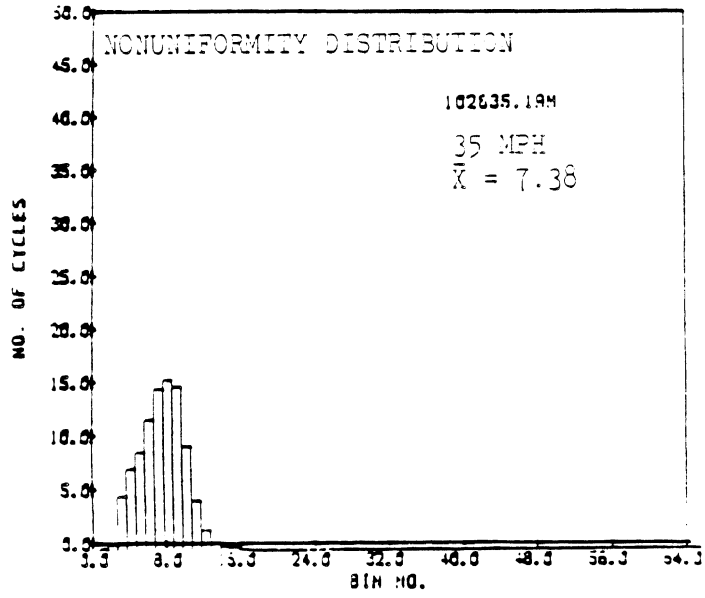
NONUNIFORMITY DISTRIBUTION
102635.1AM
35 MPH
$\bar{X}$ = 7.38
NO. OF CYCLES
BIN NO.

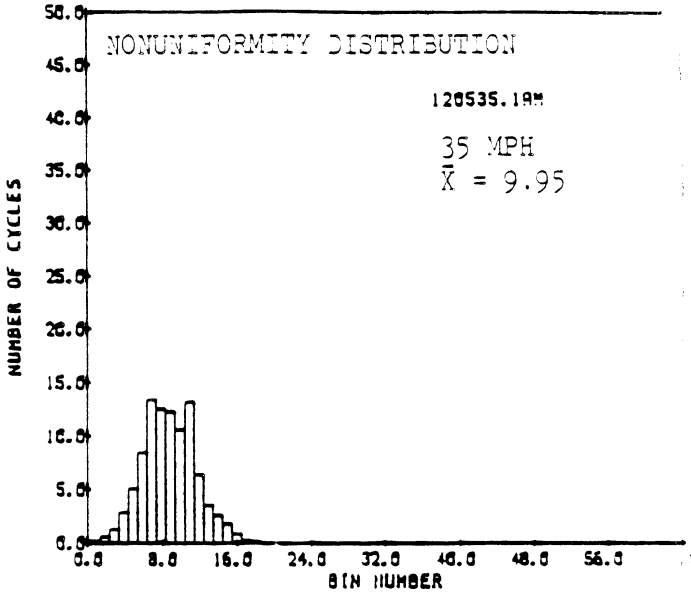
NONUNIFORMITY DISTRIBUTION
120535.1AM
35 MPH
$\bar{X}$ = 9.95
NUMBER OF CYCLES
BIN NUMBER

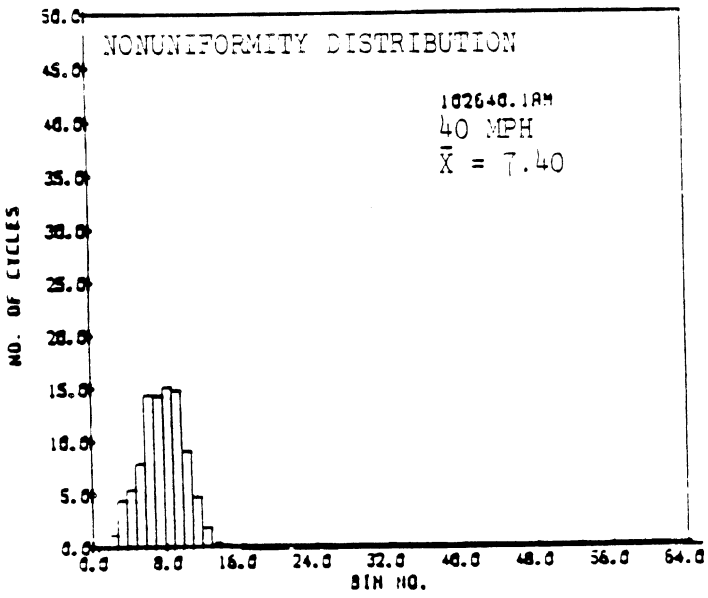
NONUNIFORMITY DISTRIBUTION
102640.1AM
40 MPH
$\bar{X}$ = 7.40
NO. OF CYCLES
BIN NO.

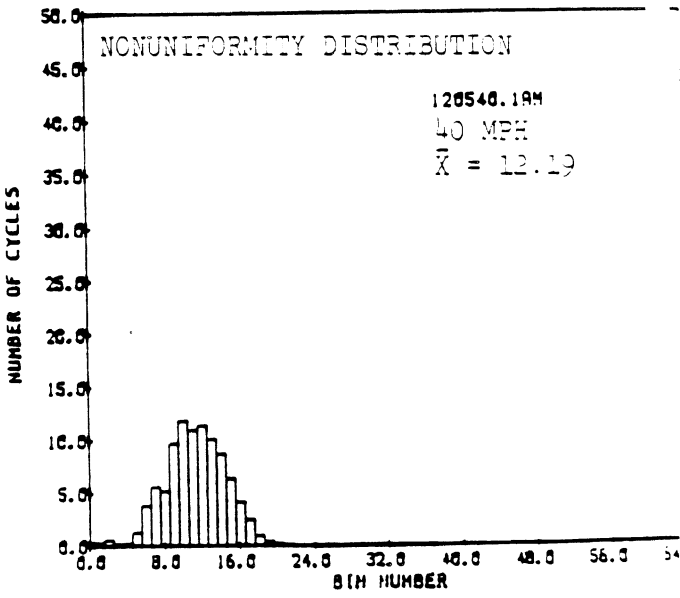
NONUNIFORMITY DISTRIBUTION
120540.1AM
40 MPH
$\bar{X}$ = 12.19
NUMBER OF CYCLES
BIN NUMBER

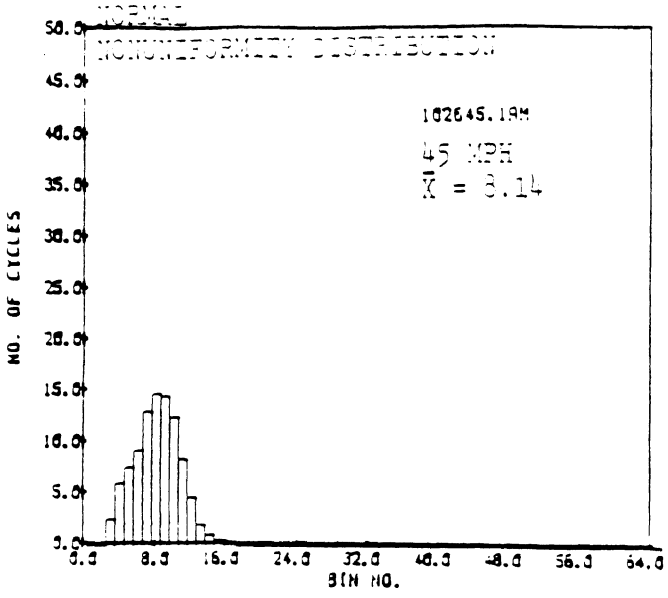
NONUNIFORMITY DISTRIBUTION
102645.1AM
45 MPH
X̄ = 8.14
NO. OF CYCLES
BIN NO.

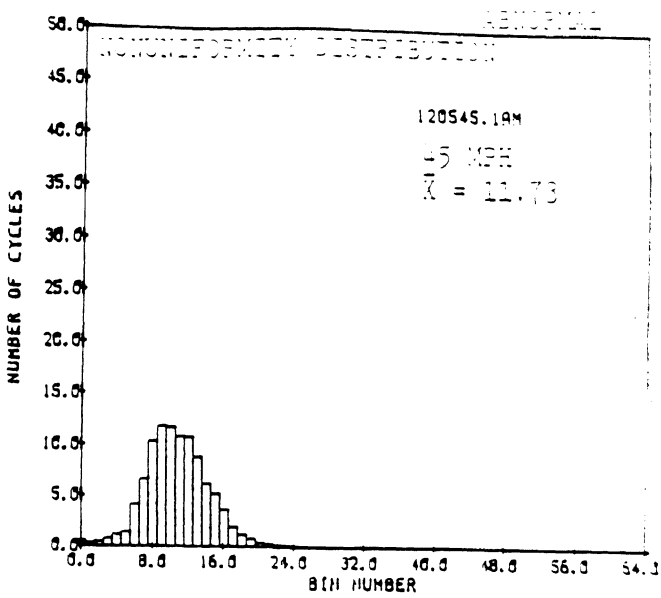
NONUNIFORMITY DISTRIBUTION
120545.1AM
45 MPH
X̄ = 11.73
NUMBER OF CYCLES
BIN NUMBER

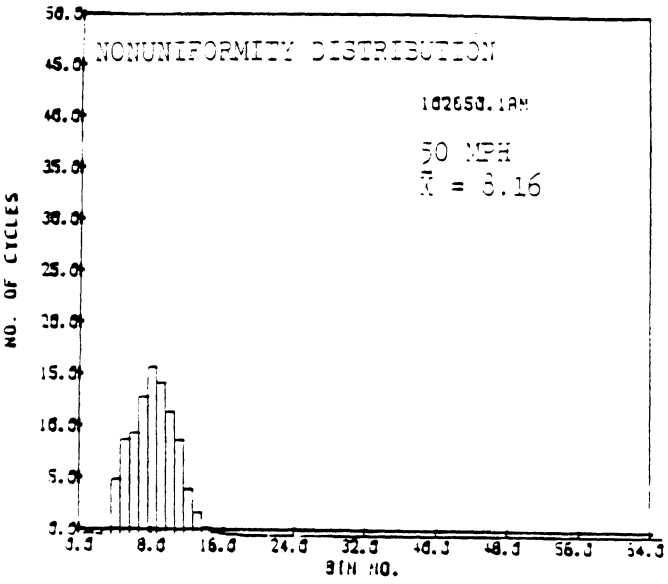
NONUNIFORMITY DISTRIBUTION
102650.1AM
50 MPH
X̄ = 8.16
NO. OF CYCLES
BIN NO.

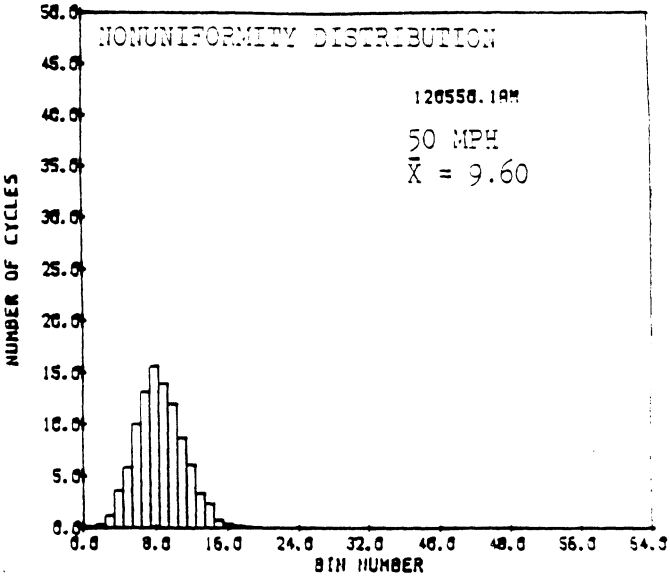
NONUNIFORMITY DISTRIBUTION
120550.1AM
50 MPH
X̄ = 9.60
NUMBER OF CYCLES
BIN NUMBER

NORMAL

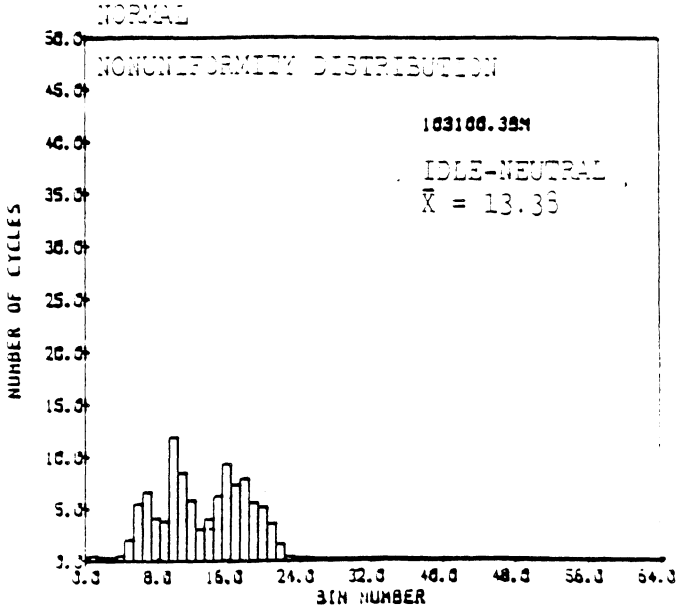

ABNORMAL

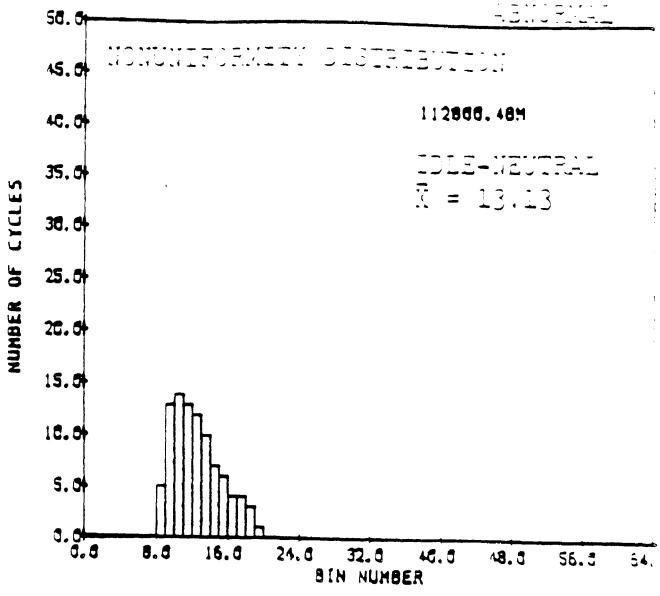

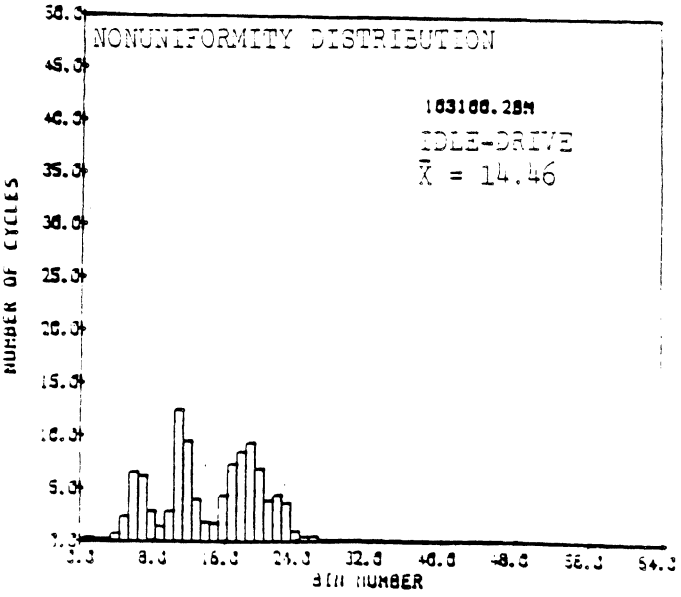

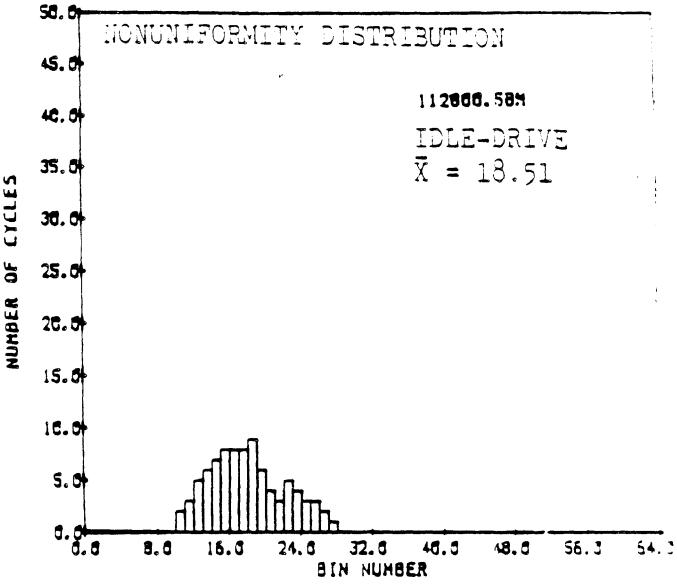

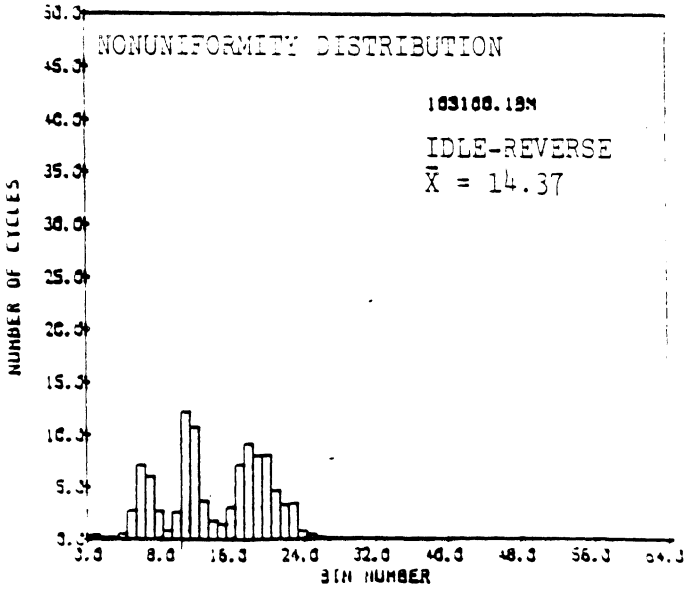

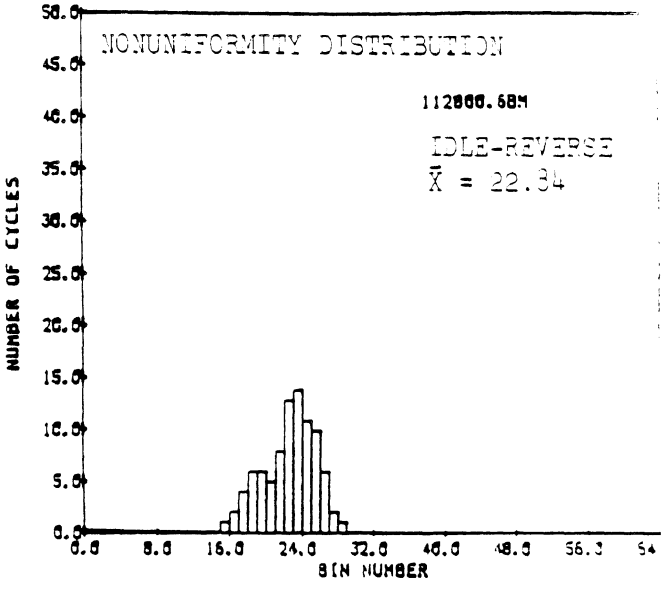

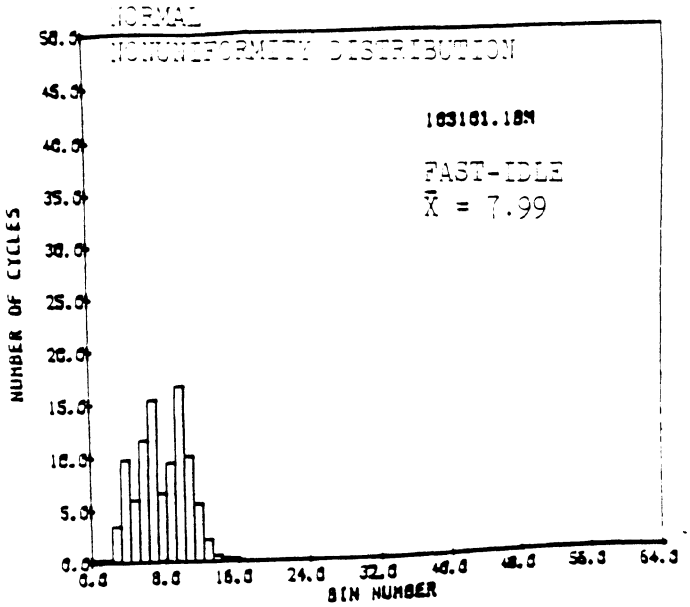
NORMAL
NONUNIFORMITY DISTRIBUTION
163161.18M
FAST-IDLE
X̄ = 7.99
NUMBER OF CYCLES
BIN NUMBER

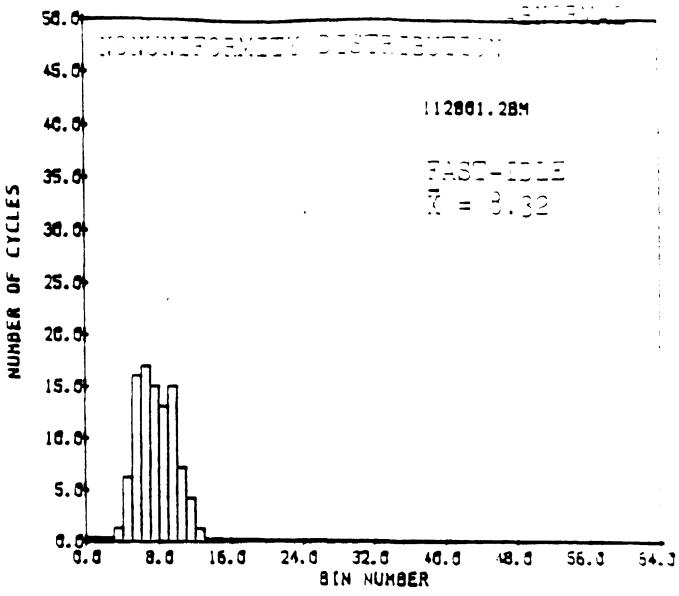
NONUNIFORMITY DISTRIBUTION
112861.28M
FAST-IDLE
X̄ = 8.32
NUMBER OF CYCLES
BIN NUMBER

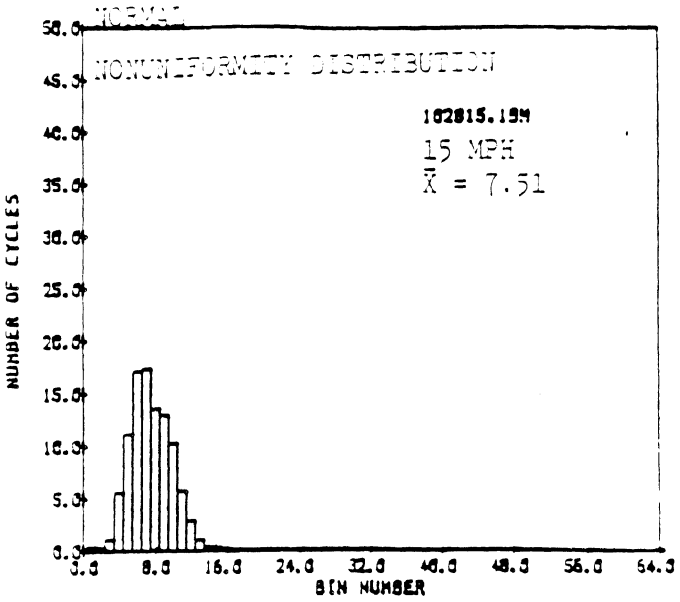
NONUNIFORMITY DISTRIBUTION
102815.19M
15 MPH
$\bar{X}$ = 7.51
NUMBER OF CYCLES
BIN NUMBER

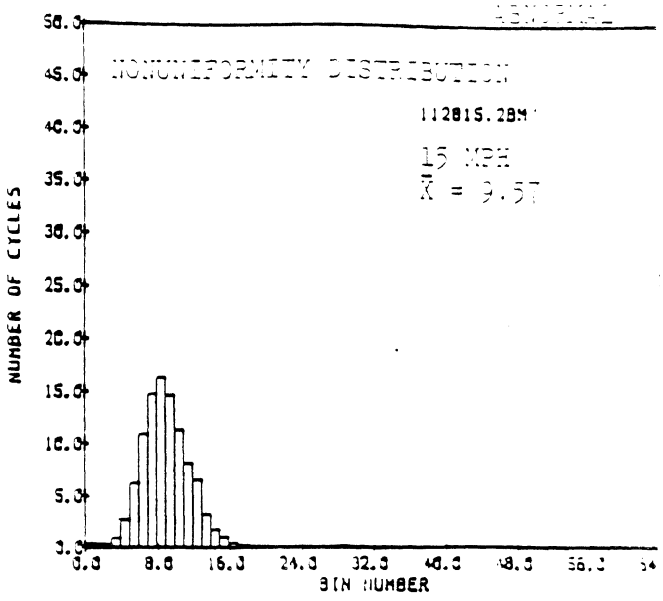
NONUNIFORMITY DISTRIBUTION
112815.28M
15 MPH
$\bar{X}$ = 9.57
NUMBER OF CYCLES
BIN NUMBER

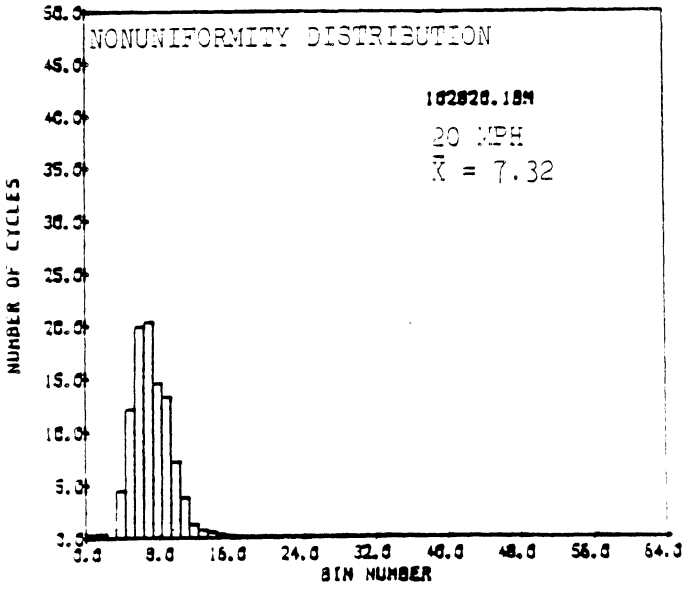
NONUNIFORMITY DISTRIBUTION
102820.18M
20 MPH
$\bar{X}$ = 7.32
NUMBER OF CYCLES
BIN NUMBER

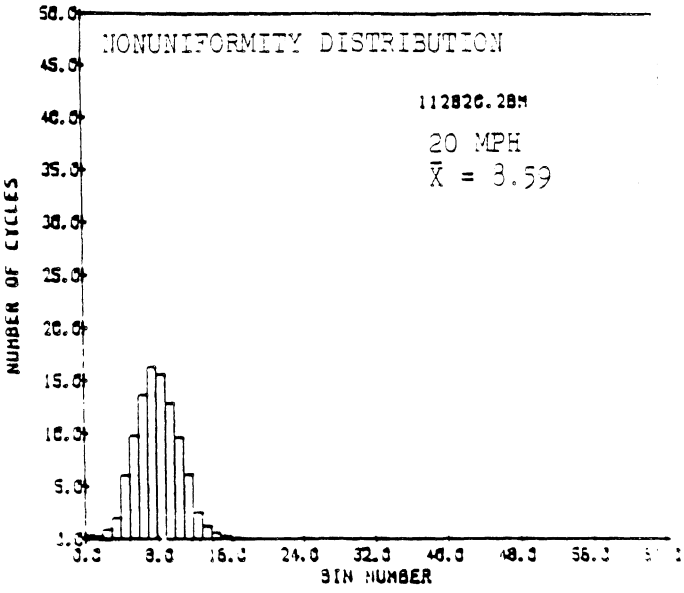
NONUNIFORMITY DISTRIBUTION
112820.28M
20 MPH
$\bar{X}$ = 8.59
NUMBER OF CYCLES
BIN NUMBER

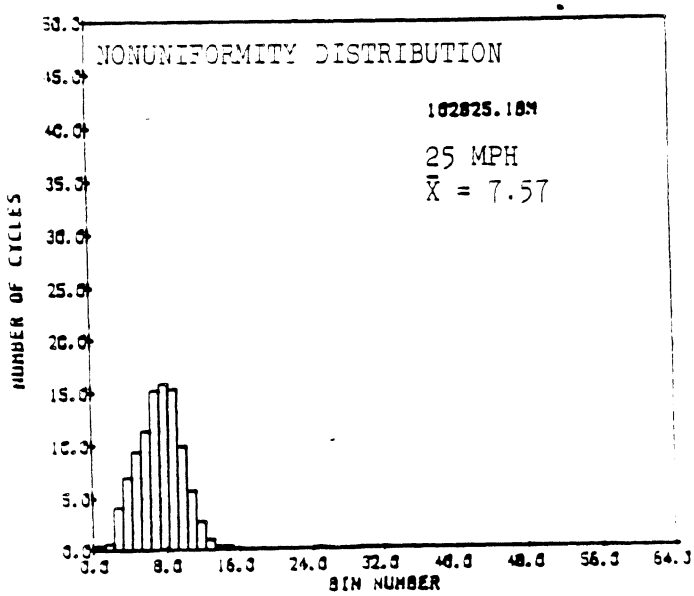
NONUNIFORMITY DISTRIBUTION
102825.18M
25 MPH
$\bar{X}$ = 7.57
NUMBER OF CYCLES
BIN NUMBER

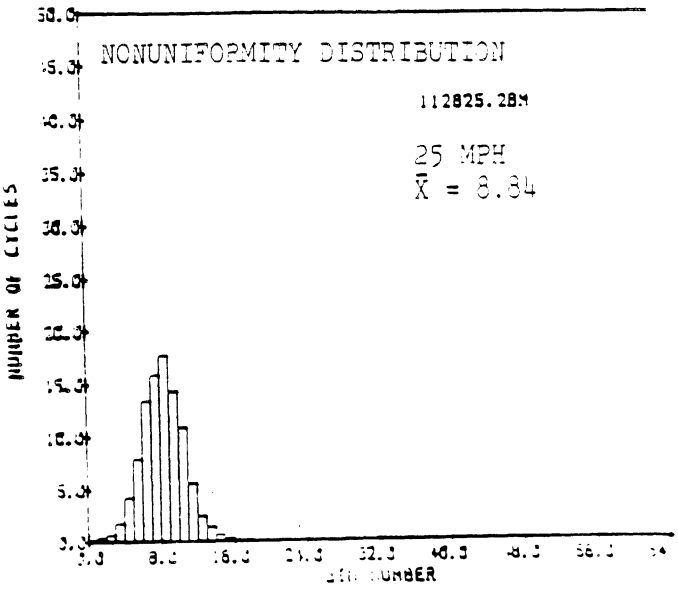
NONUNIFORMITY DISTRIBUTION
112825.28M
25 MPH
$\bar{X}$ = 8.84
NUMBER OF CYCLES

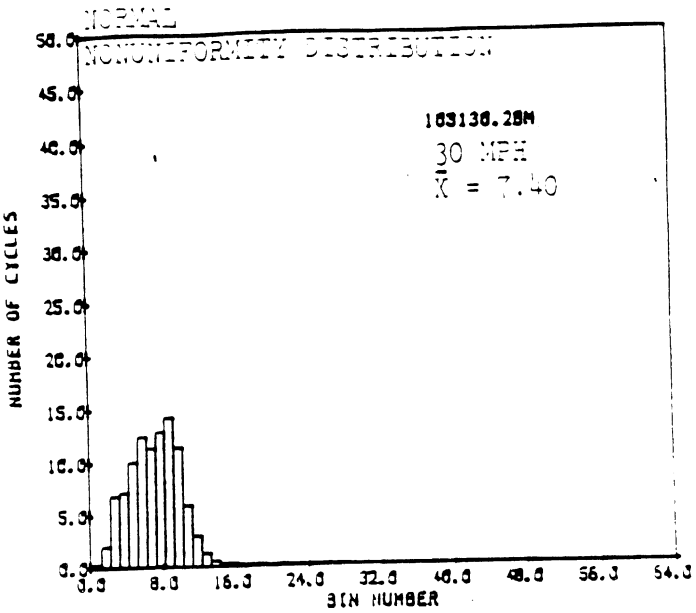
NONUNIFORMITY DISTRIBUTION
163130.2BM
30 MPH
$\bar{X}$ = 7.40
NUMBER OF CYCLES
BIN NUMBER

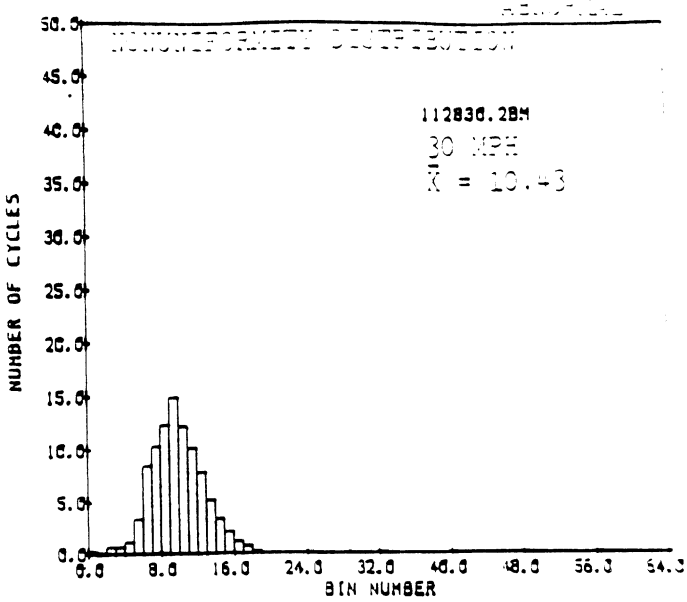
112830.2BM
30 MPH
$\bar{X}$ = 10.43
NUMBER OF CYCLES
BIN NUMBER

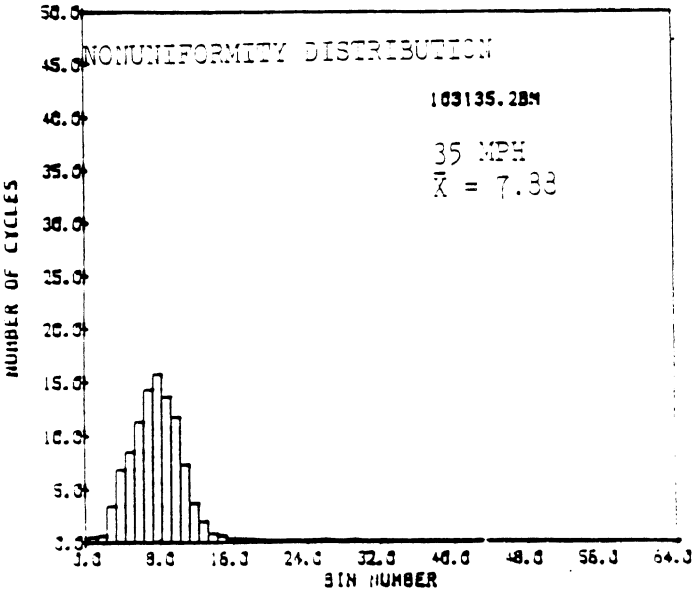
NONUNIFORMITY DISTRIBUTION
163135.2BM
35 MPH
$\bar{X}$ = 7.38
NUMBER OF CYCLES
BIN NUMBER

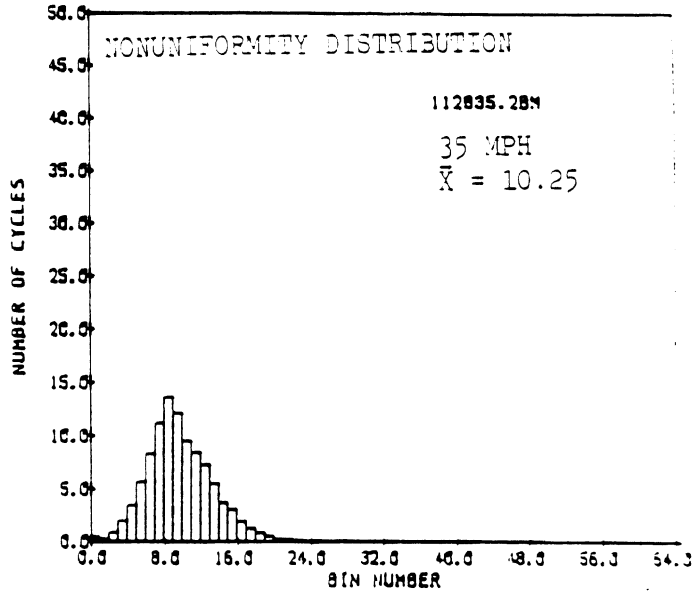
NONUNIFORMITY DISTRIBUTION
112835.2BM
35 MPH
$\bar{X}$ = 10.25
NUMBER OF CYCLES
BIN NUMBER

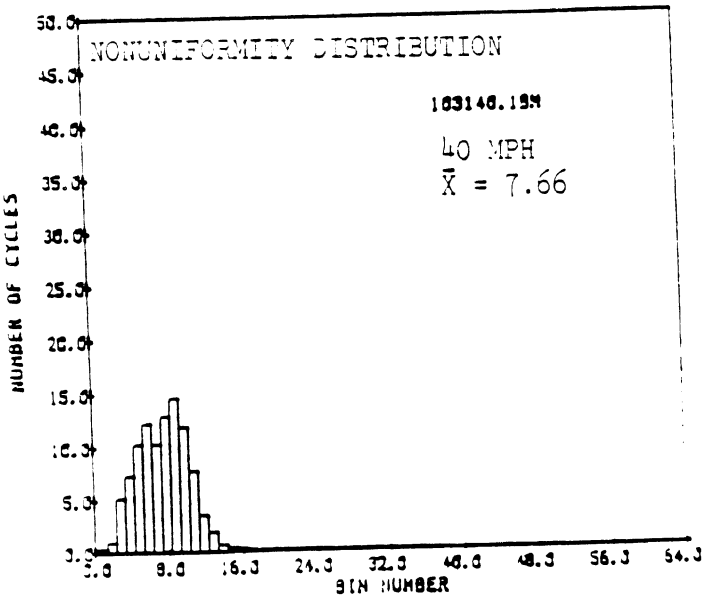
NONUNIFORMITY DISTRIBUTION
163140.1BM
40 MPH
$\bar{X}$ = 7.66
NUMBER OF CYCLES
BIN NUMBER

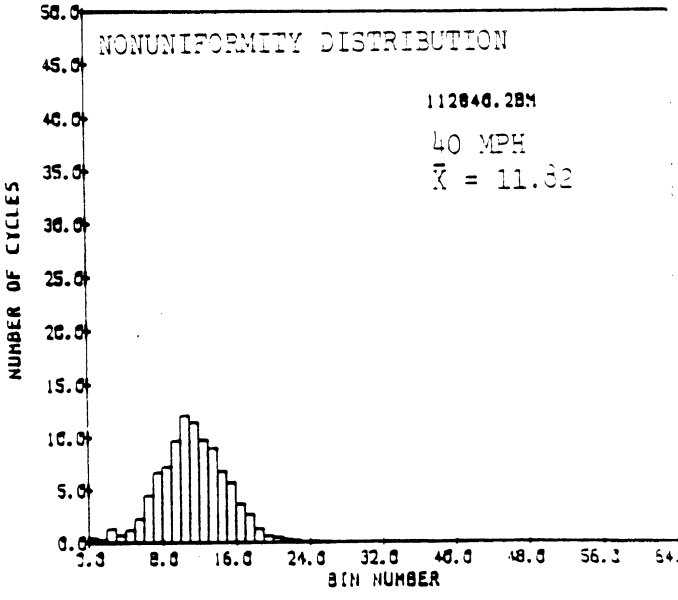
NONUNIFORMITY DISTRIBUTION
112840.2BM
40 MPH
$\bar{X}$ = 11.32
NUMBER OF CYCLES
BIN NUMBER

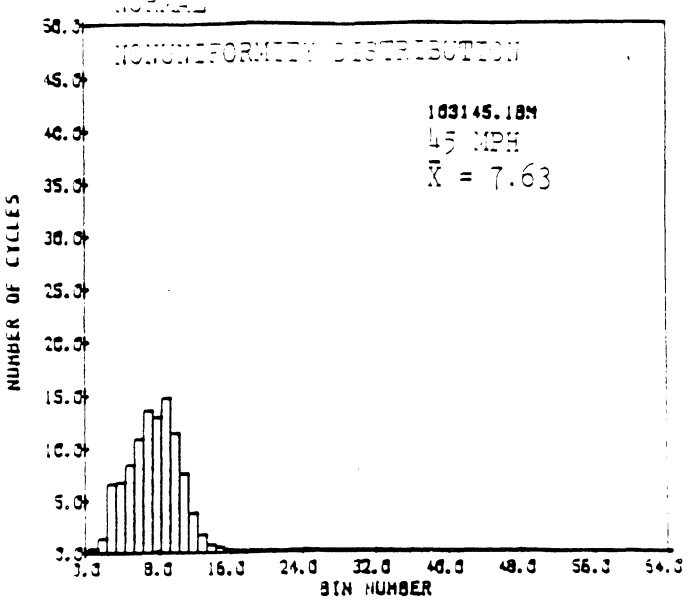
NONUNIFORMITY DISTRIBUTION
103145.18M
45 MPH
X̄ = 7.63
NUMBER OF CYCLES
BIN NUMBER

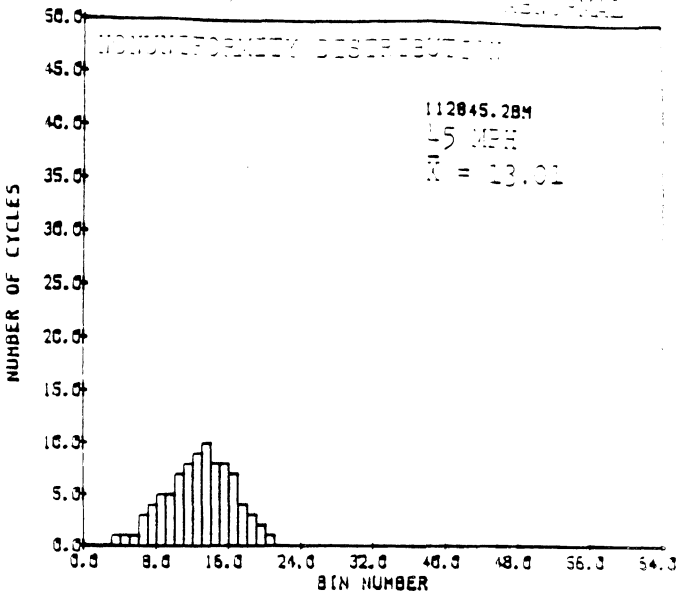
NONUNIFORMITY DISTRIBUTION
112845.28M
45 MPH
X̄ = 13.01
NUMBER OF CYCLES
BIN NUMBER

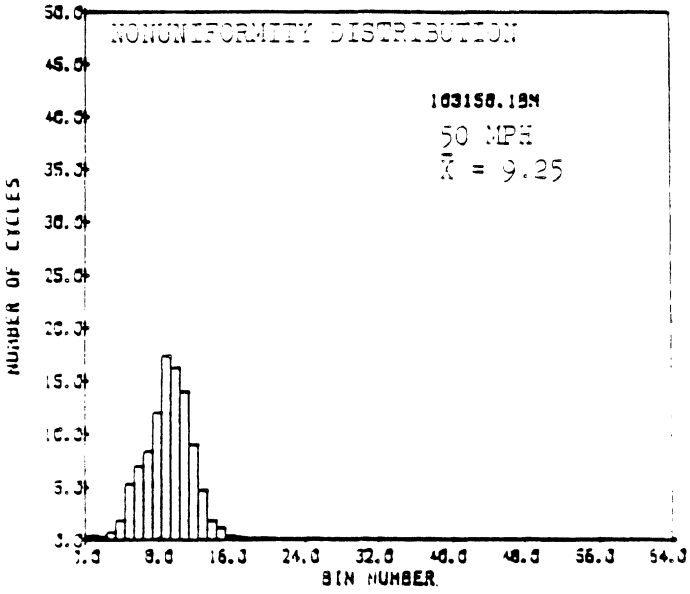
NONUNIFORMITY DISTRIBUTION
103158.18M
50 MPH
X̄ = 9.25
NUMBER OF CYCLES
BIN NUMBER

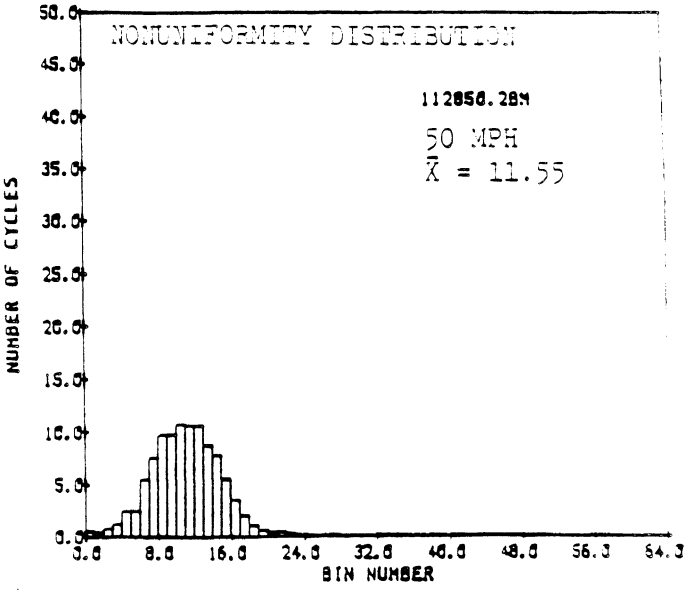
NONUNIFORMITY DISTRIBUTION
112858.28M
50 MPH
X̄ = 11.55
NUMBER OF CYCLES
BIN NUMBER

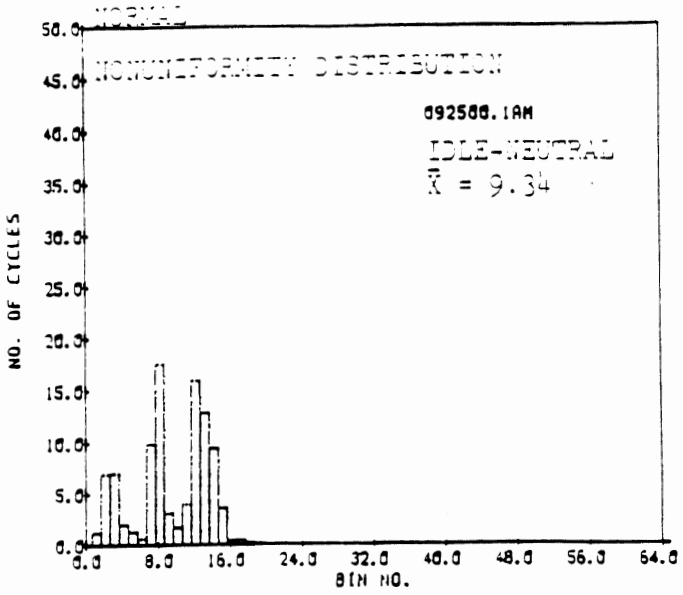
NONUNIFORMITY DISTRIBUTION
092588.1AM
IDLE-NEUTRAL
X̄ = 9.34
NO. OF CYCLES
BIN NO.

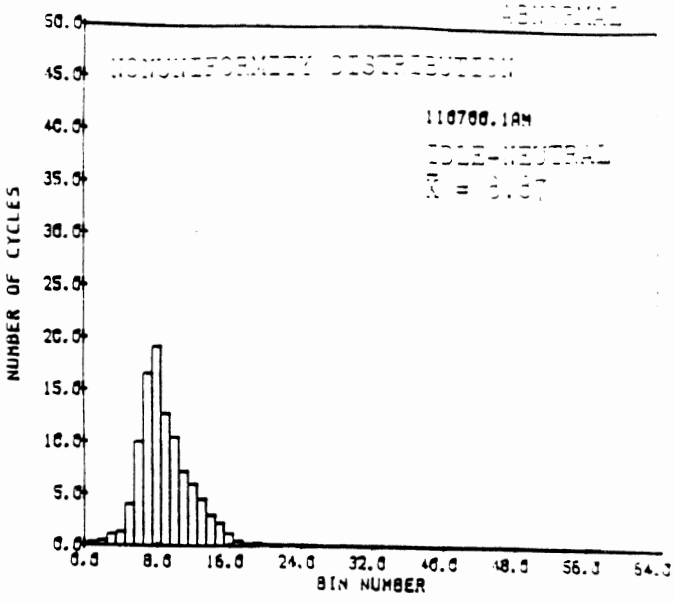
NONUNIFORMITY DISTRIBUTION
110788.1AM
IDLE-NEUTRAL
X̄ = 8.87
NUMBER OF CYCLES
BIN NUMBER

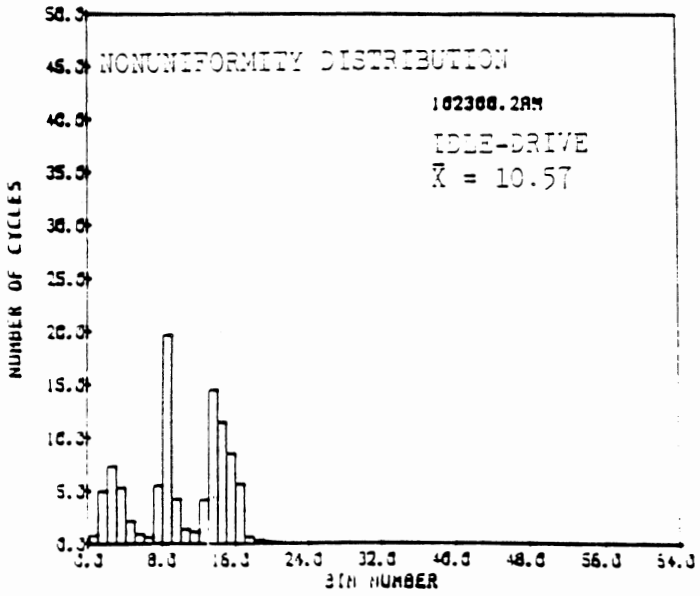
NONUNIFORMITY DISTRIBUTION
102388.2AM
IDLE-DRIVE
X̄ = 10.57
NUMBER OF CYCLES
BIN NUMBER

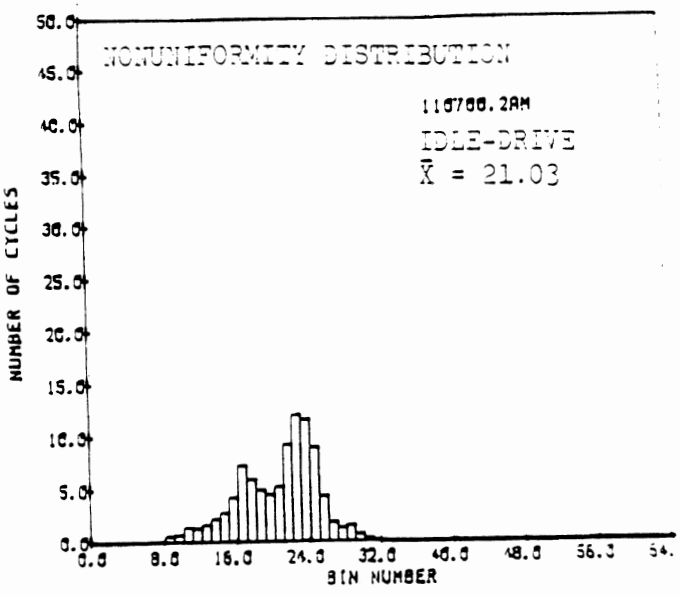
NONUNIFORMITY DISTRIBUTION
110788.2AM
IDLE-DRIVE
X̄ = 21.03
NUMBER OF CYCLES
BIN NUMBER

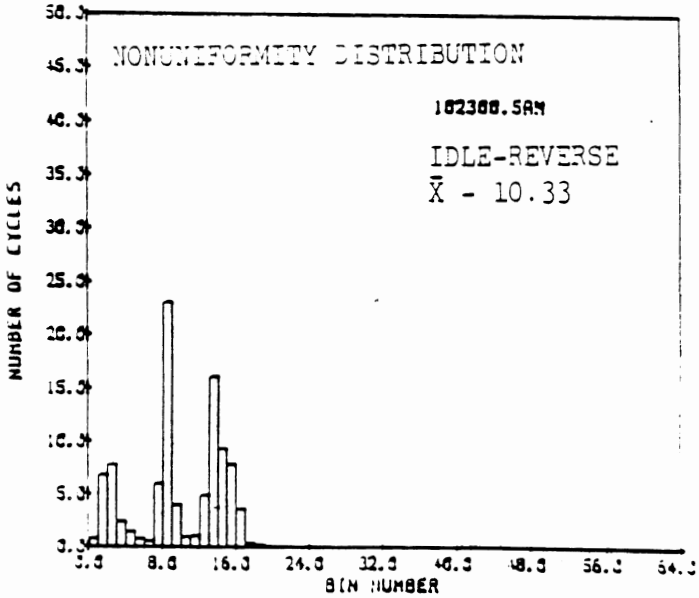
NONUNIFORMITY DISTRIBUTION
102388.5AM
IDLE-REVERSE
X̄ - 10.33
NUMBER OF CYCLES
BIN NUMBER

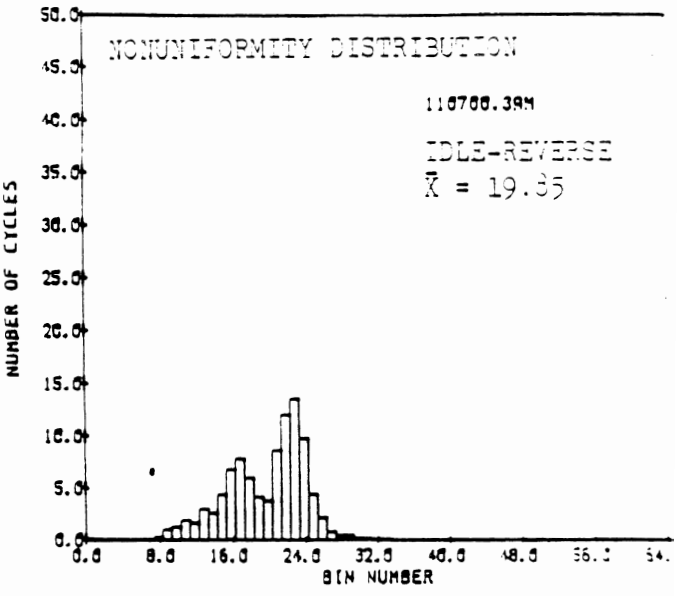
NONUNIFORMITY DISTRIBUTION
110788.3AM
IDLE-REVERSE
X̄ = 19.85
NUMBER OF CYCLES
BIN NUMBER

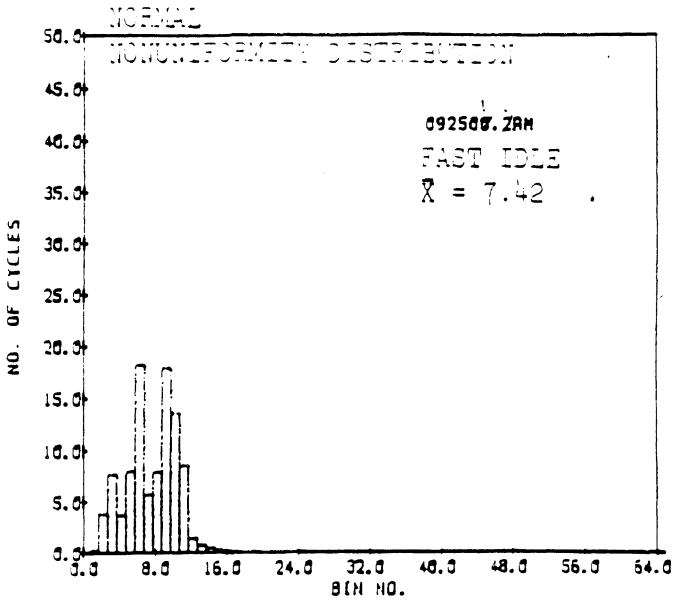
NORMAL
NONUNIFORMITY DISTRIBUTION
092500.ZAM
FAST IDLE
X̄ = 7.42
NO. OF CYCLES
50.0
45.0
40.0
35.0
30.0
25.0
20.0
15.0
10.0
5.0
0.0
0.0
8.0
16.0
24.0
32.0
40.0
48.0
56.0
64.0
BIN NO.

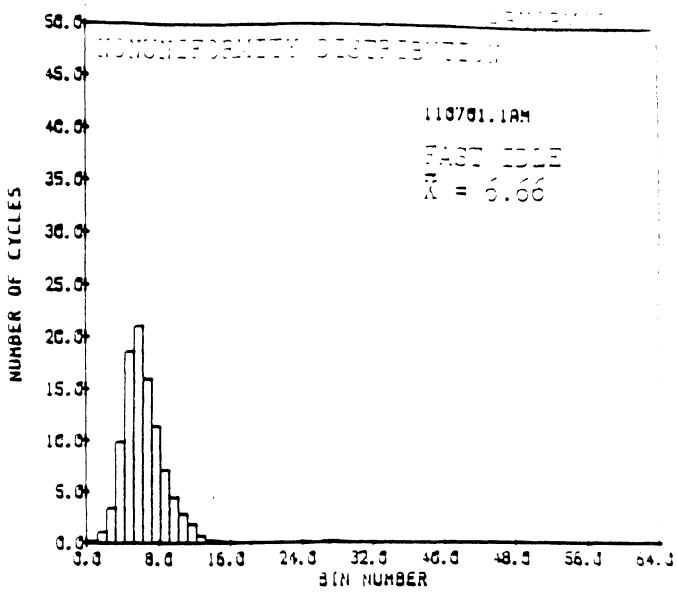
NONUNIFORMITY DISTRIBUTION
110701.1AM
FAST IDLE
X̄ = 6.66
NUMBER OF CYCLES
50.0
45.0
40.0
35.0
30.0
25.0
20.0
15.0
10.0
5.0
0.0
0.0
8.0
16.0
24.0
32.0
40.0
48.0
56.0
64.0
BIN NUMBER

NORMAL

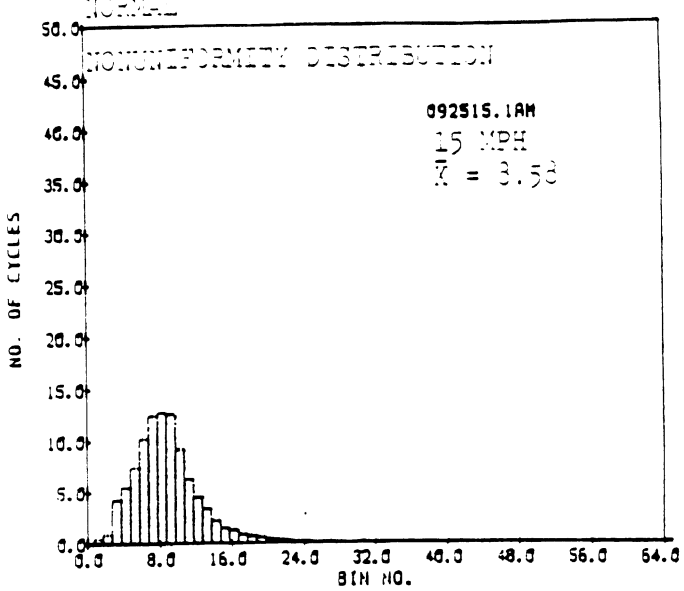

ABNORMAL

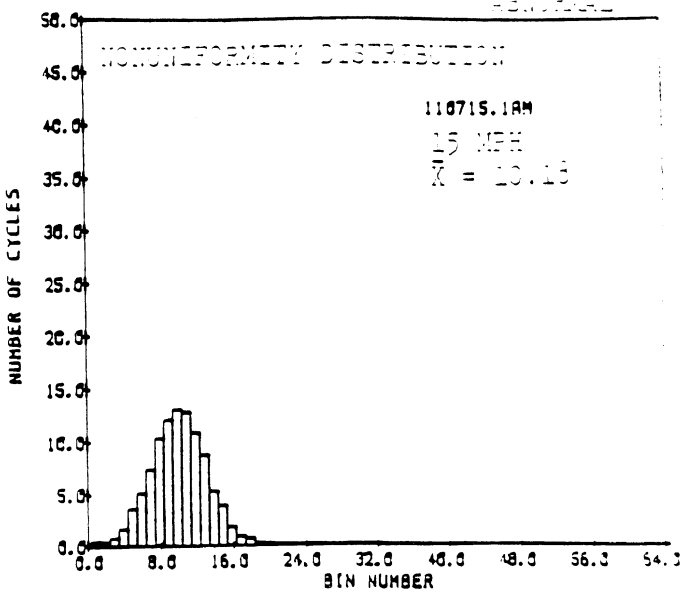

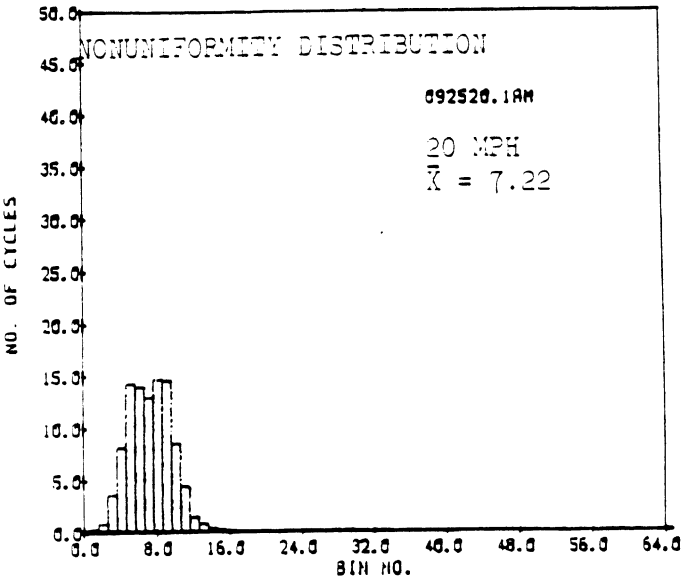

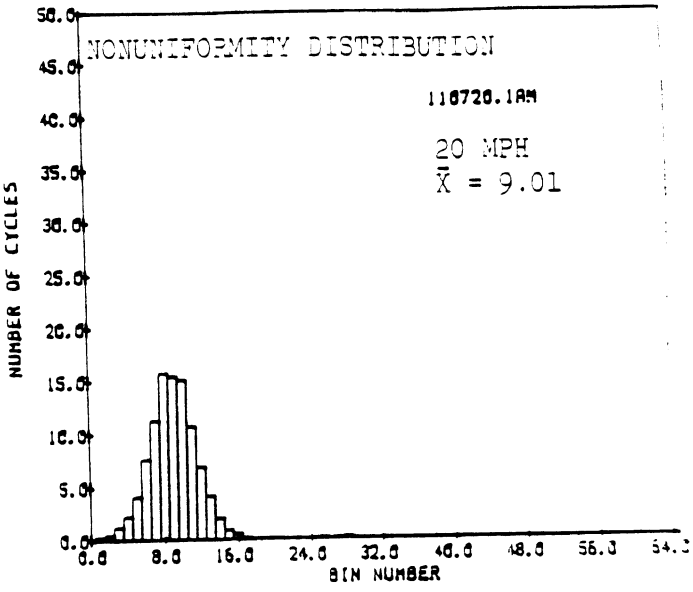

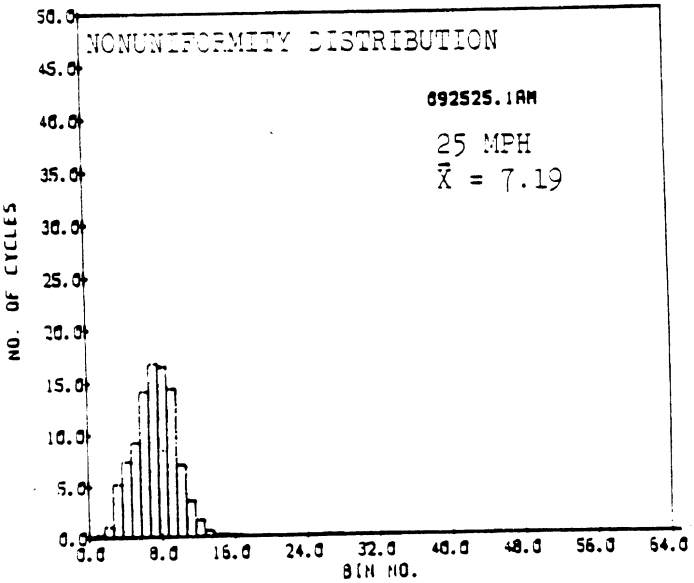

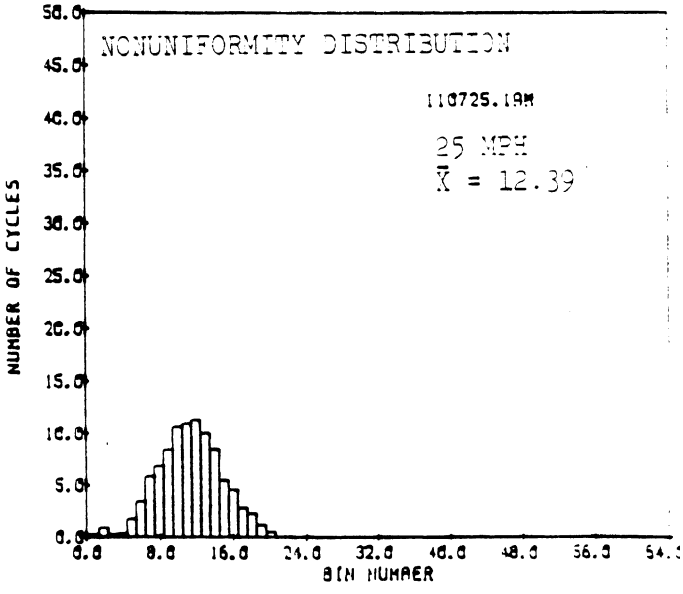

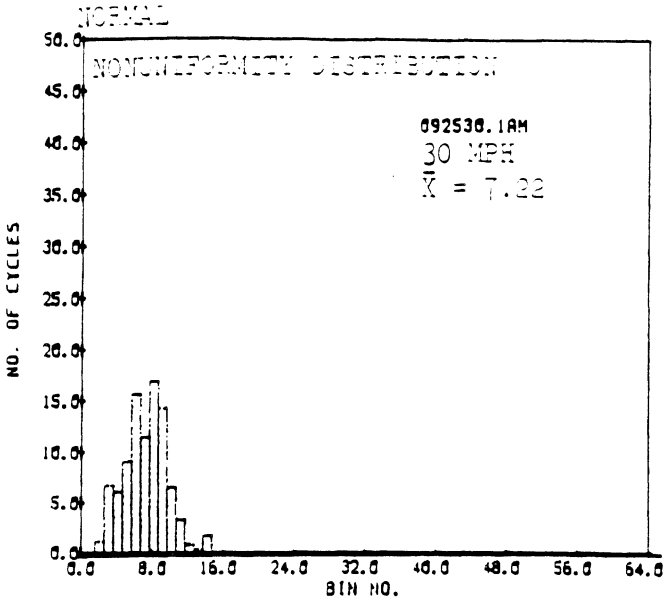
NORMAL
NONUNIFORMITY DISTRIBUTION
092536.1AM
30 MPH
X̄ = 7.22
NO. OF CYCLES
BIN NO.

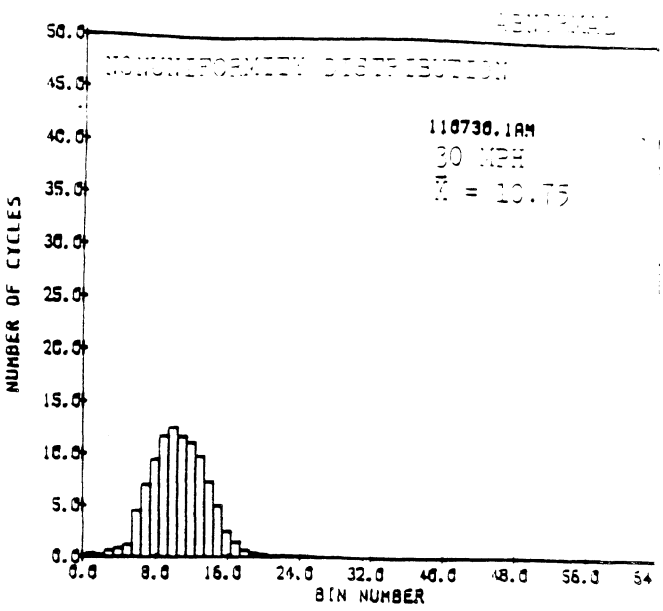
NONUNIFORMITY DISTRIBUTION
110736.1AM
30 MPH
X̄ = 10.75
NUMBER OF CYCLES
BIN NUMBER

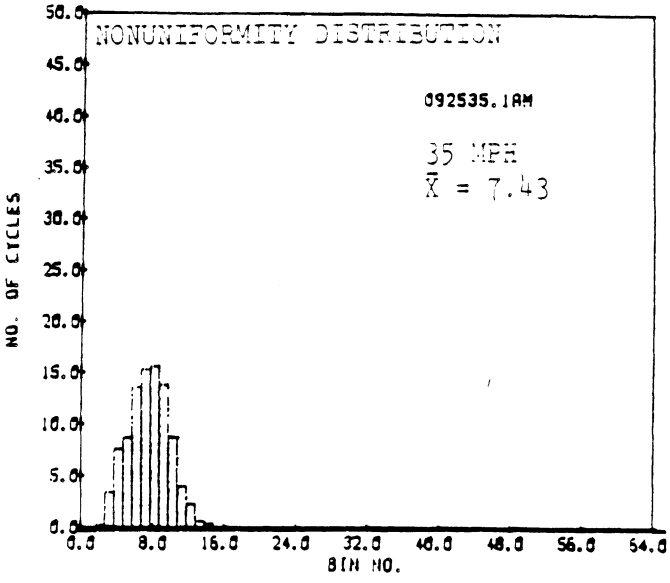
NONUNIFORMITY DISTRIBUTION
092535.1AM
35 MPH
X̄ = 7.43
NO. OF CYCLES
BIN NO.

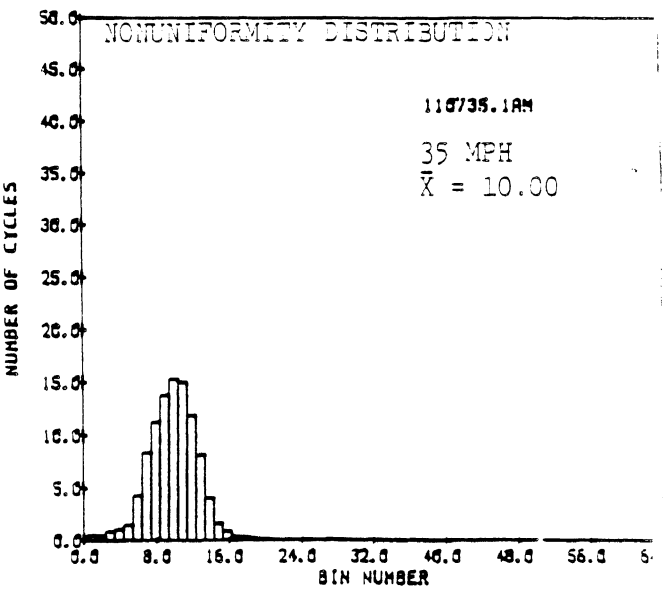
NONUNIFORMITY DISTRIBUTION
110735.1AM
35 MPH
X̄ = 10.00
NUMBER OF CYCLES
BIN NUMBER

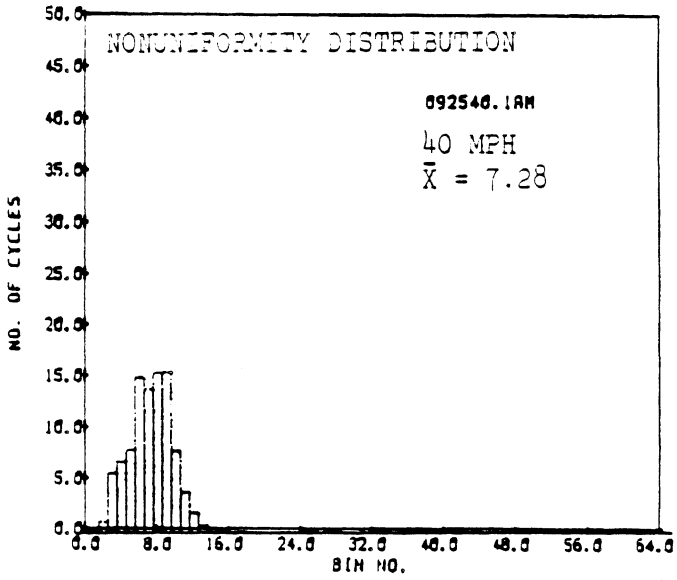
NONUNIFORMITY DISTRIBUTION
092540.1AM
40 MPH
X̄ = 7.28
NO. OF CYCLES
BIN NO.

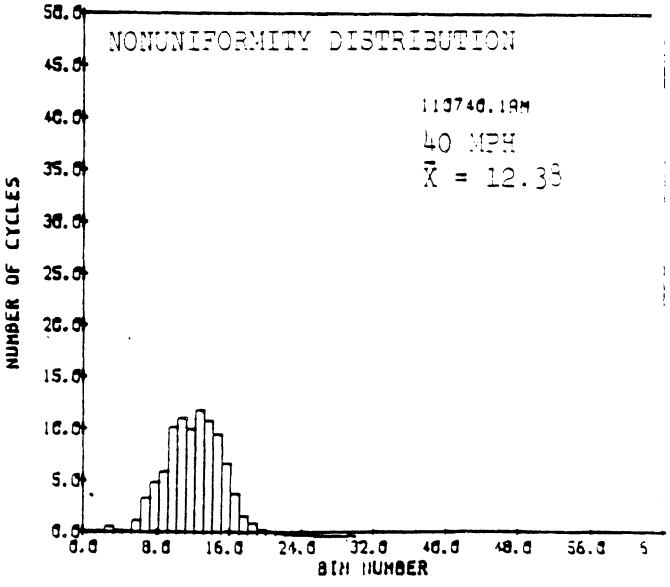
NONUNIFORMITY DISTRIBUTION
110740.1AM
40 MPH
X̄ = 12.38
NUMBER OF CYCLES
BIN NUMBER

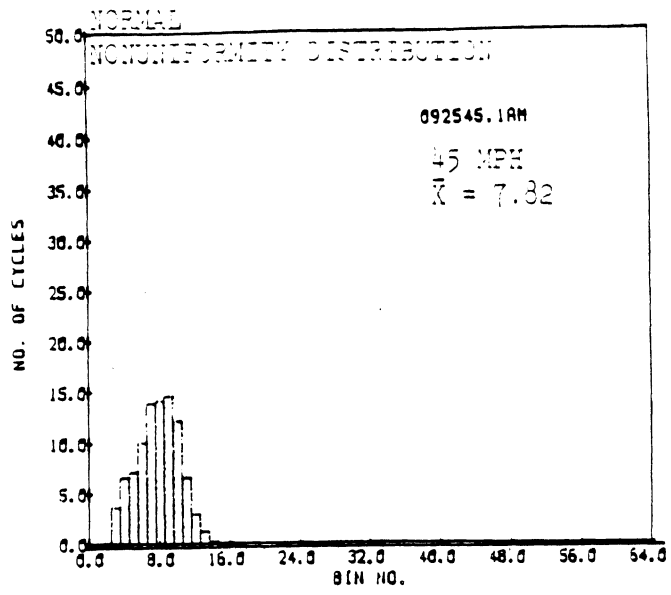
NORMAL
NONUNIFORMITY DISTRIBUTION
092545.1AM
45 MPH
X̄ = 7.82
NO. OF CYCLES
BIN NO.

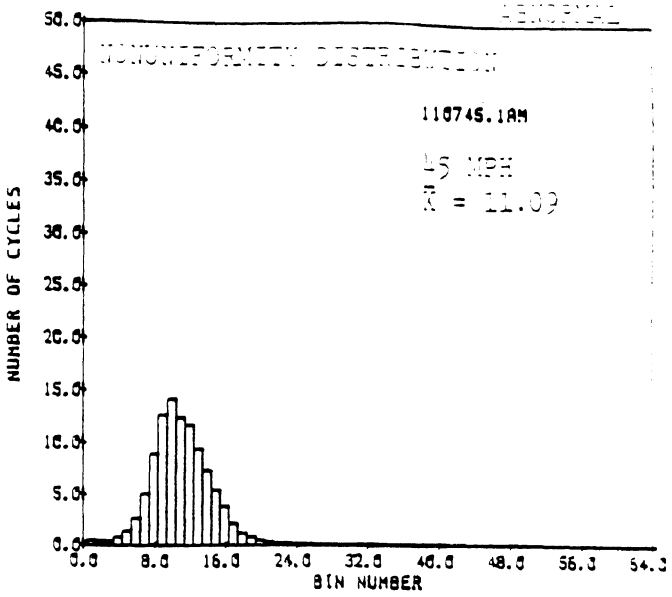
NONUNIFORMITY DISTRIBUTION
110745.1AM
45 MPH
X̄ = 11.09
NUMBER OF CYCLES
BIN NUMBER

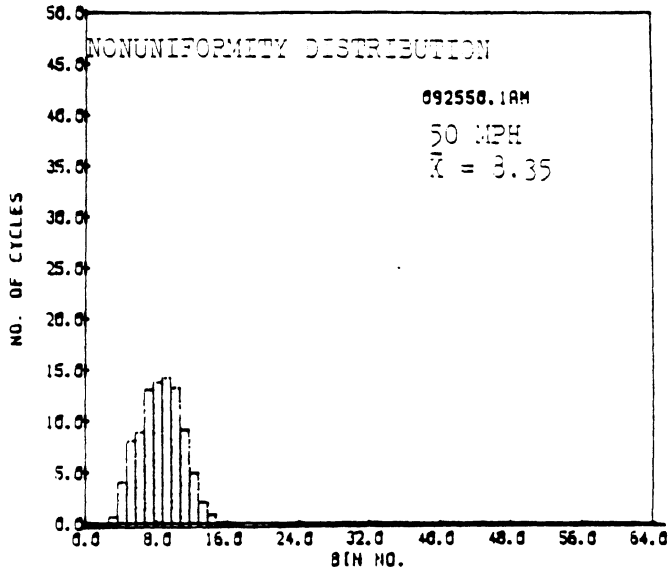
NONUNIFORMITY DISTRIBUTION
092556.1AM
50 MPH
X̄ = 8.35
NO. OF CYCLES
BIN NO.

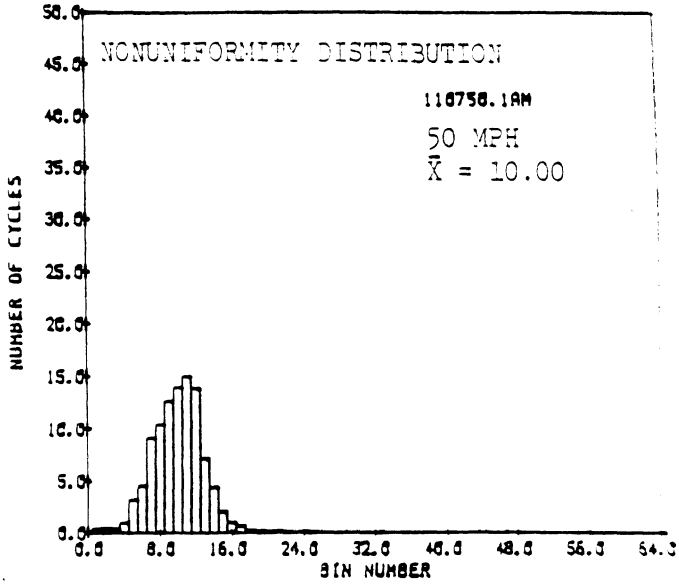
NONUNIFORMITY DISTRIBUTION
110756.1AM
50 MPH
X̄ = 10.00
NUMBER OF CYCLES
BIN NUMBER

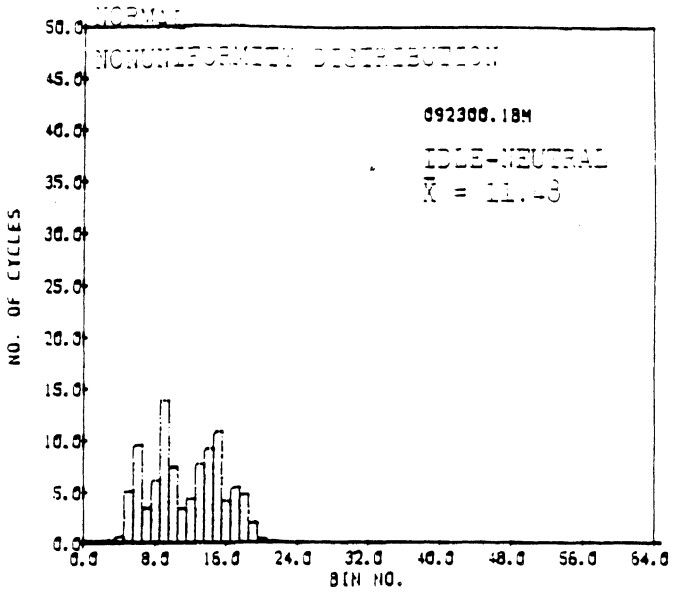
NONUNIFORMITY DISTRIBUTION
092300.18M
IDLE-NEUTRAL
X̄ = 11.43
NO. OF CYCLES
BIN NO.

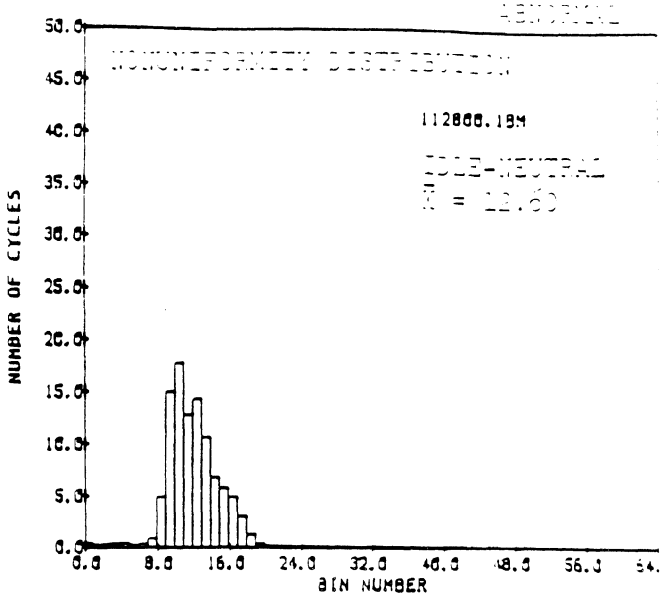
NONUNIFORMITY DISTRIBUTION
112800.18M
IDLE-NEUTRAL
X̄ = 12.60
NUMBER OF CYCLES
BIN NUMBER

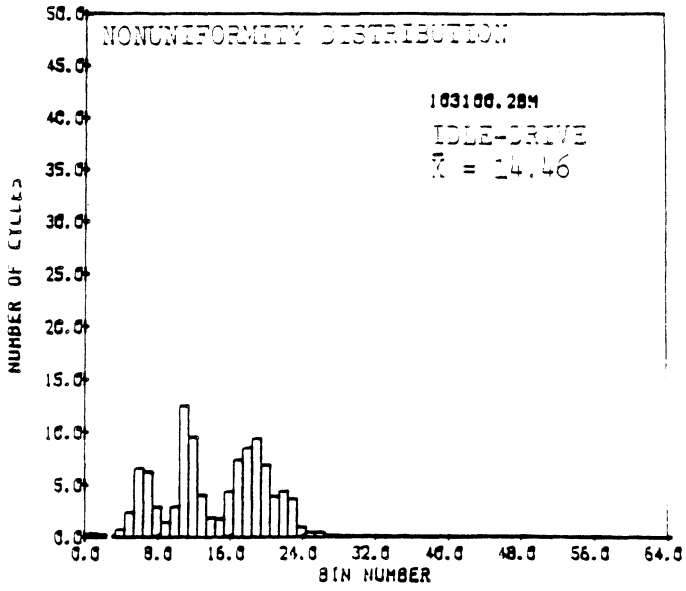
NONUNIFORMITY DISTRIBUTION
103100.28M
IDLE-DRIVE
X̄ = 14.46
NUMBER OF CYCLES
BIN NUMBER

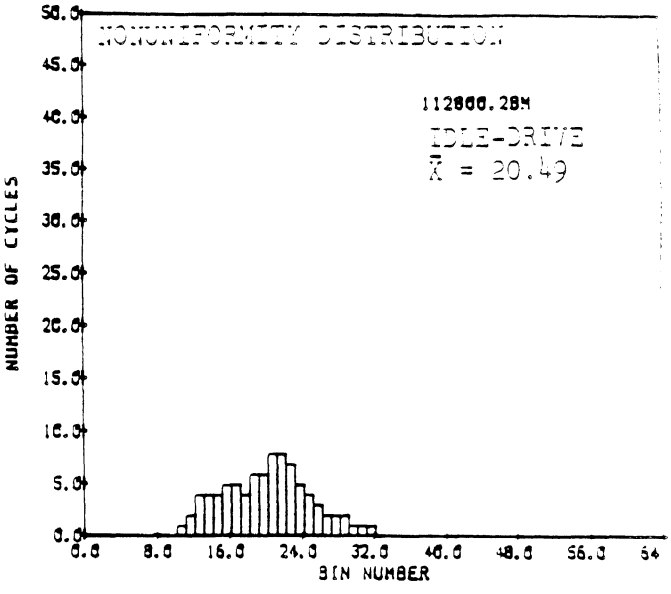
NONUNIFORMITY DISTRIBUTION
112800.28M
IDLE-DRIVE
X̄ = 20.49
NUMBER OF CYCLES
BIN NUMBER

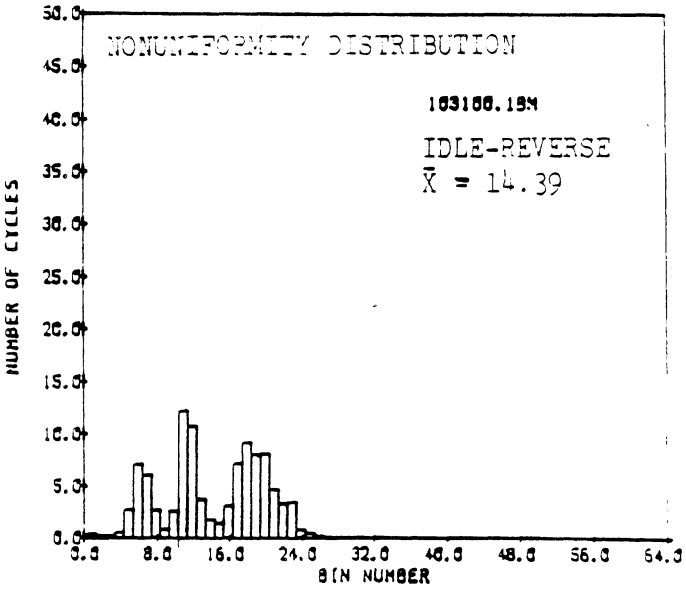
NONUNIFORMITY DISTRIBUTION
103100.18M
IDLE-REVERSE
X̄ = 14.39
NUMBER OF CYCLES
BIN NUMBER

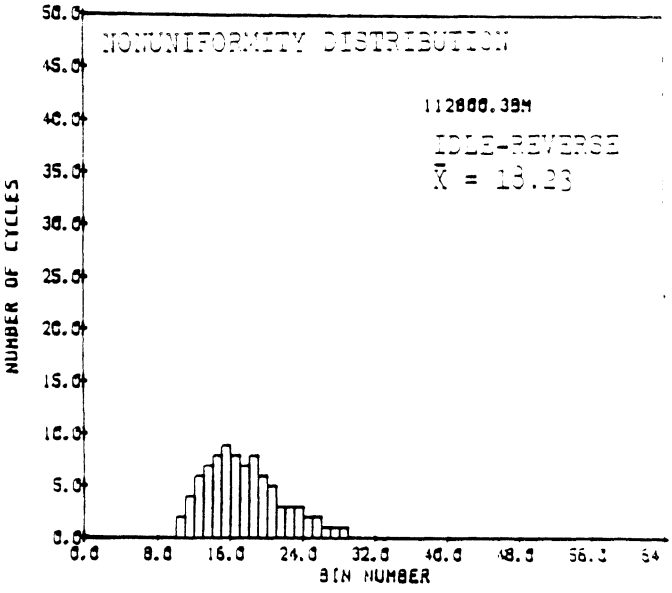
NONUNIFORMITY DISTRIBUTION
112800.38M
IDLE-REVERSE
X̄ = 18.23
NUMBER OF CYCLES
BIN NUMBER

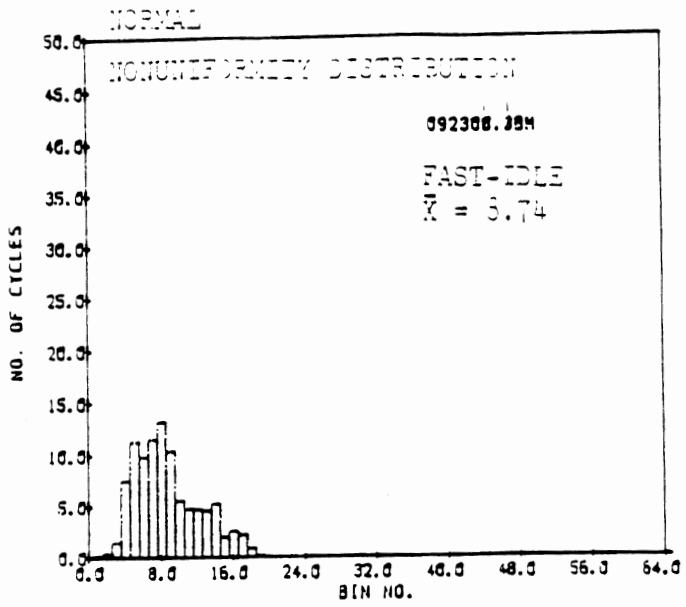
NORMAL
NONUNIFORMITY DISTRIBUTION
092306.18M
FAST-IDLE
X̄ = 6.74
NO. OF CYCLES
50.0
45.0
40.0
35.0
30.0
25.0
20.0
15.0
10.0
5.0
0.0
0.0
8.0
16.0
24.0
32.0
40.0
48.0
56.0
64.0
BIN NO.

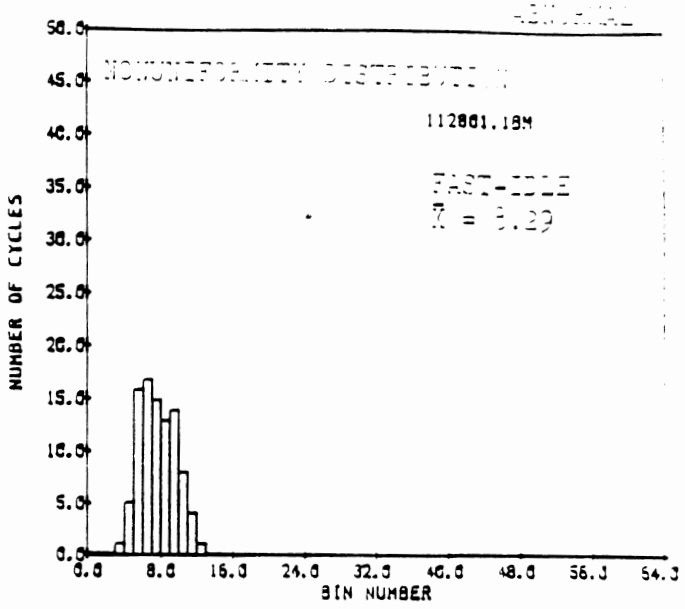
NONUNIFORMITY DISTRIBUTION
112801.18M
FAST-IDLE
X̄ = 8.29
NUMBER OF CYCLES
50.0
45.0
40.0
35.0
30.0
25.0
20.0
15.0
10.0
5.0
0.0
0.0
8.0
16.0
24.0
32.0
40.0
48.0
56.0
64.0
BIN NUMBER

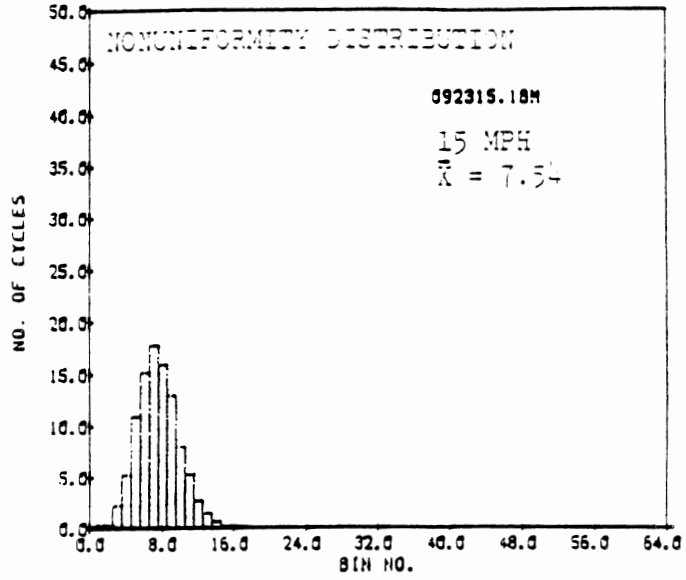
NONUNIFORMITY DISTRIBUTION
092315.18M
15 MPH
$\bar{X}$ = 7.54
NO. OF CYCLES
BIN NO.

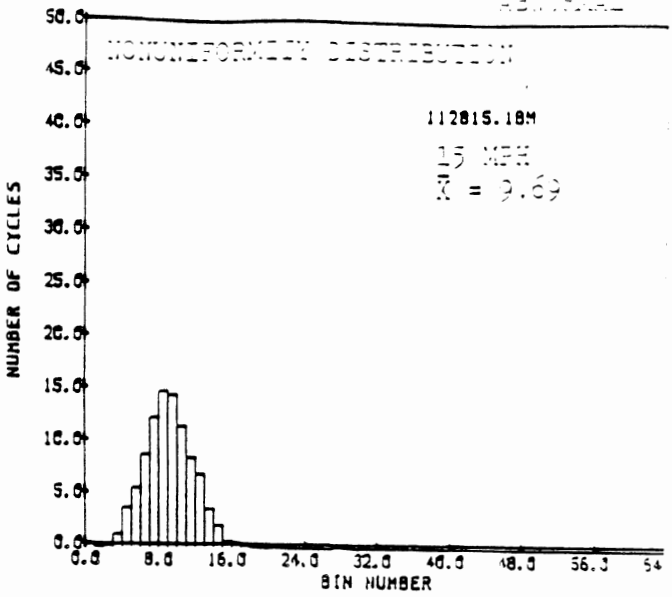
NONUNIFORMITY DISTRIBUTION
112815.18M
15 MPH
$\bar{X}$ = 9.69
NUMBER OF CYCLES
BIN NUMBER

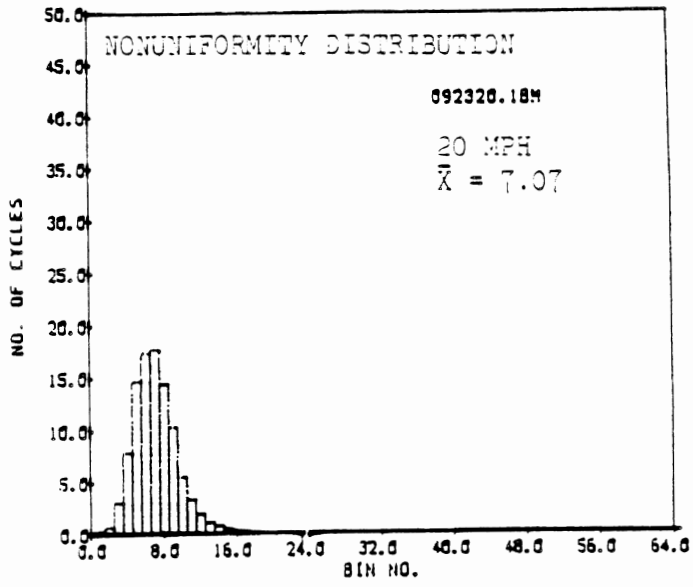
NONUNIFORMITY DISTRIBUTION
092320.18M
20 MPH
$\bar{X}$ = 7.07
NO. OF CYCLES
BIN NO.

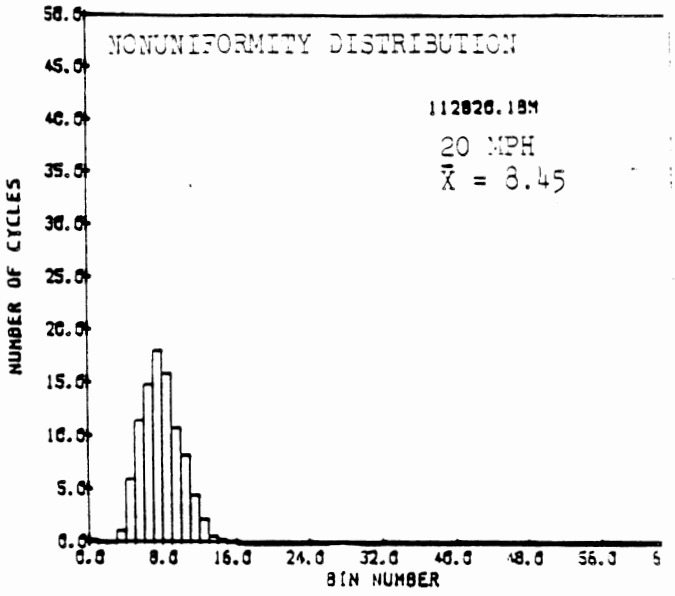
NONUNIFORMITY DISTRIBUTION
112820.18M
20 MPH
$\bar{X}$ = 8.45
NUMBER OF CYCLES
BIN NUMBER

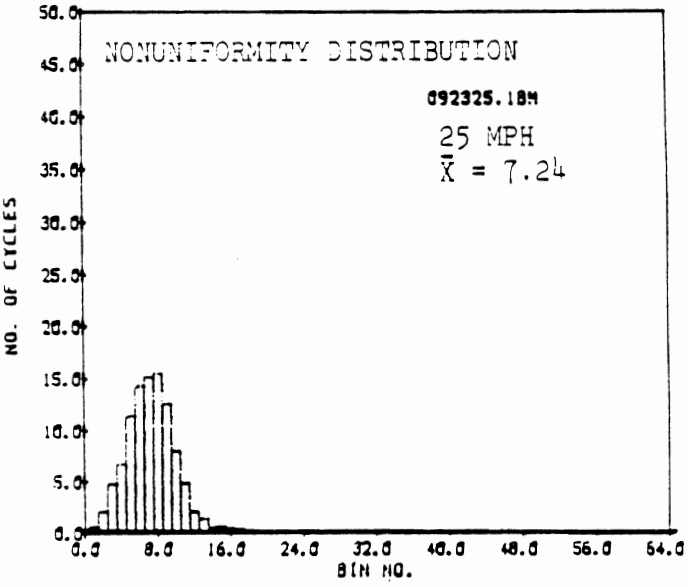
NONUNIFORMITY DISTRIBUTION
092325.18M
25 MPH
$\bar{X}$ = 7.24
NO. OF CYCLES
BIN NO.

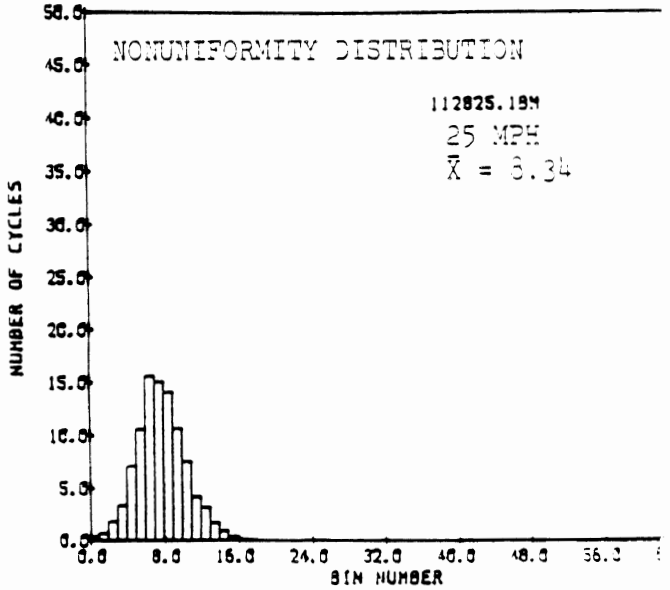
NONUNIFORMITY DISTRIBUTION
112825.18M
25 MPH
$\bar{X}$ = 8.34
NUMBER OF CYCLES
BIN NUMBER

NORMAL

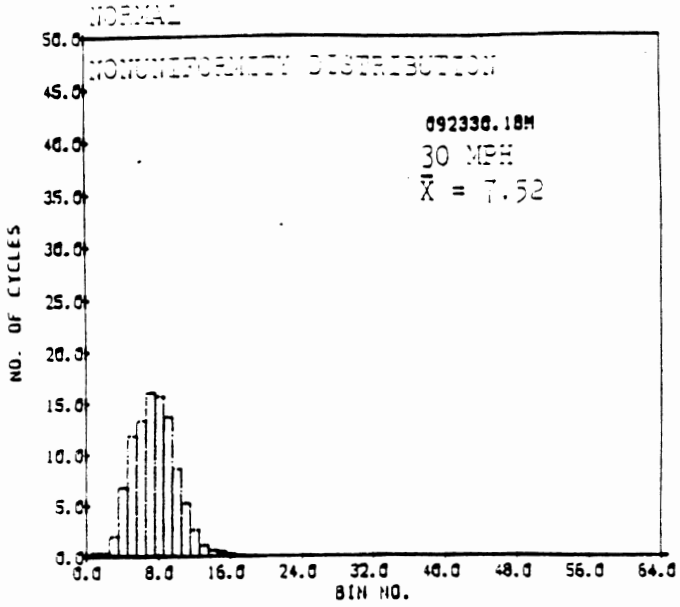

ABNORMAL

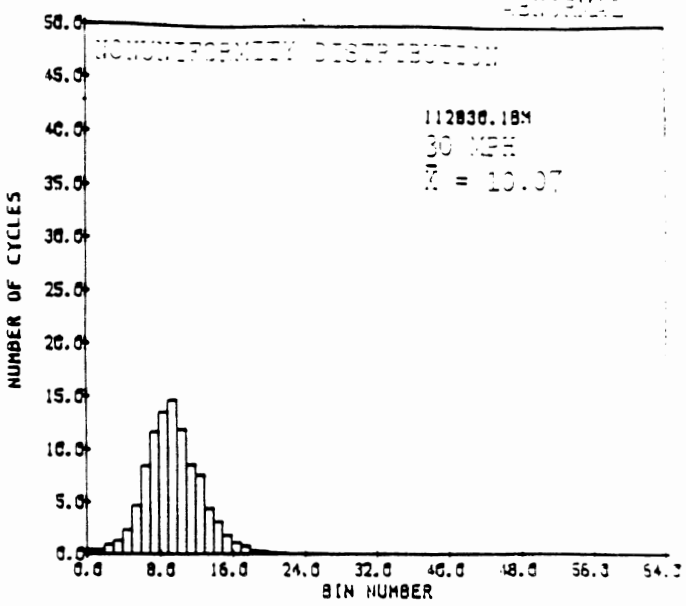

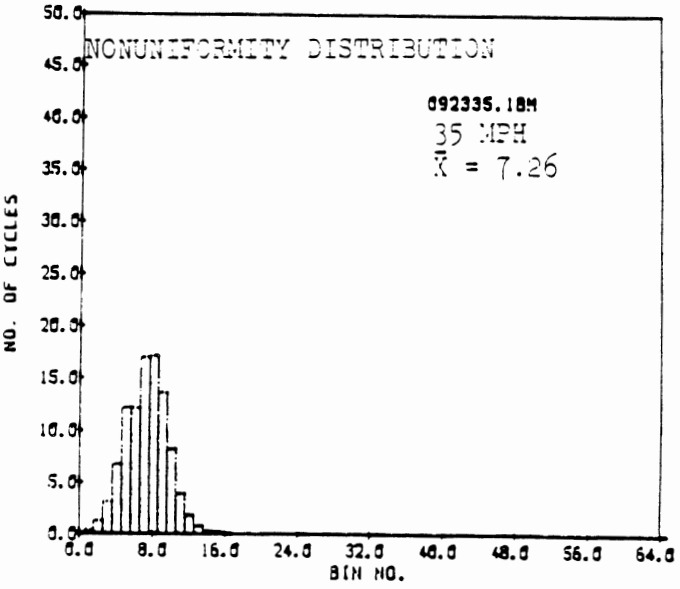

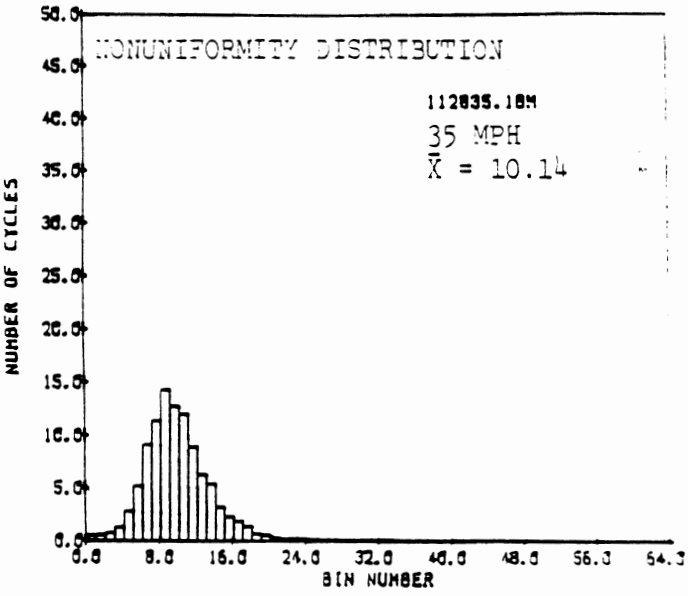

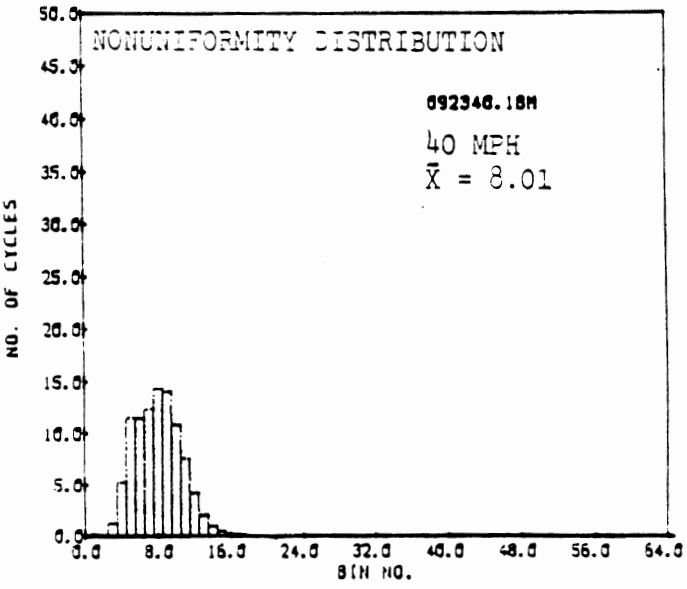

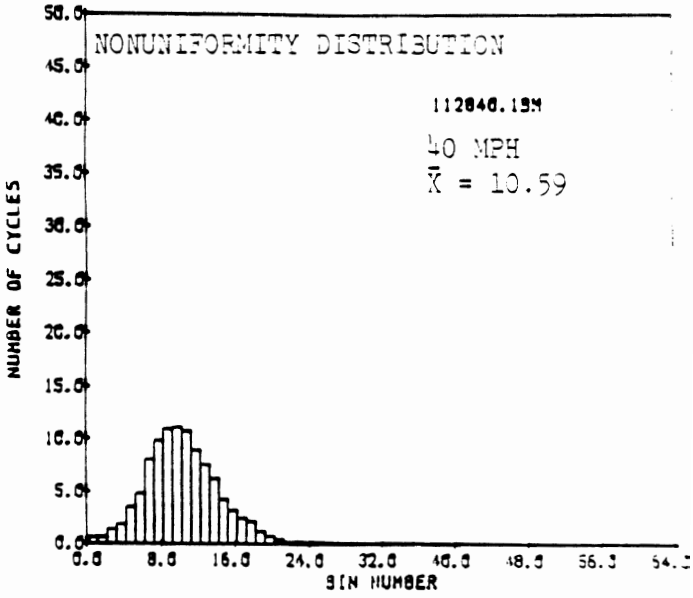

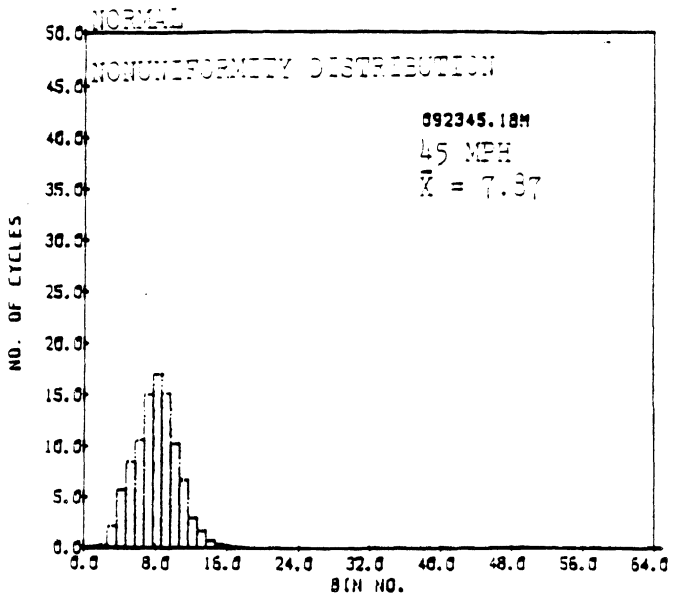
NORMAL
NONUNIFORMITY DISTRIBUTION
092345.18M
45 MPH
X̄ = 7.87
NO. OF CYCLES
BIN NO.

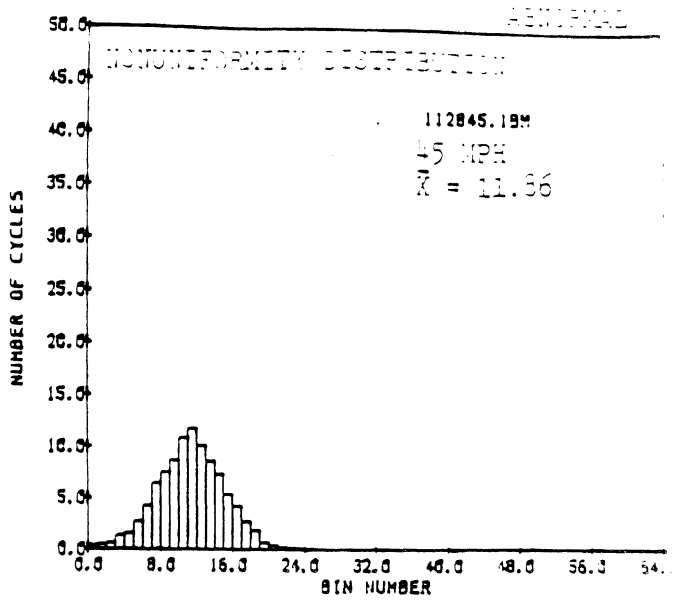
NONUNIFORMITY DISTRIBUTION
112845.18M
45 MPH
X̄ = 11.86
NUMBER OF CYCLES
BIN NUMBER

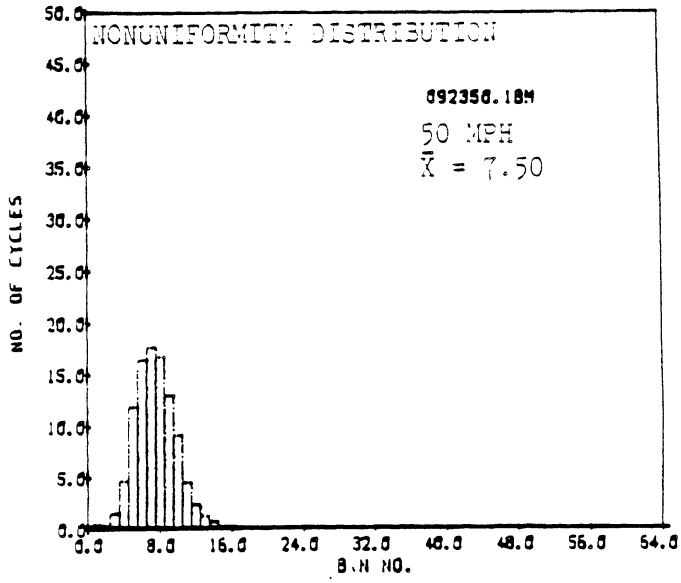
NONUNIFORMITY DISTRIBUTION
092350.18M
50 MPH
X̄ = 7.50
NO. OF CYCLES
BIN NO.

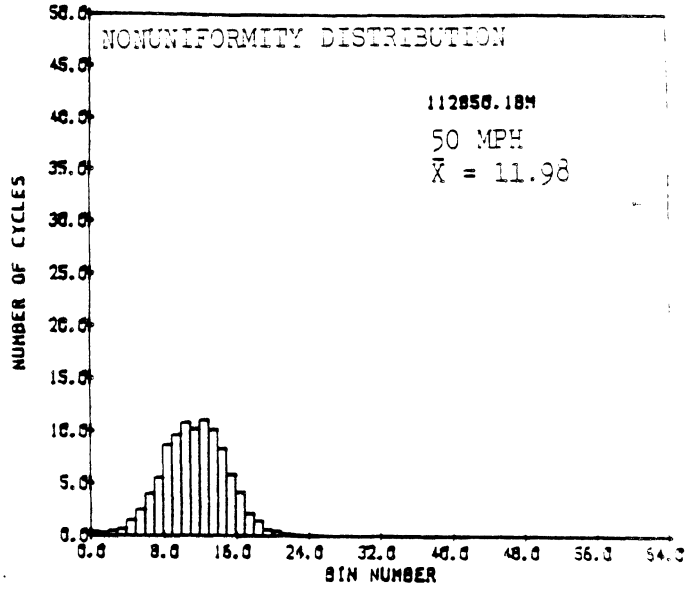
NONUNIFORMITY DISTRIBUTION
112850.18M
50 MPH
X̄ = 11.98
NUMBER OF CYCLES
BIN NUMBER

6. OBSERVATIONS OF EXPERIMENTAL DATA

Several important observations can be made from the data which has been collected on the buses operating in simulated service on the road. Perhaps the most important observation is that the shift in nonuniformity with abnormal engine operation relative to normal operation is greatest for the engine at or near idle condition. It should be recalled that it is this shift in the statistical distribution for n which serves as the 'signature' for abnormal engine operation. In making this observation it is important to recognize that the idle/near-idle condition is being compared with many operating conditions involving the bus driving on the road.

In particular a comparison of the various operating conditions is presented in Table 1. This table lists the various statistical parameters for the statistical distribution of n for each operating condition. Special attention should be given to the shift in mean value. The mean value provides a useful index of engine torque production in the sense that larger values of n indicate relatively poorer engine torque uniformity and relatively poorer engine performance. The other statistical parameters (i.e., standard deviation, skew and kurtosis) are useful primarily as indicators of the shape of the probability distribution functions.

The relatively small shift in the mean value of n for road operating conditions can be explained partly in terms of the relatively high moment of inertia of the engine rotating components. As explained in the theory section of this report, n varies inversely with this moment of inertia for any given torque nonuniformity level.

Another observation which can be made from the experimental data is that the shape of the probability distribution remains relatively unchanged as the mean value shifts. That is, in going from normal operation to abnormal operation the probability density function for n shifts to higher values but the shape remains roughly constant.

Still another important observation which can be made is that an individual cylinder producing abnormal torque can be identified directly from the vector $\underline{n}$. This identification is possible because there is a unique signature for $\underline{n}$ which is associated with failure or partial failure of each cylinder to produce rated torque. Unfortunately, the funding for the present project has not permitted an exhaustive study of this important aspect of the performance measurements.

The above observations form the basis for significant results in the present project. The most important result of these studies is the ability to conduct hypothesis testing measurements to ascertain whether the engine is operating normally or abnormally.

Figure (10) illustrates the concept for this hypothesis testing based upon measurements of n. This figure is a sketch of the probability density function for the random variable n under two hypotheses: H_0 → normal engine operation and H_1 → abnormal engine operation.

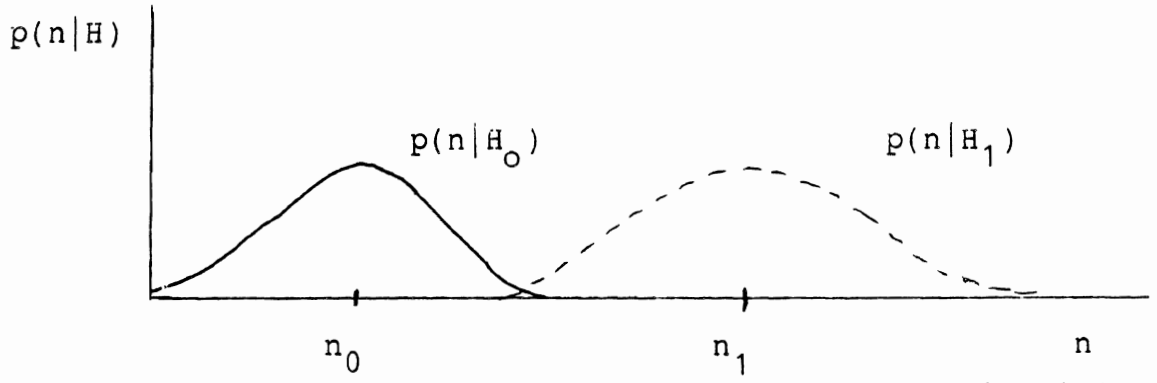

Figure 10. Conditional probability for nonuniformity index

In this figure the solid curve is the probability density function for n under hypothesis H_0 and the dashed curve corresponds to H_1. The ability to distinguish H_0 from H_1 depends upon the shift in $p(n|H_1)$ relative to $p(n|H_0)$.

The observations of the experimental results have demonstrated that the shift in these two functions is greatest for idle and near idle, in gear. Hence the probability of successfully detecting H_1 is greatest for this operating condition.

We conclude therefore that measurements of n are best made with the transmission in gear, the brakes locked, and the engine at or near idle.

We further recommend, with respect to detecting component incipient failure for gradual deterioration to failure, that one-per-day sampling of the statistics for n is probably sufficient for maintenance scheduling purposes. However, we were unable to verify this recommendation with respect to mean-times-to-failure because there were no failures on the buses on which our studies were conducted during the period of data collection. Recall, that tests were conducted using AATA buses. This transit authority has an outstanding maintenance program and has a very well maintained bus fleet.

Nevertheless, for relatively gradual deterioration to failure the once per day sampling should be adequate. In this case, it is further recommended that the instrumentation for n measurement be maintained in the garage and that the buses carry only the two flywheel sensors required to measure n. The signals from these sensors can be provided to the instrumentation via a connector.

It should be noted that if each bus is equipped with the instrumentation, then meaningful data can only be collected during the time the bus is stopped. Continuous monitoring of bus performance throughout the day in actual service is beneficial for detecting relatively rapid performance detrioration.

Measurements can be taken from the two onboard using a single garage-based instrument. This instrument will include sufficient memory to maintain a record for each bus in the fleet. From the daily measurements the time to failure can be estimated.

Another benefit of keeping the performance monitoring equipment in the shop is the ability to coordinate the diagnostic capability of the n measurements with an expert system. It is likely that over the next decade expert systems will be utilized in bus maintenance applications. There is already a strong trend toward such development in automotive maintenance (e.g., GM's CAMs system). The performance data available from measurements of $\underline{n}$ is well suited for expert system diagnosis.

7. SUMMARY AND CONCLUSIONS

We have concluded from our study that the concept for detecting incipient engine component failures based upon measurements of n is feasible. Experimental verification of real time engine performance measurements has been completed. The instrumentation for these measurements has been designed so that on-board measurements can be made for a bus in actual operation.

However, we recommend, based upon experimental studies, that the instrumentation for performance measurements be maintained in the shop. The required sensors for performance measurements should be maintained on each bus.

In addition, we have concluded that the optimum engine operating condition for detecting abnormal operation is at or near idle with the transmission in gear and the brakes locked. This operating condition yields the greatest "signature" for abnormal engine operation.

We recommend sampling the statistics once per day by connecting the sensors to the garage based instrument and collecting data for 2-5 min. This measurement could be conducted during fueling operations. The computer based garage instrument then calculates estimated time-to-failure from present and past measurements of n each day. In addition to time-to-failure, the computer can identify individual cylinders with low performance based upon the vector $\underline{n}$.

A criterion for optimum maintenance scheduling can readily be formulated from the time-to-failure estimates.

APPENDIX A

Detailed Schematic for the Analog Instrument and the Computer Interface

List of IC's used for the instrument

IC-1	LM2907
IC-2	14538
IC-3	3260
IC-4	3260
IC-5	MF-10
IC-6	3260
IC-7	3080
IC-8	3260
IC-9	3260
IC-10	4011
IC-11	4011
IC-12	14538
IC-13	4106
IC-14	4066
IC-15	AC800
IC-16	4106
IC-17	4106
IC-18	3260
IC-19	3260
IC-20	3260
IC-21	LM319N

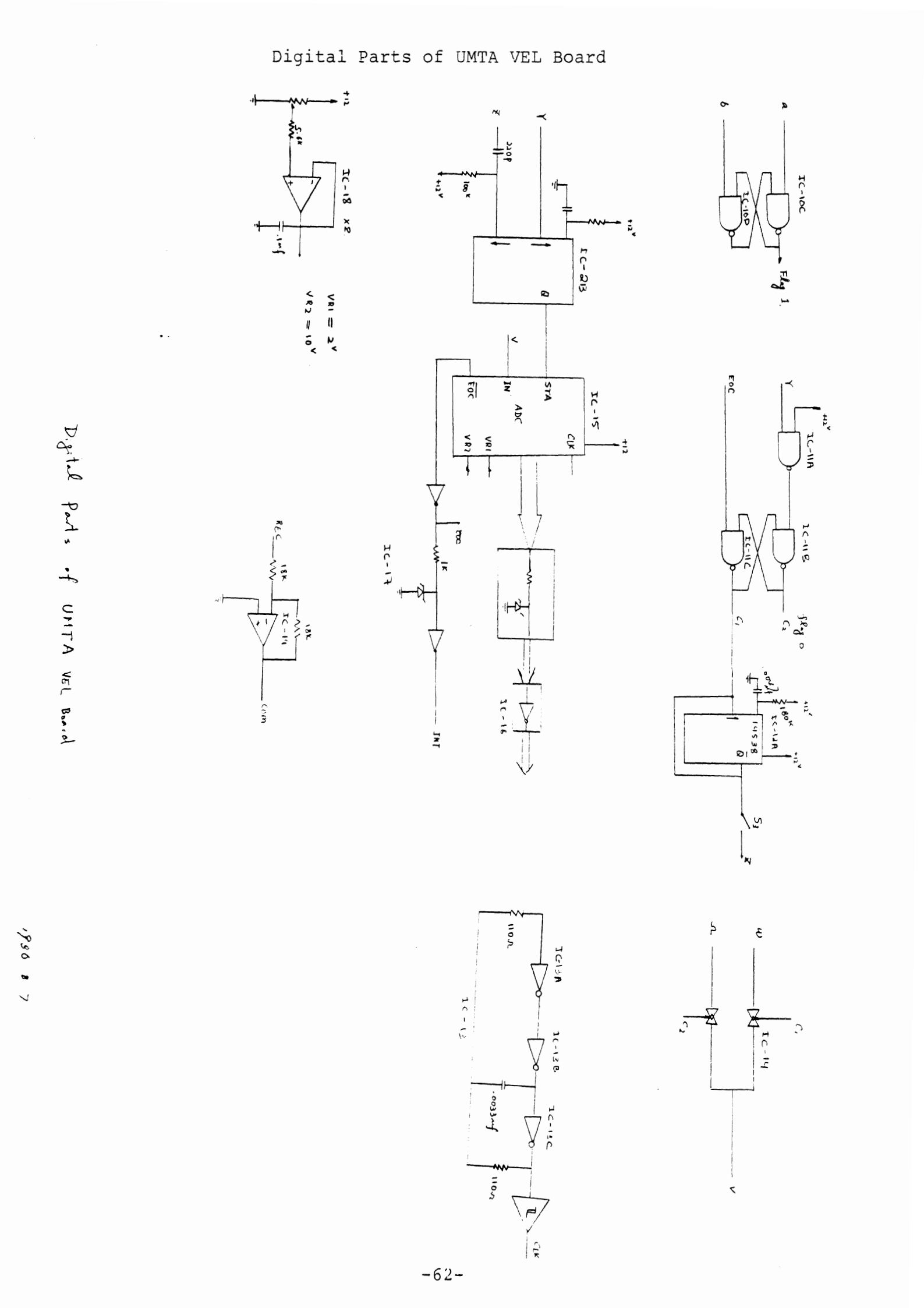

Digital Parts of UMTA VEL Board

1980 8 7

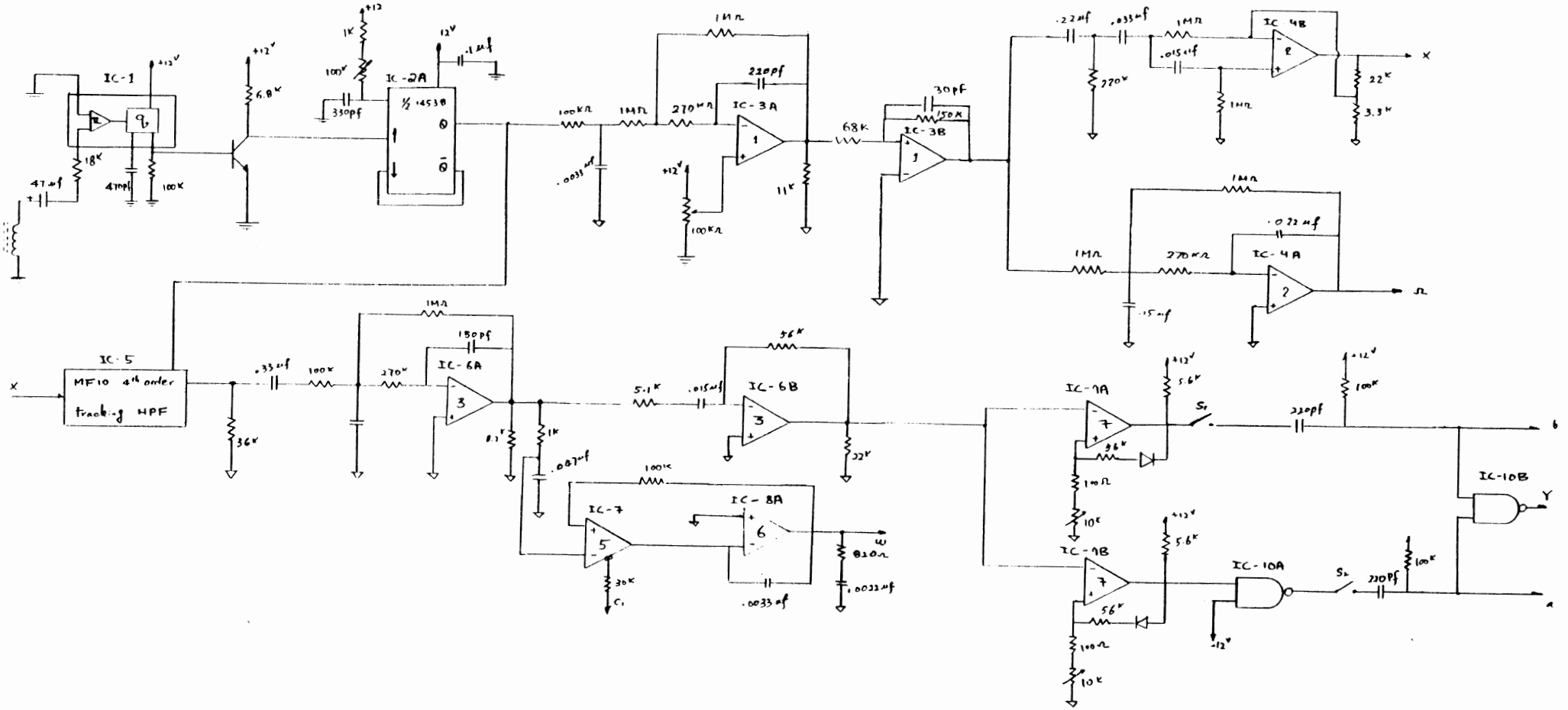

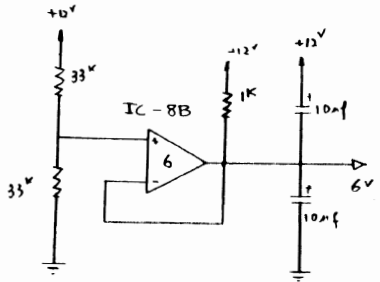

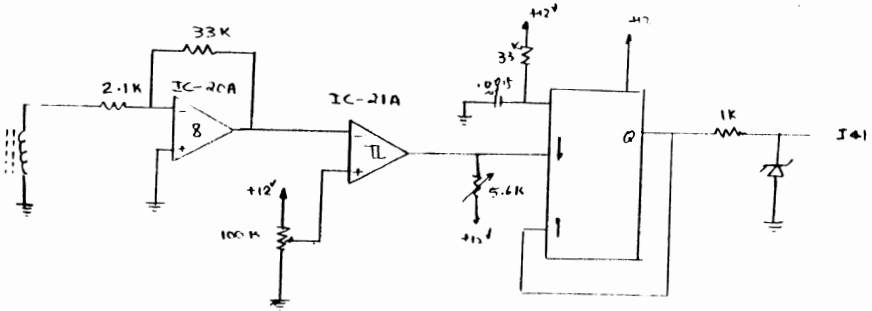

Analog parts of

Analog Parts of the UMTA Vel Board

1986. 8. 7

APPENDIX B

Pulse Generator Output Proportional to Sensor Frequency

If we picture the waveform from the sensor as follows

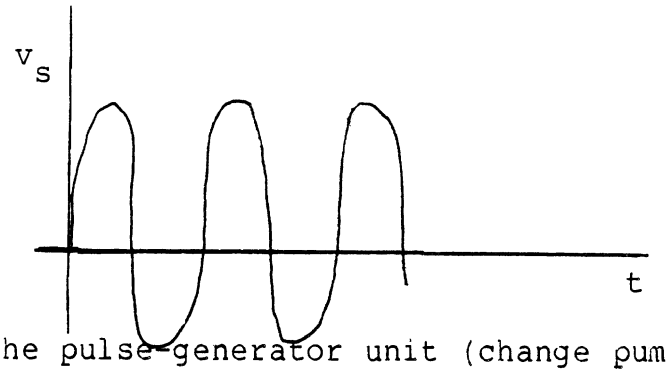

Then the output of the pulse-generator unit (change pump and one shot) would be as follows:

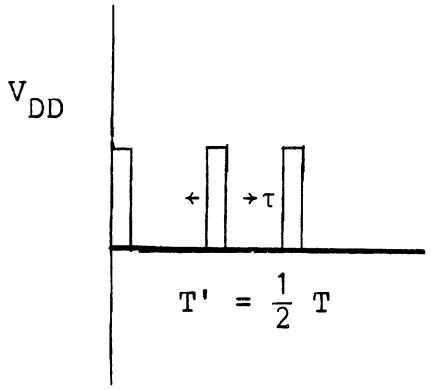

For every zero-crossing of the sensor signal there is a pulse with the width of τ insensitive to variations. The pulse has an average value equivalent to:

$$V_{out} = \frac{1}{T'} \int_0^{\tau} V_{DD}\, dt \qquad T' = \frac{T}{2}$$

$$= \frac{2}{T} \tau V_{DD}$$

$$= 2 \tau V_{DD} \text{ fin} \qquad \text{fin} = \frac{1}{T}$$

where

τ = fixed pulse width of one-shot

V_{DD} = supply voltage

fin = input signal frequency ($\frac{1}{T}$)

APPENDIX C

Circuitry and theory of design for the switched capacitor filter (MF-10)

Requirements:

1) f_c (overall-cutoff frequency) - f_f (firing frequency)
2) $f_s = 10\ f_c$
3) $A_{max} \triangleq 1.0$ dB
4) $A_{min} \triangleq 80$ dB

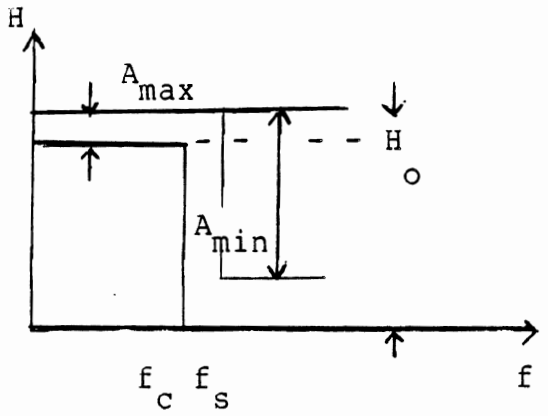

Order Calculations:

$$n = \log_{10} \left(\frac{10^{A_{min}/10} - 1}{10^{A_{max}/10} - 1}\right) / 2 \log_{10} \left(\frac{f_s}{f_c}\right)$$

$$\doteq 4.3$$

Since MF-10 is constituted of two 2nd-order filters, order of n=4 was used.

For n=4, $A_{max} = 1$ dB $f_c = f_f$ and $f_s = 10\ f_c$, we have

$$A_{min} = 10 \log_{10} \left[1 + (10^{0.1A_{max}} - 1) \left(\frac{f_s}{f_c}\right)^{2n}\right]$$

$$= 74.13 \text{ dB}$$

and

$$\frac{f3dB}{f_c} = \left(\frac{10^{0.3} - 1}{10^{0.1A_{max}} - 1}\right)^{1/2n}$$

$$= 1.1833 \quad 1.2$$

thus

$$f3dB = 1.2\ f_c$$

The two Butterworth Low Pass Filters are chosen as follows:

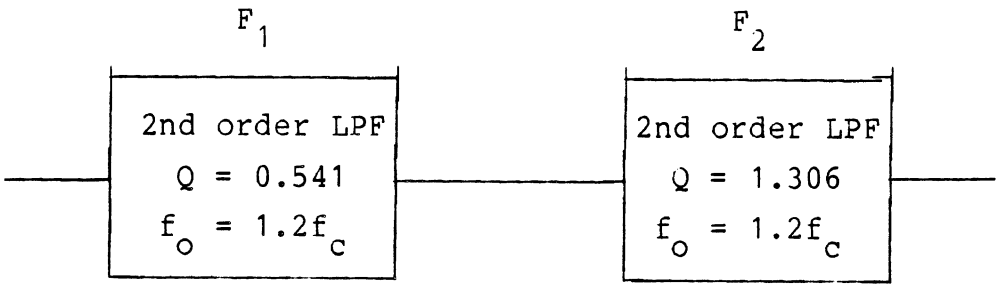

Using model II on the spec. sheet for MF-10

$$f_o = \frac{f_{clk}}{100}\left(\frac{R_2}{R_4} + 1\right)^{1/2} \quad \text{or} \quad f_o = \frac{f_{clk}}{50}\left(\frac{R_2}{R_1} + 1\right)^{1/2}$$

$$f_{notch} = \frac{f_{clock}}{100} \quad \text{or} \quad \frac{f_{clock}}{50}$$

$$Q = \left((R_3/R_4 + 1)/R_2/R_3\right)^{1/2} \qquad H_{olp} = -R_2/R_1 \;/\; (R_2/R_4 + 1)$$

$$f_o = 1.2\, f_c = 1.2\, f_f$$

$$f_{clock} = 2f_s = 34f_f$$

$$\therefore\ 1.2\, f_f = \frac{34f_f}{100}\,(R_2/R_4 + 1)^{1/2}$$

Design Calculations

1) First Filter (F_1)

$Q = 0.54$, $f_o = 1.2\, f_c$

$$\frac{R_2}{R_4} = 11.5$$

$$\frac{R_2}{R_3} = 42.7$$

$$\frac{R_2}{R_1} = 24.9$$

Chosen values $R_1 = 8.2K$, $R_2 = 22K$

$R_3 = 5K$, $R_4 = 18K$

2) Second Filter (F_2)

$Q = 1.306$ $\quad f_o = 1.2\ f_c$

$$\frac{R_2}{R_4} = 11.5$$

$$\frac{R_2}{R_3} = 7.3$$

$$\frac{R_2}{R} = 24.9$$

Chosen values $R_1' = 8.6K$ $\quad R_2' = 38.5K$

$R_3' = 5K$ $\quad R_4' = 18.6K$

MF-10 IC connection diagram

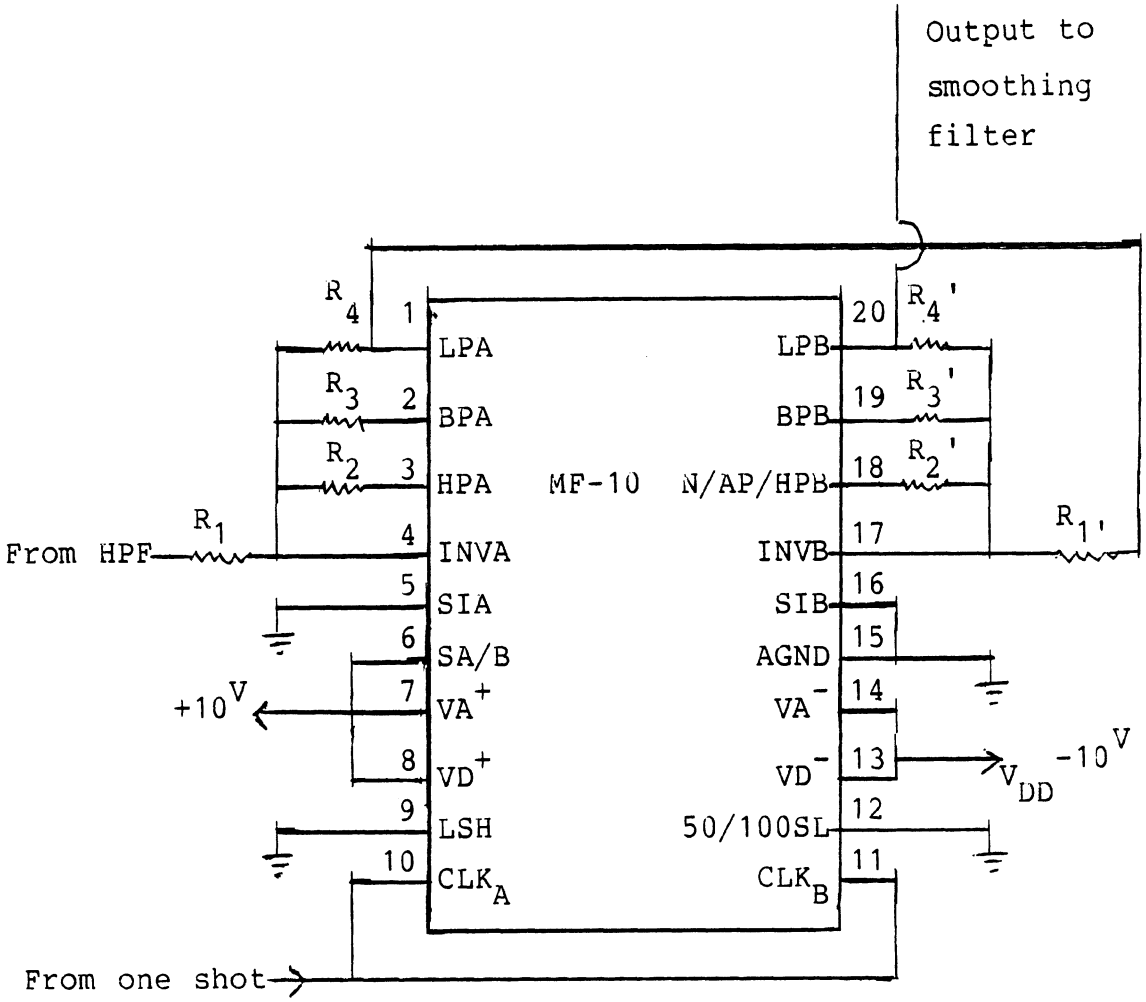

APPENDIX D

Listing of the Program in

Assembler 68000 Language

```
$2000    MOVE.W    #8192,SR
         MOVE.B    #0,$10001
         MOVE.B    #255,$1005
         MOVE.B    #0,$10007
         MOVE.L    #12288,$003C
         MOVE.B    #68,$1000D
         MOVE.B    #4,$1000F
         MOVE.B    #29,$10003
         MOVE.L    #16384, Aϕ
         MOVE.B    #1,$998
         MOVE.L    #0,$1000
         MOVE.L    #0,$1004
         MOVE.W    #10,$1008
         MOVE.W    #12,D7
         MOVE.W    #0,D6
         MOVE.L    #20480,A3
$206C    MOVE.W    #0,(A3)+
         ADDI.W    #1,D6
         CMPI.W    #256,D6
         BMI       $206C
         MOVE.B    #52,$10001
$2082    BRA,      $2082
```

Main Routine

```
$3000    BTST      #1,$1001B
         BNE       $3028
         MOVE.B    $10013,(Aϕ)+
         ADD.W     #1,$1002
         MOVE.B    #0,$10001
         MOVE.B    #52,$10001
         RTE
```

```
$3028    BTST      #0,$998
         BNE       $3044
         MOVE.L    #16384,Aϕ
         MOVE.B    #1,$998
         MOVE.L    #17664,A1
         BRA       $3056
$3044    MOVE.L    #17664,Aϕ
         MOVE.B    #0,$998
         MOVE.L    #16384,A1
$3056    MOVE.L    #0,D5
         MOVE.W    $1002,D5
         MOVE.W    #0,$1002
         MOVE.B    #0,$10001
         MOVE.B    #52,$10001
         CMP.W     #12,D5
         BGT       $3084
         CMP.W     #5,D5
         BLT       $3084
         BRA       $308C
$3084    ADDI.W    #1,$1004
         BRA       $30F8
$308C    MOVE.L    #0,Dϕ
         MOVE.W    #0,D2
$3096    MOVE.W    #0,D1
         MOVE.B    (A1)+,D1
         ADD.W     D1,Dϕ
         ADDI.W    #1,D2
         CMP.W     D5,D2
         BEQ       $30A8
         BRA       $3096
$308A    DIVS.W    D5,Dϕ
         MOVE.L    #0,D3
         MOVE.W    #0,D2
```

```
$30B4    MOVE.W    #0,D1
         MOVE.B    -(A1),D1
         SUB.W     Dϕ,D1
         BPL       $30C0
         NEG.W     D1
$30C0    ADD.W     D1,D3
         ADDI.W    #1,D2
         CMP.W     D5,D2
         BEQ       $30CC
         BRA       $30B4
$30CC    DIVS.W    D5,D3
         MOVE.L    #0,D1
         MOVE.W    D3,D1
         ADD.W     D1,D1
         MOVE.L    #20480,A2
         ADDA.W    D1,A2
         ADDI.W    #1,(A2)
         ADDI.W    #1,$1000
         ADDI.W    #1,$1006
         CMPI.W    #4,$1006
         BEQ       $30FA
$30F8    RTE
$30FA    MOVE.W    #0,$1006
         MOVE.L    #0,D6
         MOVE.W    D3,D6
         DIVS.W    $1008,D6
         SWAP      D6
         LSL.W     D7,D6
         LSR.L     D7,D6
         MOVE.B    D6,$10011
$3118    RET
```

BIBLIOGRAPY

1. "A Noncontacting Torque Sensor for the Internal Combustion Engine," W. B. Ribbens, SAE International Congress & Exposition, Cobo Hall, Detroit, Mich., Feb. 23-27, 1981, SAE 810155.

2. "Experimental Road Test of A Noncontacting Method of Measuring I-C Engine Torque Nonuniformity," W. B.Ribbens, SAE International Congress & Exposition, Cobo Hall, Detroit, Mich., Feb. 27-Mar. 2, 1984, SAE 840136.

3. "An On-line Engine Roughness Measurement Technique," S. Citron & W. Mihekc, SAE International Congress and Exposition, Cobo Hall, Detroit, Mich., Feb. 22-Mar. 2, 1984, SAE 840136.

4. "A New Metric for Torque Nonuniformity," W. B. Ribbens, SAE International Congress & Exposition, Cobo Hall, Detroit, Mich., Feb. 28-Mar. 4, 1983, SAE 830425.